

---

# Safe Pontryagin Differentiable Programming

---

**Wanxin Jin**  
University of Pennsylvania  
wanxinjin@gmail.com

**Shaoshuai Mou**  
Purdue University  
mous@purdue.edu

**George J. Pappas**  
University of Pennsylvania  
pappasg@seas.upenn.edu

## Abstract

We propose a Safe Pontryagin Differentiable Programming (Safe PDP) methodology, which establishes a theoretical and algorithmic framework to solve a broad class of safety-critical learning and control tasks—problems that require the guarantee of safety constraint satisfaction at any stage of the learning and control progress. In the spirit of interior-point methods, Safe PDP handles different types of system constraints on states and inputs by incorporating them into the cost or loss through barrier functions. We prove three fundamentals of the proposed Safe PDP: first, both the solution and its gradient in the backward pass can be approximated by solving their more efficient unconstrained counterparts; second, the approximation for both the solution and its gradient can be controlled for arbitrary accuracy by a barrier parameter; and third, importantly, all intermediate results throughout the approximation and optimization strictly respect the constraints, thus guaranteeing safety throughout the entire learning and control process. We demonstrate the capabilities of Safe PDP in solving various safety-critical tasks, including safe policy optimization, safe motion planning, and learning MPCs from demonstrations, on different challenging systems such as 6-DoF maneuvering quadrotor and 6-DoF rocket powered landing.

## 1 Introduction

Safety is usually a priority in the deployment of a learning or control algorithm to real-world systems. For a physical system (agent), safety is normally given in various constraints on system states and inputs, which must not be violated by the algorithm at *any stage* of the learning and control process, otherwise will cause irrevocable or unacceptable failure/damage. Those systems are referred to as *safety-critical*. The constraints in a safety-critical system can include the immediate ones, which are directly imposed on the system state and input at certain or all-time instances, and the long-term ones, which are defined on the trajectory of system states and inputs over a long period.

Compared to the abundant results that focus on system optimality [1–3], systematic and principled treatments for safety-critical learning and control problems seem largely insufficient, particularly in the following gaps (detailed in Section 1.1). First, existing safety strategies are either too conservative, which may restrict the task performance, or violation-tolerable, which only pursues the near-constraint guarantee and thus are not strictly constraint-respecting. Second, a systematic safety paradigm capable of handling different types of constraints, including system state and input (or mixed), immediate, or/and long-term constraints, is still lacked. Third, some existing safety strategies suffer from huge computational- and data- complexity, difficult to be integrated into any differentiable programming frameworks to solve large-scale learning and continuous control tasks.

To address the above research gaps, this paper aims to develop a *safe differentiable programming* framework with the following key capabilities. First, the framework provides a systematic treatment for *different types of constraints* in a safety-critical problem; second, it attains *provable safety- and accuracy- guarantees* throughout the learning and control process; third, it is flexible to perform *safe learning* of any unknown aspects of a constrained decision-making system, including policy, dynamics, state and input constraints, and control cost; finally, it can be integrated to any *differentiable programming framework* to efficiently solve large-scale safe learning and control tasks.

## 1.1 Related Work

In machine learning and control fields, safety has been defined by different criteria, such as worst-case [4, 5], risk-sensitive [6], ergodicity [7], robust [8, 9], etc., most of which are formulated by directly altering an objective function [10]. In this paper, we focus only on constrained learning and control problems, where constraints are *explicitly formulated and must be satisfied*. We categorize existing techniques into *at-convergence safety* methods, which only concern constraint satisfaction at convergence, or *in-progress safety* methods, which attempt to ensure constraint satisfaction during the entire optimization process.

**At-convergence safety methods.** In reinforcement learning (RL), a constrained agent is typically formulated as a Constrained Markov Decision Process (CMDP) [11], seeking a policy that not only optimizes a reward but also satisfies an upper bound for a cumulative cost. A common strategy [12–17] to solve CMDPs is to use the primal-dual method, by establishing the unconstrained Lagrangian and performing saddle-point optimization. In deep learning, the primal-dual method has been recently used [18] to train deep neural networks with constraints. In control, the primal-dual method has been used to solve constrained optimal control (constrained trajectory) problems [19–21]. While proved to satisfy constraints at convergence [22, 23], the primal-dual type methods cannot guarantee constraint satisfaction during optimization, as shown in [13, 24], thus are not suitable for safety-critical tasks.

**In-progress safety methods.** To enforce safety during training, [25] and [26] solve CMDPs by introducing additional constraints into the Trust Region Policy Optimization (TRPO) [27]. Since these methods only obtain the ‘near constraint’ guarantee, constraint violation is not fully eliminated. Another line of constrained RL [24, 28–30] leverages the Lyapunov theory [31] to bound behavior of an agent. But how to choose a valid Lyapunov function for general tasks is still an open problem to date [32], particularly for constrained RL, since it requires a Lyapunov function to be consistent with the constraints and to permit optimal policies [28]. Some other work also attempts to handle immediate constraints — the constraints imposed on agent state and input at any time. In [33], a safe exploration scheme is proposed to produce a safe reachable region; and it only considers finite state space. [34] develops a method that learns safety constraints and then optimizes a reward within the certified safe region; the method defines constraints purely on agent state and thus may not be readily applicable to mixed state-input constraints.

In control, in-progress safety can be achieved via two model-based frameworks: reachability theory [35] and control barrier functions [36, 37]. Safe control based on reachability theory [35, 38–40] explicitly considers adversarial factors and seeks a strategy that maintains the constraints despite the adversarial factors. This process typically requires solving the Hamilton-Jacobi-Isaacs equations [41], which become computationally difficult for high-dimensional systems [35]. Control barrier functions [36, 37] constrain a system only on safety boundaries, making it a less-conservative strategy for safety-critical tasks [42–44]. Most of the methods consider affine dynamics and directly use the given constraint function as a control barrier function. Such a choice could be problematic when a system is uncontrollable at the boundary of the sublevel set. Thus, how to find a valid control barrier function is still an ongoing research topic [45–47]. The above two control safety frameworks favorably focus on pure state constraints and cannot be readily extended to other constraints, such as mixed state-input constraints or the cumulative constraints defined on the system trajectory.

**Interior-point methods and control.** Interior-point methods (IPMs) [48–50] solve constrained optimization by sequentially finding solutions to unconstrained problems with the objective combining the original objective and a barrier that prevents from leaving the feasible regions. IPMs have been used for *constrained* linear quadratic regular (LQR) control in [51–57]. While IPMs for nonlinear constrained optimal control are studied in [58–62], they mostly focus on developing algorithms to solve the unconstrained approximation (from the perturbed KKT conditions) and lack of performance analysis. Most recently, [63] uses the IPM to develop a zero-th order non-convex optimization method; and [64] uses IPMs to solve reinforcement learning with only cumulative constraints. Despite the promise of the trend, the theoretical results and systematic algorithms regarding the *differentiability of general constrained control systems based on IPMs* have not been studied and established.

**Differentiable projection layer.** In machine learning, a recent line of work considers embedding a differentiable projection layer [65–67] into a general training process to ensure safety. Particularly, [67] and [66] enforce safety by constructing a dedicated projection layer, which projects the unsafe actions outputted from a neural policy into a safe region (satisfying safety constraints). This projection layer is a differentiable convex layer [68, 69], which can be trained end-to-end. In [65], safety is

defined as robustness in the case of the worst adversarial disturbance, and the set of robust policies is solved by classic robust control (solving LMIs). An RL neural policy with a differentiable projection layer is learned such that the action from the neural policy lies in the robust policy set. Different from the above work, Safe PDP does not enforce safety by projection; instead, Safe PDP uses *barrier functions* to guarantee safety constraint satisfaction. More importantly, we have shown, in both theory and experiments, that *with barrier functions, differentiability can also be attained*.

**Sensitivity analysis and differentiable MPCs.** Other work related to Safe PDP includes the recent results for sensitivity analysis [70], which focuses on differentiation of a solution to a general nonlinear program, and differentiable MPCs [68], which is based on differentiable quadratic programming. In long-horizon control settings, directly applying [70] and [68] can be inefficient: the complexity of [68, 70] for differentiating a solution to a general optimal control system is at least  $\mathcal{O}(T^2)$  ( $T$  is the time horizon) due to computing the inverse of Jacobian of the KKT conditions. Since an optimal control system has more sparse structures than general nonlinear or quadratic programs, by exploiting those structures and proposing the *Auxiliary Control System*, Safe PDP enjoys the complexity of  $\mathcal{O}(T)$  for differentiating a solution to a general control system. Such advantages have been discussed and shown in the foundational PDP work [71] and will also be shown later (in Section 8) in this paper.

## 1.2 Paper Contributions

We propose a safe differentiable programming methodology named as *Safe Pontryagin Differentiable Programming* (Safe PDP). Safe PDP provides a systematic treatment of different types of system constraints, including state and inputs (or mixed), immediate, and long-term constraints, with provable safety- and performance-guarantee. Safe PDP is also a unified differentiable programming framework, which can be used to efficiently solve a broad class of safety-critical learning and control tasks.

In the spirit of interior-point methods, Safe PDP incorporates different types of system constraints into control cost and loss through barrier functions, approximating a constrained control system and task using their unconstrained counterparts. Contributions of Safe PDP are theoretical and algorithmic. Theoretically, we prove in Theorem 2 and Theorem 3 that (I) not only a solution but also the gradient of the solution can be safely approximated by solving a more efficient unconstrained counterpart; (II) any intermediate results throughout the approximation and optimization are strictly safe, that is, never violating the original system/task constraints; and (III) the approximations for both solution and its gradient can be controlled for arbitrary accuracy by barrier parameters. Arithmetically, (IV) we prove in Theorem 1 that if a constrained control system is differentiable, the gradient of its trajectory is a globally unique solution to an Auxiliary Control System [71], which can be solved efficiently with the complexity of only  $\mathcal{O}(T)$ ,  $T$  is control horizon; (V) in Section 7, we experimentally demonstrate the capability of Safe PDP for efficiently solving various safety-critical learning and control problems, including safe neural policy optimization, safe motion planning, learning MPCs from demonstrations.

## 2 Safe PDP Problem Formulation

Consider a class of constrained optimal control systems (models)  $\Sigma(\theta)$ , which are parameterized by a tunable parameter  $\theta \in \mathbb{R}^r$  in its control cost function, dynamics, initial condition, and constraints:

$$\Sigma(\theta) : \begin{array}{l} \text{control cost: } J(\theta) = \sum_{t=0}^{T-1} c_t(\mathbf{x}_t, \mathbf{u}_t, \theta) + c_T(\mathbf{x}_T, \theta) \\ \text{subject to} \\ \text{dynamics: } \mathbf{x}_{t+1} = \mathbf{f}(\mathbf{x}_t, \mathbf{u}_t, \theta) \quad \text{with } \mathbf{x}_0 = \mathbf{x}_0(\theta), \quad \forall t, \\ \text{terminal constraints: } \mathbf{g}_T(\mathbf{x}_T, \theta) \leq \mathbf{0}, \quad \mathbf{h}_T(\mathbf{x}_T, \theta) = \mathbf{0}, \\ \text{path constraints: } \mathbf{g}_t(\mathbf{x}_t, \mathbf{u}_t, \theta) \leq \mathbf{0}, \quad \mathbf{h}_t(\mathbf{x}_t, \mathbf{u}_t, \theta) = \mathbf{0}, \quad \forall t. \end{array} \quad (1)$$

Here,  $\mathbf{x}_t \in \mathbb{R}^n$  is the system state;  $\mathbf{u}_t \in \mathbb{R}^m$  is the control input;  $c_t : \mathbb{R}^n \times \mathbb{R}^m \times \mathbb{R}^r \rightarrow \mathbb{R}$  and  $c_T : \mathbb{R}^n \times \mathbb{R}^r \rightarrow \mathbb{R}$  are the stage and final costs, respectively;  $\mathbf{f} : \mathbb{R}^n \times \mathbb{R}^m \times \mathbb{R}^r \rightarrow \mathbb{R}^n$  is the dynamics with initial state  $\mathbf{x}_0 = \mathbf{x}_0(\theta) \in \mathbb{R}^n$ ;  $t = 0, 1, \dots, T$  is the time step with  $T$  the time horizon;  $\mathbf{g}_T : \mathbb{R}^n \times \mathbb{R}^r \rightarrow \mathbb{R}^{q_T}$  and  $\mathbf{h}_T : \mathbb{R}^n \times \mathbb{R}^r \rightarrow \mathbb{R}^{s_T}$  are the final inequality and equality constraints, respectively;  $\mathbf{g}_t : \mathbb{R}^n \times \mathbb{R}^m \times \mathbb{R}^r \rightarrow \mathbb{R}^{q_t}$  and  $\mathbf{h}_t : \mathbb{R}^n \times \mathbb{R}^m \times \mathbb{R}^r \rightarrow \mathbb{R}^{s_t}$  are the immediate inequality and equality constraints at time  $t$ , respectively. All inequalities (here and below) are entry-wise. We consider that all functions in  $\Sigma(\theta)$  are three-times continuously differentiable (i.e.,  $C^3$ ) with respect to its arguments. Although we here have parameterized all aspects of  $\Sigma(\theta)$ , for a specific application (see Section 7), one only needs to parameterize the unknown aspects in  $\Sigma(\theta)$  and keep others given.

Any unknown aspects in  $\Sigma(\theta)$  can be implemented by differentiable neural networks. For a given  $\theta$ ,  $\Sigma(\theta)$  produces a trajectory  $\xi_\theta = \{x_{0:T}^\theta, u_{0:T-1}^\theta\}$  by solving the following Problem **B**( $\theta$ ):

$$\begin{aligned} \xi_\theta = \{x_{0:T}^\theta, u_{0:T-1}^\theta\} \in \arg \min_{\{x_{0:T}, u_{0:T-1}\}} & J(\theta) \\ \text{subject to} & \quad x_{t+1} = f(x_t, u_t, \theta) \quad \text{with } x_0 = x_0(\theta), \quad \forall t, \\ & \quad g_T(x_T, \theta) \leq 0 \quad \text{and } h_T(x_T, \theta) = 0, \\ & \quad g_t(x_t, u_t, \theta) \leq 0 \quad \text{and } h_t(x_t, u_t, \theta) = 0, \quad \forall t. \end{aligned} \quad \mathbf{B}(\theta)$$

Here, we use  $\in$  since  $\xi_\theta$  to Problem **B**( $\theta$ ) may not be unique in general, thus constituting a solution set  $\{\xi_\theta\}$ . We will discuss the existence and uniqueness of  $\{\xi_\theta\}$  in Section 4.

For a specific task, we aim to find a specific model  $\Sigma(\theta^*)$ , i.e., searching for a specific  $\theta^*$ , such that its trajectory  $\xi_{\theta^*}$  from **B**( $\theta^*$ ) meets the following two *given* requirements. First,  $\xi_{\theta^*}$  minimizes a *given task loss*  $\ell(\xi_\theta, \theta)$ ; and second,  $\xi_{\theta^*}$  satisfies the *given task constraints*  $R_i(\xi_\theta, \theta) \leq 0, i = 1, 2, \dots, l$ . Note that, we need to distinguish between the two types of objectives: task loss  $\ell(\xi_\theta, \theta)$  and control cost  $J(\theta)$ , and also the two types of constraints: task constraints  $R_i(\xi_\theta, \theta)$  and model constraints  $g_t(\theta)$ . In fact,  $J(\theta)$  and  $g_t(\theta)$  in  $\Sigma(\theta)$  are *unknown and parameterized by  $\theta$*  and can represent the unknown inherent aspects of a physical agent, while  $\ell(\xi_\theta, \theta)$  and  $R_i(\xi_\theta, \theta)$  are *given and known* depending on the specific task (they also explicitly depend on  $\theta$  since  $\theta$  needs to be regularized in some learning cases). Assume  $\ell(\xi_\theta, \theta)$  and  $R_i(\xi_\theta, \theta)$  are both twice-continuously differentiable. The problem of searching for  $\theta^*$  can be formally written as:

$$\begin{aligned} \theta^* = \arg \min_{\theta} & \ell(\xi_\theta, \theta) \\ \text{subject to} & \quad R_i(\xi_\theta, \theta) \leq 0, \quad i = 1, 2, \dots, l, \\ & \quad \xi_\theta \text{ solves Problem } \mathbf{B}(\theta). \end{aligned} \quad \mathbf{P}$$

For a specific learning and control task, one only needs to specify the details of  $\Sigma(\theta)$  and give a task loss  $\ell(\xi_\theta, \theta)$  and constraints  $R_i(\xi_\theta, \theta) \leq 0$ . Section 7 will give representative examples.

### 3 Challenges to Solve Problem **P**

Problem **P** belongs to bi-level optimization [72]—each time  $\theta$  is updated in the outer-level (including task loss  $\ell$  and task constraint  $R_i$ ) of Problem **P**, the corresponding trajectory  $\xi_\theta$  needs to be solved from the inner-level Problem **B**( $\theta$ ). Similar to PDP [71], one could approach Problem **P** using gradient-based methods by ignoring the process of solving inner-level Problem **B**( $\theta$ ) and just viewing  $\xi_\theta$  as an explicit differentiable function of  $\theta$ . Then, based on interior-point methods [48], one can introduce a logarithmic barrier function for each task constraint,  $-\ln(-R_i)$ , and a barrier parameter  $\epsilon > 0$ . This leads to solving the following unconstrained Problem **SP**( $\epsilon$ ) sequentially

$$\theta^*(\epsilon) = \arg \min_{\theta} \ell(\xi_\theta, \theta) - \epsilon \sum_{i=1}^l \ln(-R_i(\xi_\theta, \theta)) \quad \mathbf{SP}(\epsilon)$$

for a fixed  $\epsilon$ . By controlling  $\epsilon \rightarrow 0$ ,  $\theta^*(\epsilon)$  is expected to converge to the solution  $\theta^*$  to Problem **P**. Although plausible, the above process has the following technical challenges to be addressed:

- (1) As  $\xi_\theta$  is a solution to the constrained optimal control Problem **B**( $\theta$ ), is  $\xi_\theta$  differentiable? Does the auxiliary control system [71] exist for solving  $\frac{\partial \xi_\theta}{\partial \theta}$ ?
- (2) Since we want to obtain  $\xi_\theta$  and  $\frac{\partial \xi_\theta}{\partial \theta}$  at as low cost as possible, instead of solving the constrained Problem **B**( $\theta$ ), can we use an *unconstrained* system to approximate both  $\xi_\theta$  and  $\frac{\partial \xi_\theta}{\partial \theta}$ ? Importantly, can the accuracy of the approximations for  $\xi_\theta$  and  $\frac{\partial \xi_\theta}{\partial \theta}$  be arbitrarily and safely controlled?
- (3) Can we guarantee that the approximation for  $\xi_\theta$  is safe in a sense that the approximation always respects the system original inequality constraints  $g_t \leq 0$  and  $g_T \leq 0$ ?
- (4) With the safe approximations for both  $\xi_\theta$  and  $\frac{\partial \xi_\theta}{\partial \theta}$ , can accuracy of the solution to the outer-level unconstrained optimization **SP**( $\epsilon$ ) be arbitrarily controlled towards  $\theta^*$ ?
- (5) With the safe approximations for both  $\xi_\theta$  and  $\frac{\partial \xi_\theta}{\partial \theta}$ , can we guarantee the safety of the outer-level inequality constraints  $R_i \leq 0$  during the optimization for the outer-level **SP**( $\epsilon$ )?

The following paper will address the above challenges. For reference, we give a quick overview: Challenge (1) will be addressed in Section 4 and the result is in Theorem 1; Challenges (2) and (3) will be addressed in Section 5 and the result is in Theorem 2; Challenges (4) and (5) will be addressed in Section 6 and the result is in Theorem 3; and Section 7 gives some representative applications.

## 4 Differentiability for $\Sigma(\theta)$ and its Auxiliary Control System

### 4.1 Differentiability of $\xi_\theta$

For the constrained optimal control system  $\Sigma(\theta)$  in (1), we define the following Hamiltonian  $L_t$  for  $t = 0, 1, \dots, T-1$  and  $L_T$ , respectively,

$$L_t = c_t(x_t, u_t, \theta) + \lambda'_{t+1} f(x_t, u_t, \theta) + v'_t g_t(x_t, u_t, \theta) + w'_t h_t(x_t, u_t, \theta), \quad (2a)$$

$$L_T = c_T(x_T, \theta) + v'_T g_T(x_T, \theta) + w'_T h_T(x_T, \theta), \quad (2b)$$

where  $\lambda_t \in \mathbb{R}^n$  is the costate,  $v_t \in \mathbb{R}^{q_t}$  and  $w_t \in \mathbb{R}^{s_t}$  are multipliers for the inequality and equality constraints, respectively. The well-known second-order condition for  $\xi_\theta$  to be a *local isolated (locally unique) minimizing trajectory* to  $\Sigma(\theta)$  in Problem B( $\theta$ ) has been well-established in [73]. For completeness, we present it in Lemma A.2 in Appendix A. Lemma A.2 states that there exist costate sequence  $\lambda_{1:T}^\theta$ , and multiplier sequences  $v_{0:T}^\theta$  and  $w_{0:T}^\theta$ , such that  $(\xi_\theta, \lambda_{1:T}^\theta, v_{0:T}^\theta, w_{0:T}^\theta)$  satisfies the well-known Constrained Pontryagin Minimum Principle (C-PMP) given in (S.5) in Lemma A.2. Based on the above, one can have the following result for the differentiability of  $\xi_\theta$ .

**Lemma 1** (Differentiability of  $\xi_\theta$ ). *Given a fixed  $\bar{\theta}$ , assume the following conditions hold for  $\Sigma(\bar{\theta})$ :*

- (i) *the second-order condition (Lemma A.2) is satisfied for  $\Sigma(\bar{\theta})$ ;*
- (ii) *the gradients of all binding constraints at  $\xi_{\bar{\theta}}$  are linearly independent (binding constraints include all equality constraints and all active inequality constraints);*
- (iii) *strict complementarity holds at  $\xi_{\bar{\theta}}$ , i.e., active inequality constraint has positive multiplier.*

*Then, for all  $\theta$  in a neighborhood of  $\bar{\theta}$ , there exists a unique once-continuously differentiable function  $(\xi_\theta, \lambda_{1:T}^\theta, v_{0:T}^\theta, w_{0:T}^\theta)$  that satisfies the second-order condition (Lemma A.2) for the constrained optimal control system  $\Sigma(\theta)$  with  $(\xi_\theta, \lambda_{1:T}^\theta, v_{0:T}^\theta, w_{0:T}^\theta) = (\xi_{\bar{\theta}}, \lambda_{1:T}^{\bar{\theta}}, v_{0:T}^{\bar{\theta}}, w_{0:T}^{\bar{\theta}})$  at  $\theta = \bar{\theta}$ . Hence,  $\xi_\theta$  is a local isolated minimizing trajectory to  $\Sigma(\theta)$ . Further, for all  $\theta$  near  $\bar{\theta}$ , the strict complementarity is preserved, and the linear independence of the gradients of all binding constraints at  $\xi_\theta$  hold.*

The proof of Lemma 1 can directly follow the well-known first-order sensitivity result in Theorem 2.1 in [74]. Here, conditions (i)-(iii) are the sufficient conditions to guarantee the applicability of the well-known implicit function theorem [75] to the C-PMP. Condition (ii) is well-known and serves as a sufficient condition for the constraint qualification to establish the C-PMP (see Corollary 3, pp. 22, [48]). Condition (iii) is necessary to ensure that the Jacobian matrix in the implicit function theorem is invertible, and it also leads to the persistence of strict complementarity, saying that the inactive inequalities remain inactive and active ones remain active and there is no ‘switching’ between them near  $\bar{\theta}$ . Both our practice and previous works [68, 69, 71, 74, 76] show that the conditions (i)-(iii) are very mild and the differentiability of  $\xi_\theta$  can be attained almost everywhere in the space of  $\theta$ .

### 4.2 Auxiliary Control System to Solve $\frac{\partial \xi_\theta}{\partial \theta}$

If the conditions (i)-(iii) in Lemma 1 for differentiability of  $\xi_\theta$  hold, we next show that  $\frac{\partial \xi_\theta}{\partial \theta}$  can also be efficiently solved by an auxiliary control system, which is originally proposed in the foundational work [71]. First, we define the new state and input (matrix) variables  $X_t \in \mathbb{R}^{n \times r}$  and  $U_t \in \mathbb{R}^{m \times r}$ , respectively. Then, we introduce the following *auxiliary control system*,

$$\begin{aligned} \bar{\Sigma}(\xi_\theta) : \quad & \text{control cost: } \bar{J} = \text{Tr} \sum_{t=0}^{T-1} \left( \frac{1}{2} \begin{bmatrix} X_t \\ U_t \end{bmatrix}' \begin{bmatrix} L_t^{xx} & L_t^{xu} \\ L_t^{ux} & L_t^{uu} \end{bmatrix} \begin{bmatrix} X_t \\ U_t \end{bmatrix} + \begin{bmatrix} L_t^{x\theta} \\ L_t^{u\theta} \end{bmatrix}' \begin{bmatrix} X_t \\ U_t \end{bmatrix} \right) \\ & + \text{Tr} \left( \frac{1}{2} X_T' L_T^{xx} X_T + (L_T^{x\theta})' X_T \right) \\ & \text{subject to} \\ & \text{dynamics: } X_{t+1} = F_t^x X_t + F_t^u U_t + F_t^\theta \quad \text{with } X_0 = X_0^\theta \\ & \text{terminal constraint: } \bar{G}_T^x X_T + \bar{G}_T^\theta = \mathbf{0}, \quad H_T^x X_T + H_T^\theta = \mathbf{0}, \\ & \text{path constraint: } \bar{G}_t^x X_t + \bar{G}_t^u U_t + \bar{G}_t^\theta = \mathbf{0}, \quad H_t^x X_t + H_t^u U_t + H_t^\theta = \mathbf{0}. \end{aligned} \quad (3)$$

Here,  $L_t^x$  and  $L_t^{xx}$  denote the first- and second- order derivatives, respectively, of the Hamiltonian  $L_t$  in (2) with respect to  $x$ ;  $F_t^x$ ,  $H_t^x$ ,  $\bar{G}_t^x$  denote the first-order derivatives of  $f_t$ ,  $h_t$ ,  $\bar{g}_t$  with respect

to  $\mathbf{x}$ , respectively, where  $\bar{\mathbf{g}}_t$  is the vector of stacking all active inequality constraints in  $\mathbf{g}_t$ ; and the similar convention applies to the other notations. All derivative matrices defining  $\bar{\Sigma}(\xi_\theta)$  are evaluated at  $(\xi_\theta, \lambda_{1:T}^\theta, \mathbf{v}_{0:T}^\theta, \mathbf{w}_{0:T}^\theta)$ , where  $\lambda_{1:T}^\theta$ ,  $\mathbf{v}_{0:T}^\theta$ , and  $\mathbf{w}_{0:T}^\theta$  are usually the byproducts of a constrained optimal control solver [77] or can be easily solved from the C-PMP given  $\xi_\theta$ , as done in [71]. We note that  $\bar{\Sigma}(\xi_\theta)$  is a *Equality-constrained Linear Quadratic Regulator (LQR)* system, as its control cost function is quadratic and dynamics and constraints are linear. For the above  $\bar{\Sigma}(\xi_\theta)$ , we have the following important result *without additional assumptions*.

**Theorem 1** ( $\frac{\partial \xi_\theta}{\partial \theta}$  is a globally unique minimizing trajectory to  $\bar{\Sigma}(\xi_\theta)$ ). *Let the conditions (i)-(iii) in Lemma 1 for differentiability of  $\xi_\theta$  hold. Then, the auxiliary control system  $\bar{\Sigma}(\xi_\theta)$  in (3) has a globally unique minimizing trajectory, denoted as  $\{X_{0:T}^\theta, U_{0:T-1}^\theta\}$ , which is exactly  $\frac{\partial \xi_\theta}{\partial \theta}$ , i.e.,*

$$\{X_{0:T}^\theta, U_{0:T-1}^\theta\} = \frac{\partial \xi_\theta}{\partial \theta} \quad \text{with} \quad X_t^\theta = \frac{\partial \mathbf{x}_t}{\partial \theta} \quad \text{and} \quad U_t^\theta = \frac{\partial \mathbf{u}_t}{\partial \theta}. \quad (4)$$

The proof of the above theorem is in Appendix B. Theorem 1 states that as long as the conditions (i)-(iii) in Lemma 1 for differentiability of  $\xi_\theta$  are satisfied, without additional assumptions, the auxiliary control system  $\bar{\Sigma}(\xi_\theta)$  always has a globally unique minimizing trajectory, which is exactly  $\frac{\partial \xi_\theta}{\partial \theta}$ . Thus, obtaining  $\frac{\partial \xi_\theta}{\partial \theta}$  is equivalent to solving  $\bar{\Sigma}(\xi_\theta)$ , which be efficiently done thanks to the recent development of the equality-constrained LQR algorithms [78–80], all of which have a complexity of  $\mathcal{O}(T)$ . The algorithm that implements Theorem 1 is given in Algorithm 1 in Appendix E.1.

## 5 Safe Unconstrained Approximations for $\xi_\theta$ and $\frac{\partial \xi_\theta}{\partial \theta}$

From Section 4, we know that one can solve the constrained system  $\Sigma(\theta)$  to obtain  $\xi_\theta$  and solve its auxiliary control system  $\bar{\Sigma}(\xi_\theta)$  to obtain  $\frac{\partial \xi_\theta}{\partial \theta}$ . Although theoretically appealing, there are several difficulties in implementation. First, solving a constrained optimal control Problem B( $\theta$ ) is not as easy as solving an unconstrained optimal control, for which many trajectory optimization algorithms, e.g., iLQR [81] and DDP [82], are available. Second, establishing  $\bar{\Sigma}(\xi_\theta)$  requires the values of the multipliers  $\mathbf{v}_{0:T}^\theta$  and  $\mathbf{w}_{0:T}^\theta$ . And third, to construct  $\bar{\Sigma}(\xi_\theta)$ , one also needs to identify all active inequality constraints  $\bar{\mathbf{g}}_t$ , which can be numerically difficult due to numerical error (we will show this in later experiments). All those difficulties motivate us to develop a more efficient paradigm to obtain both  $\xi_\theta$  and  $\frac{\partial \xi_\theta}{\partial \theta}$ , which is the goal of this section.

To proceed, we first convert the constrained system  $\Sigma(\theta)$  to an unconstrained system  $\Sigma(\theta, \gamma)$  by adding all constraints to its control cost via barrier functions. Here, we use quadratic barrier function for each equality constraint and logarithm barrier functions for each inequality constraint; and all barrier functions are associated with the same barrier parameter  $\gamma > 0$ . This leads to  $\Sigma(\theta, \gamma)$  to be

$$\Sigma(\theta, \gamma) : \quad \begin{aligned} \text{control cost:} \quad J(\theta, \gamma) &= \sum_{t=0}^{T-1} \left( c_t(\mathbf{x}_t, \mathbf{u}_t, \theta) - \gamma \sum_{i=1}^{q_t} \ln(-g_{t,i}(\mathbf{x}_t, \mathbf{u}_t, \theta)) + \right. \\ &\quad \left. \frac{1}{2\gamma} \sum_{i=1}^{s_t} (h_{t,i}(\mathbf{x}_t, \mathbf{u}_t, \theta))^2 \right) + c_T(\mathbf{x}_T, \theta) - \\ &\quad \gamma \sum_{i=1}^{q_T} \ln(-g_{T,i}(\mathbf{x}_T, \theta)) + \frac{1}{2\gamma} \sum_{i=1}^{s_T} (h_{T,i}(\mathbf{x}_T, \theta))^2, \end{aligned} \quad (5)$$

subject to

dynamics:  $\mathbf{x}_{t+1} = \mathbf{f}(\mathbf{x}_t, \mathbf{u}_t, \theta)$  with  $\mathbf{x}_0 = \mathbf{x}_0(\theta)$ ,  $\forall t$ .

The trajectory  $\xi_{(\theta, \gamma)} = \{\mathbf{x}_{0:T}^{(\theta, \gamma)}, \mathbf{u}_{0:T-1}^{(\theta, \gamma)}\}$  produced by the above unconstrained system  $\Sigma(\theta, \gamma)$  is

$$\begin{aligned} \xi_{(\theta, \gamma)} &= \left\{ \mathbf{x}_{0:T}^{(\theta, \gamma)}, \mathbf{u}_{0:T-1}^{(\theta, \gamma)} \right\} \in \arg \min_{\{\mathbf{x}_{0:T}, \mathbf{u}_{0:T-1}\}} J(\theta, \gamma) && \text{SB}(\theta, \gamma) \\ \text{s.t.} \quad &\mathbf{x}_{t+1} = \mathbf{f}(\mathbf{x}_t, \mathbf{u}_t, \theta) \quad \text{with} \quad \mathbf{x}_0 = \mathbf{x}_0(\theta), \end{aligned}$$

that is,  $\xi_{(\theta, \gamma)}$  is minimizing the new control cost  $J(\theta, \gamma)$  subject to only dynamics. Then we have the following important result about the safe unconstrained approximation for  $\xi_\theta$  and  $\frac{\partial \xi_\theta}{\partial \theta}$  using  $\Sigma(\theta, \gamma)$ .

**Theorem 2.** Let conditions (i)-(iii) in Lemma 1 for differentiability of  $\xi_\theta$  hold. For any small  $\gamma > 0$ ,

(a) there exists a local isolated minimizing trajectory  $\xi_{(\theta, \gamma)}$  that solves Problem  $SB(\theta, \gamma)$ , and  $\Sigma(\theta, \gamma)$  is well-defined at  $\xi_{(\theta, \gamma)}$ , i.e.,  $\mathbf{g}_t(\mathbf{x}_t^{(\theta, \gamma)}, \mathbf{u}_t^{(\theta, \gamma)}, \theta) < \mathbf{0}$  and  $\mathbf{g}_T(\mathbf{x}_T^{(\theta, \gamma)}, \theta) < \mathbf{0}$ ;

(b)  $\xi_{(\theta, \gamma)}$  is once-continuously differentiable with respect to  $(\theta, \gamma)$ , and

$$\xi_{(\theta, \gamma)} \rightarrow \xi_\theta \quad \text{and} \quad \frac{\partial \xi_{(\theta, \gamma)}}{\partial \theta} \rightarrow \frac{\partial \xi_\theta}{\partial \theta} \quad \text{as } \gamma \rightarrow 0; \quad (6)$$

(c) the trajectory derivative  $\frac{\partial \xi_{(\theta, \gamma)}}{\partial \theta}$  is a globally unique minimizing trajectory to the auxiliary control system  $\bar{\Sigma}(\xi_{(\theta, \gamma)})$  corresponding to  $\Sigma(\theta, \gamma)$ .

The proof of the above theorem is given in Appendix C. It is worth noting that the above assertions require no additional assumption except the same conditions (i)-(iii) for differentiability of  $\xi_\theta$ . We make the following comments on the above results, using an illustrative cartpole example in Fig. 1. First, assertion (b) states that by choosing a small  $\gamma > 0$ , one can simply use  $\xi_{(\theta, \gamma)}$  and  $\frac{\partial \xi_{(\theta, \gamma)}}{\partial \theta}$  of the *unconstrained optimal control system*  $\Sigma(\theta, \gamma)$  to approximate  $\xi_\theta$  and  $\frac{\partial \xi_\theta}{\partial \theta}$  of the original constrained system  $\Sigma(\theta)$ , respectively. Second, notably, assertion (b) also states that the above approximations can be controlled for arbitrary accuracy by simply letting  $\gamma \rightarrow 0$ , as illustrated in the upper panels in Fig. 1. Third, more importantly, assertion (a) states that the above approximations are always safe in a sense that the approximation  $\xi_{(\theta, \gamma)}$  with any small  $\gamma > 0$  is guaranteed to satisfy all inequality constraints in the original  $\Sigma(\theta)$ , as illustrated in the bottom panels in Fig. 1. Finally, similar to Theorem 1, assertion (c) states that the derivative  $\frac{\partial \xi_{(\theta, \gamma)}}{\partial \theta}$  for  $\Sigma(\theta, \gamma)$  is a globally unique minimizing trajectory to its corresponding auxiliary control system  $\bar{\Sigma}(\xi_{(\theta, \gamma)})$ , thus PDP [71] directly applies here.

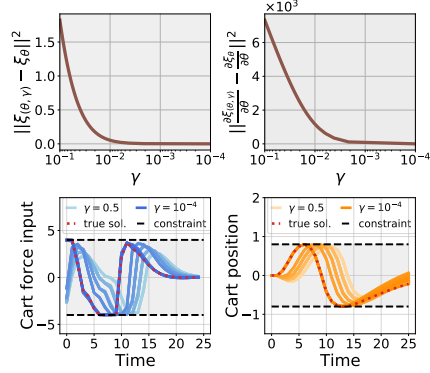


Figure 1:  $\xi_{(\theta, \gamma)}$  and  $\frac{\partial \xi_{(\theta, \gamma)}}{\partial \theta}$  approximate  $\xi_\theta$  and  $\frac{\partial \xi_\theta}{\partial \theta}$  under different  $\gamma > 0$ .

In addition to the theoretical importance of Theorem 2, we also summarize its algorithmic advantage compared to directly handling the original constrained system  $\Sigma(\theta)$  and its auxiliary control system  $\bar{\Sigma}(\xi_\theta)$ . First, solving the unconstrained  $\Sigma(\theta, \gamma)$  is easier than solving the constrained  $\Sigma(\theta)$  as off-the-shelf algorithms are available for unconstrained trajectory optimization than for constrained one. Second, when solving  $\frac{\partial \xi_{(\theta, \gamma)}}{\partial \theta}$  using  $\bar{\Sigma}(\xi_{(\theta, \gamma)})$ , there is no need to identify the inactive and active inequality constraints, as opposed to solving  $\frac{\partial \xi_\theta}{\partial \theta}$  using  $\bar{\Sigma}(\xi_\theta)$ ; thus it is easier to implement and more numerically stable (we will show this later in experiments). Third, in contrast to Theorem 1, the unconstrained  $\Sigma(\theta, \gamma)$  and  $\bar{\Sigma}(\xi_{(\theta, \gamma)})$  avoid dealing with the multipliers  $\mathbf{v}_{0:T}$  and  $\mathbf{w}_{0:T}$ . Finally, by absorbing hard inequality constraints into the control cost through barrier functions,  $\Sigma(\theta, \gamma)$  introduces the ‘softness’ of constraints and mitigates the discontinuous ‘switching’ between inactive/active inequalities over a large range of  $\theta$ . This leads to a more numerically stable algorithm, as we will show in later experiments. Implementation of Theorem 2 is given in Algorithm 2 in Appendix E.2.

## 6 Safe PDP to Solve Problem P

According to Theorem 2, we use the safe unconstrained approximation system  $\Sigma(\theta, \gamma)$  in (5) to replace the original inner-level constrained system  $\Sigma(\theta)$  in (1). Then, we give the following important result for solving Problem P, which addresses the Challenges (4) and (5) in Section 3.

**Theorem 3.** Consider all functions defining the constrained optimal control system  $\Sigma(\theta)$  are at least three-times continuously differentiable, and let the conditions (i)-(iii) in Lemma 1 for differentiability of  $\xi_\theta$  hold in a neighborhood of  $\theta^*$ . Suppose that the second-order condition for a local isolated minimizer  $\theta^*$  to Problem P is satisfied, that the gradients  $\nabla_\theta R_i(\xi_{\theta^*}, \theta^*)$  of all binding constraints  $R_i(\xi_\theta, \theta) = 0$  are linearly independent at  $\theta^*$ , and that the strict complementary holds at  $\theta^*$ . Then, for any small  $\epsilon > 0$  and any small  $\gamma > 0$ , the following outer-level unconstrained approximation

$$\theta^*(\epsilon, \gamma) = \arg \min_{\theta} \ell(\xi_{(\theta, \gamma)}, \theta) - \epsilon \sum_{i=1}^l \ln(-R_i(\xi_{(\theta, \gamma)}, \theta)), \quad \text{SP}(\epsilon, \gamma)$$

with  $\xi_{(\theta, \gamma)}$  being the optimal trajectory to the inner-level safe unconstrained approximation system  $\Sigma(\theta, \gamma)$  in (5), has the following assertions:

- (a) there exists a local isolated minimizer  $\theta^*(\epsilon, \gamma)$  to the above  $\text{SP}(\epsilon, \gamma)$ , and the corresponding trajectory  $\xi_{(\theta^*(\epsilon, \gamma), \gamma)}$  from the inner-level approximation system  $\Sigma(\theta^*(\epsilon, \gamma), \gamma)$  is safe with respect to the original outer-level constraints, i.e.,  $R_i(\xi_{(\theta^*(\epsilon, \gamma), \gamma)}, \theta^*(\epsilon, \gamma)) < 0, i = 1, 2, \dots, l$ ;
- (b)  $\theta^*(\epsilon, \gamma)$  is once-continuously differentiable with respect to both  $\epsilon$  and  $\gamma$ , and

$$\theta^*(\epsilon, \gamma) \rightarrow \theta^* \quad \text{as} \quad (\epsilon, \gamma) \rightarrow (0, 0); \quad (7)$$

- (c) for any  $\theta$  near  $\theta^*(\epsilon, \gamma)$ ,  $\xi_{(\theta, \gamma)}$  from the inner-level approximation system  $\Sigma(\theta, \gamma)$  is safe with respect to the original outer-level constraints, i.e.,  $R_i(\xi_{(\theta, \gamma)}, \theta) < 0, i = 1, 2, \dots, l$ .

The proof of the above theorem is given in Appendix D. The above result says that instead of solving the original constrained Problem P with the inner-level constrained system  $\Sigma(\theta)$  in (1), one can solve an unconstrained approximation Problem  $\text{SP}(\epsilon, \gamma)$  with the inner-level safe unconstrained approximation system  $\Sigma(\theta, \gamma)$  in (5). Particularly, we make the following comments on the importance of the above theorem. First, claim (a) affirms that although the inner-level trajectory  $\xi_{(\theta, \gamma)}$  is an approximation (recall Theorem 2), the outer-level unconstrained Problem  $\text{SP}(\epsilon, \gamma)$  always has a locally unique solution  $\theta^*(\epsilon, \gamma)$ ; furthermore, at  $\theta^*(\epsilon, \gamma)$ , the corresponding inner-level trajectory  $\xi_{(\theta^*(\epsilon, \gamma), \gamma)}$  is safe with respect to the original outer-level constraints, i.e.,  $R_i(\xi_{(\theta^*(\epsilon, \gamma), \gamma)}, \theta^*(\epsilon, \gamma)) < 0, i = 1, 2, \dots, l$ . Second, claim (b) asserts that the accuracy of the solution  $\theta^*(\epsilon, \gamma)$  to the outer-level approximation Problem  $\text{SP}(\epsilon, \gamma)$  is controlled jointly by the inner-level barrier parameter  $\gamma$  and outer-level barrier parameter  $\epsilon$ : as both barrier parameters approach zero,  $\theta^*(\epsilon, \gamma)$  is converging to the true solution  $\theta^*$  to the original Problem P. Third, claim (c) says that during the local search of the outer-level solution  $\theta^*(\epsilon, \gamma)$ , the corresponding inner-level trajectory  $\xi_{(\theta, \gamma)}$  is always safe with respect to the original outer-level constraints, i.e.,  $R_i(\xi_{(\theta, \gamma)}, \theta) < 0, i = 1, 2, \dots, l$ . The above Theorem 3, together with Theorem 2 provide the safety- and accuracy- guarantees for the whole Safe PDP framework. Then entire Safe PDP algorithm is given in Algorithm 3 in Appendix E.3.

## 7 Applications to Different Safety-Critical Tasks

We apply Safe PDP to solve some representative safety-critical learning/control tasks. For a specific task, one only needs to specify the parameterization detail of  $\Sigma(\theta)$ , a task loss  $\ell(\xi_\theta, \theta)$ , and task constraints  $R_i(\xi_\theta, \theta)$  in Problem P. The experiments are performed on the systems of different complexities in Table 1. All codes are available at <https://github.com/wanxinjin/Safe-PDP>.

Table 1: Experimental environments [71]

| System $\Sigma(\theta)$ | Dynamics $f(\theta_{\text{dyn}})$ | Control cost $J(\theta_{\text{obj}})$                                  | Constraints $g(\theta_{\text{cstr}})$                       |
|-------------------------|-----------------------------------|------------------------------------------------------------------------|-------------------------------------------------------------|
| Cartpole                | cart & pole masses and length     | $c_t = \ \mathbf{u}\ _2^2 +$                                           | $g_x(\mathbf{x}) \leq X_{\text{max}},$                      |
| Two-link Robot arm      | length and mass of links          | $\ \theta'_{\text{obj}}(\mathbf{x} - \mathbf{x}_{\text{goal}})\ _2^2,$ | $\ \mathbf{u}\ _{2/\infty} \leq U_{\text{max}},$            |
| 6-DoF quadrotor         | mass, wing length, inertia        | $c_T =$                                                                | $\theta_{\text{cstr}} = \{X_{\text{max}}, U_{\text{max}}\}$ |
| 6-DoF rocket landing    | rocket mass, length, inertia      | $\ \theta'_{\text{obj}}(\mathbf{x} - \mathbf{x}_{\text{goal}})\ _2^2$  |                                                             |

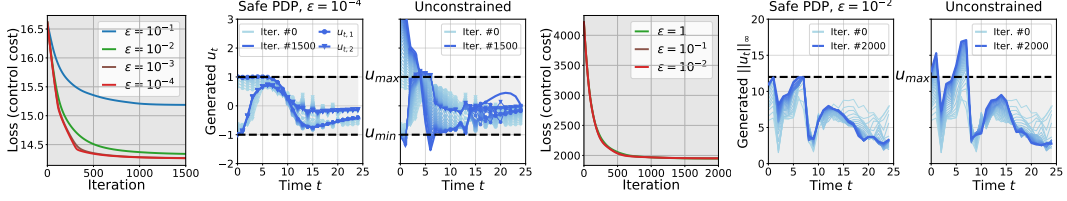
Note that for each system,  $g(\theta_{\text{cstr}})$  includes the immediate constraints on system input  $\mathbf{u}$  and state  $\mathbf{x}$  at any time instance;  $g_x$  is known;  $\|\cdot\|_{2/\infty}$  is the 2 or  $\infty$  norm; and time horizon  $T$  is around 50 for all systems.

**Problem I: Safe Policy Optimization** aims to find a policy that minimizes a control cost  $J$  subject to constraints  $g$  while guaranteeing that *any intermediate policy during optimization should never violate the constraints*. To apply Safe PDP to solve such a problem for the systems in Table 1, we set:

$$\Sigma(\theta) : \quad \begin{array}{l} \text{dynamics: } \mathbf{x}_{t+1} = \mathbf{f}(\mathbf{x}_t, \mathbf{u}_t) \quad \text{with } \mathbf{x}_0, \\ \text{policy: } \mathbf{u}_t = \pi_t(\mathbf{x}_t, \theta), \end{array} \quad (8)$$

where dynamics  $\mathbf{f}$  is learned from demonstrations in Problem III, and  $\pi(\theta)$  is represented by a (deep) feedforward neural network (NN) with  $\theta$  the NN parameter. In Problem P, the task loss  $\ell(\xi_\theta, \theta)$  is set as  $J(\theta_{\text{obj}})$ , and task constraints  $R_i(\xi_\theta, \theta)$  as  $g(\theta_{\text{cstr}})$ , with both  $\theta_{\text{obj}}$  and  $\theta_{\text{cstr}}$  known. Then, safe policy optimization is to solve Problem P using Safe PDP. The results for the robot arm and 6-DoF maneuvering quadrotor are in Fig. 2, and the other results and details are in Appendix F.1.



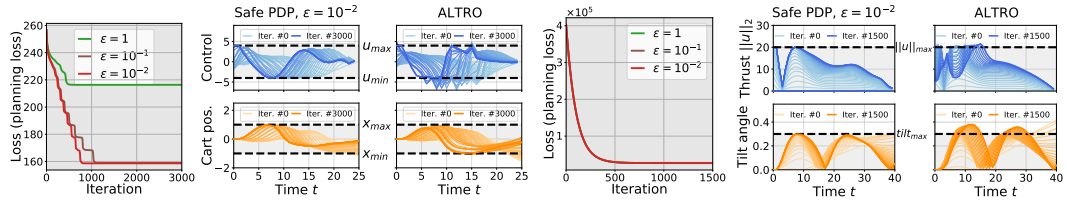


(a) Robot-arm loss (b) Constraint violation during opt. (c) Quadrotor loss (d) Constraint violation during opt.

Figure 2: Safe neural policy optimization for robot-arm (a)-(b) and 6-DoF quadrotor (c)-(d).

Fig. 2a and 2c plot loss (control cost) versus gradient-descent iteration under different  $\epsilon$ , showing that the NN policy achieves a good convergence when  $\epsilon \leq 10^{-2}$  (as asserted by Theorem 3). Fig. 2b and 2d show all indeterminate control trajectories generated from the NN policy during entire iterations; we also mark the constraints  $U_{\max}$  and compare with the unconstrained policy optimization under the same settings. The results confirm that Safe PDP enables to *achieve an optimal policy while guaranteeing that any intermediate policy throughout optimization is safe*.

**Problem II: Safe Motion Planning** searches for a dynamics-feasible trajectory that optimizes a criterion and avoids unsafe regions (obstacles), meanwhile guaranteeing that any intermediate motion trajectory during search must avoid the unsafe regions. To apply Safe PDP to solve such problem, we specialize  $\Sigma(\theta)$  as (8) except that policy here is  $u_t = u(t, \theta)$ , which is represented by Lagrangian polynomial [83] with  $\theta$  the parameters (pivots). In Problem P, task loss is set as  $J(\theta_{\text{obj}})$ , and task constraints as  $g(\theta_{\text{cstr}})$ , with  $\theta_{\text{obj}}$  and  $\theta_{\text{cstr}}$  known in Table 1. The safe planning results using Safe PDP for cartpole and 6-DoF rocket landing are in Fig. 2, in comparison with ALTRO, a state-of-the-art constrained trajectory optimization method [21]. Other results and more details are in Appendix F.2.



(a) Cartpole loss (b) Constraint violation during opt. (c) Rocket loss (d) Constraint violation during opt.

Figure 3: Safe motion planning for cartpole (a)-(b) and 6-DoF rocket powered landing (c)-(d).

Fig. 3a and 3c plot the task loss versus gradient-descent iteration, showing that the trajectory achieves a good convergence with  $\epsilon \leq 10^{-2}$ . Fig. 3b and 3d show all intermediate motion trajectories during entire optimization, with constraints marked. The results confirm that Safe PDP can find an optimal trajectory while always respecting constraints throughout planning process.

**Problem III: Learning MPC from Demonstrations.** Suppose for all systems in Table 1, the control cost  $J(\theta_{\text{cost}})$ , dynamics  $f(\theta_{\text{dyn}})$  and constraints  $g_t(\theta_{\text{cstr}})$  are all unknown and parameterized as in Table 1. We aim to jointly learn  $\theta = \{\theta_{\text{cost}}, \theta_{\text{dyn}}, \theta_{\text{cstr}}\}$  from demonstrations  $\xi^{\text{demo}} = \{x_{0:T}^{\text{demo}}, u_{0:T-1}^{\text{demo}}\}$  of a true expert system. In Problem P, set  $\Sigma(\theta)$  as (1), consisting of  $J(\theta_{\text{cost}})$ ,  $f(\theta_{\text{dyn}})$ , and  $g_t(\theta_{\text{cstr}})$  parameterized; set task loss  $\ell(\xi_{\theta}, \theta) = \|\xi^{\text{demo}} - \xi_{\theta}\|^2$ , which quantifies the *reproducing loss* between  $\xi^{\text{demo}}$  and  $\xi_{\theta}$ ; and there is no task constraints. By solving Problem P, we can learn  $\Sigma(\theta)$  such that its reproduced  $\xi_{\theta}$  is closest to given  $\xi^{\text{demo}}$ . The demonstrations  $\xi^{\text{demo}}$  here are generated with  $\theta$  known (two episode trajectories for each system with time horizon  $T=50$ ). The plots of the loss versus gradient-descent iteration are in Fig. 4, and more details and results are in Appendix F.3.

In Fig. 4a-4d, for each system, we use three strategies to obtain  $\xi_{\theta}$  and  $\frac{\partial \xi_{\theta}}{\partial \theta}$  for  $\Sigma(\theta)$ : (A) use a solver [77] to obtain  $\xi_{\theta}$  and use Theorem 1 to obtain  $\frac{\partial \xi_{\theta}}{\partial \theta}$ ; (B) use Theorem 2 to approximate both  $\xi_{\theta}$  and  $\frac{\partial \xi_{\theta}}{\partial \theta}$  by  $\xi_{(\theta, \gamma)}$  and  $\frac{\partial \xi_{(\theta, \gamma)}}{\partial \theta}$ , respectively,  $\gamma=10^{-2}$ ; and (C) use a solver to obtain  $\xi_{\theta}$  and Theorem 2 only for  $\frac{\partial \xi_{\theta}}{\partial \theta}$ . Fig. 4a-4d show that for Strategies (B) and (C), the reproducing loss quickly converges to zeros, indicating that the dynamics, constraints, and control cost are successfully learned to reproduce the demonstrations. Fig. 4a-4d also show numerical instability for strategy (A); this is due to the discontinuous ‘switching’ of active inequalities between iterations, and also the error in correctly identifying active inequalities (we identify them by checking  $g_{t,i} > -\delta$  with  $\delta > 0$  a small

threshold), as analyzed in Section 5. More analysis is given in Appendix F.3. Note that we are not aware of any existing methods that can handle jointly learning of cost, dynamics, and constraints here, and thus we have not given benchmark comparison. Fig. 4e gives timing results of Safe PDP.

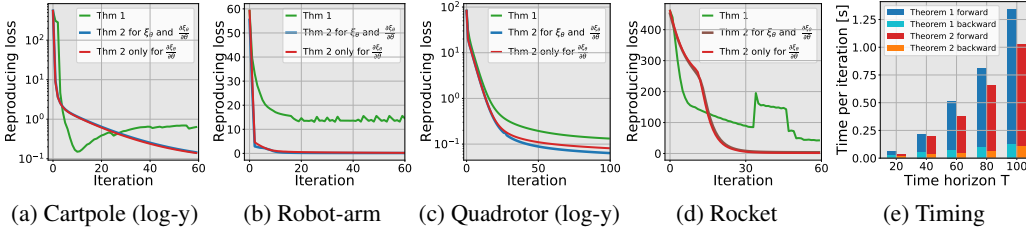


Figure 4: Jointly learning dynamics, constraints, and control cost from demonstrations.

## 8 Discussion

**Comparisons with other differentiable frameworks.** Fig. 5 compares Safe PDP, CasADi [70], and Differentiable MPC [68] for the computational efficiency of differentiating an optimal trajectory of a constrained optimal control system with different control horizons  $T$ . The results show a significantly computational advantage of Safe PDP over CasADi and Differentiable MPC. Specifically, Safe PDP has a complexity of  $\mathcal{O}(T)$ , while CasADi and Differentiable MPC have at least  $\mathcal{O}(T^2)$ . This is because both CasADi and differentiable MPC are based on the implicit function theorem [75] and need to compute the inverse of a Hessian matrix of the size proportional to  $T \times T$ . In contrast, Safe PDP solves the gradient of a trajectory by constructing an Auxiliary Control System, which can be solved using the Riccati equation.

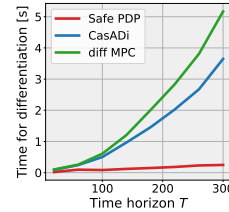


Figure 5: Time for differentiating optimal trajectory with different  $T$ .

**Limitation of Safe PDP.** Safe PDP requires a safe (feasible) initialization such that the log-barrier control cost or loss is well-defined. While restrictive, safe initialization is common in safe learning [63, 84]. We have the following empiricism on how to provide safe initializations for different types of problems, as adopted in our experiments in Section 7. In safe policy optimization, one could first use supervised learning to learn a safe policy from some safe trajectories/demonstrations (not necessarily be optimal) and then use the learned safe policy to initialize Safe PDP. In safe motion planning, one could arbitrarily provide a safe trajectory (not necessarily optimal) to initialize Safe PDP. In learning MPCs, the goal includes learning of constraint itself, and there is no such requirement.

**Strategies to accelerate forward pass of Safe PDP.** There are many strategies to accelerate a long-horizon trajectory optimization (optimal control) in the forward pass of Safe PDP. (I) One effective way is to scale the (continuous) long-horizon problem into a smaller one (e.g., a unit) by applying a time-warping function to the dynamics and cost function [85]. After solving the scaled short-horizon problem, re-scale the trajectory back. (II) There are also ‘warm-up’ tricks, e.g., one can initialize the trajectory at the next iteration using the result of the previous iteration. (III) One can also use a hierarchical strategy to solve trajectory optimization from coarse to fine resolutions. We have tested and provided the comparison for the above three acceleration strategies in Appendix G.2.

Please refer to Appendix G for more discussion, which includes G.1: comparison between Safe-PDP and non-safe PDP; G.2: comparison of different strategies for accelerating long-horizon trajectory optimization; G.3: trade-offs between accuracy and computational efficiency using barrier penalties; G.4: learning MPCs from non-optimal data; and G.5: detailed discussion on limitation of Safe PDP.

## 9 Conclusions

This paper proposes a Safe Pontryagin Differentiable Programming methodology, which establishes a provable and systematic safe differentiable framework to solve a broad class of safety-critical control and learning tasks with different types of safety constraints. For a constrained system and task, Safe PDP approximates both the solution and its gradient in backward pass by solving their more efficient unconstrained counterparts. Safe PDP has established two results: one is the *controlled accuracy guarantee* for approximations of the solution and its gradient, and the other is the *safety guarantee* for constraint satisfaction throughout the control and learning process. We envision the potential of Safe PDP for addressing various safety-critical problems in machine learning, control, and robotics fields.

## Acknowledgments and Disclosure of Funding

This work is supported by the NASA University Leadership Initiative (ULI) under grant number 80NSSC20M0161. The research of Prof. George J. Pappas is supported by the AFOSR Assured Autonomy in Congested Environments under grant number FA9550-19-1-0265. This work has been done primarily in the last semester of Wanxin Jin’s Ph.D. study at Purdue University. Wanxin Jin thanks Prof. Zhaoran Wang for some discussion about this work.

## References

- [1] Volodymyr Mnih, Koray Kavukcuoglu, David Silver, Andrei A Rusu, Joel Veness, Marc G Bellemare, Alex Graves, Martin Riedmiller, Andreas K Fidjeland, Georg Ostrovski, et al. Human-level control through deep reinforcement learning. *Nature*, 518(7540):529–533, 2015.
- [2] David Silver, Aja Huang, Chris J Maddison, Arthur Guez, Laurent Sifre, George Van Den Driessche, Julian Schrittwieser, Ioannis Antonoglou, Veda Panneershelvam, Marc Lanctot, et al. Mastering the game of go with deep neural networks and tree search. *Nature*, 529(7587):484–489, 2016.
- [3] Timothy P Lillicrap, Jonathan J Hunt, Alexander Pritzel, Nicolas Heess, Tom Erez, Yuval Tassa, David Silver, and Daan Wierstra. Continuous control with deep reinforcement learning. In *International Conference on Learning Representations*, 2016.
- [4] Arnab Nilim and Laurent El Ghaoui. Robust control of markov decision processes with uncertain transition matrices. *Operations Research*, 53(5):780–798, 2005.
- [5] Matthias Heger. Consideration of risk in reinforcement learning. In *International Conference on Machine Learning*, pages 105–111, 1994.
- [6] Ronald A Howard and James E Matheson. Risk-sensitive markov decision processes. *Management science*, 18(7):356–369, 1972.
- [7] Teodor Mihai Moldovan and Pieter Abbeel. Safe exploration in markov decision processes. *International Conference on Machine Learning*, 2012.
- [8] Aleksander Madry, Aleksandar Makelov, Ludwig Schmidt, Dimitris Tsipras, and Adrian Vladu. Towards deep learning models resistant to adversarial attacks. *arXiv preprint arXiv:1706.06083*, 2017.
- [9] Kemin Zhou and John Comstock Doyle. *Essentials of robust control*, volume 104. Prentice hall Upper Saddle River, NJ, 1998.
- [10] Javier Garcia and Fernando Fernández. A comprehensive survey on safe reinforcement learning. *Journal of Machine Learning Research*, 16(1):1437–1480, 2015.
- [11] Eitan Altman. *Constrained Markov decision processes*, volume 7. CRC Press, 1999.
- [12] Eitan Altman. Constrained markov decision processes with total cost criteria: Lagrangian approach and dual linear program. *Mathematical methods of operations research*, 48(3):387–417, 1998.
- [13] Ming Yu, Zhuoran Yang, Mladen Kolar, and Zhaoran Wang. Convergent policy optimization for safe reinforcement learning. *Advances in Neural Information Processing Systems*, 2019.
- [14] Yinlam Chow, Mohammad Ghavamzadeh, Lucas Janson, and Marco Pavone. Risk-constrained reinforcement learning with percentile risk criteria. *International Conference on Machine Learning*, 18(1):6070–6120, 2017.
- [15] Shalabh Bhatnagar and K Lakshmanan. An online actor–critic algorithm with function approximation for constrained markov decision processes. *Journal of Optimization Theory and Applications*, 153(3):688–708, 2012.

- [16] Dongsheng Ding, Kaiqing Zhang, Tamer Basar, and Mihailo Jovanovic. Natural policy gradient primal-dual method for constrained markov decision processes. *Advances in Neural Information Processing Systems*, 33, 2020.
- [17] Miguel Calvo-Fullana, Santiago Paternain, Luiz FO Chamon, and Alejandro Ribeiro. State augmented constrained reinforcement learning: Overcoming the limitations of learning with rewards. *arXiv preprint arXiv:2102.11941*, 2021.
- [18] Yatin Nandwani, Abhishek Pathak, Parag Singla, et al. A primal dual formulation for deep learning with constraints. *Advances in Neural Information Processing Systems*, 2019.
- [19] Maïtine Bergounioux, Kazufumi Ito, and Karl Kunisch. Primal-dual strategy for constrained optimal control problems. *SIAM Journal on Control and Optimization*, 37(4):1176–1194, 1999.
- [20] Matthew R Kirchner, Gary Hewer, Jérôme Darbon, and Stanley Osher. A primal-dual method for optimal control and trajectory generation in high-dimensional systems. In *Conference on Control Technology and Applications*, pages 1583–1590, 2018.
- [21] Taylor A Howell, Brian E Jackson, and Zachary Manchester. Altro: A fast solver for constrained trajectory optimization. In *IEEE/RSJ International Conference on Intelligent Robots and Systems*, pages 7674–7679, 2019.
- [22] Simon S Du and Wei Hu. Linear convergence of the primal-dual gradient method for convex-concave saddle point problems without strong convexity. In *International Conference on Artificial Intelligence and Statistics*, pages 196–205. PMLR, 2019.
- [23] Chi Jin, Praneeth Netrapalli, and Michael Jordan. What is local optimality in nonconvex-nonconcave minimax optimization? In *International Conference on Machine Learning*, pages 4880–4889. PMLR, 2020.
- [24] Yinlam Chow, Ofir Nachum, Aleksandra Faust, Edgar Duenez-Guzman, and Mohammad Ghavamzadeh. Lyapunov-based safe policy optimization for continuous control. *arXiv preprint arXiv:1901.10031*, 2019.
- [25] Joshua Achiam, David Held, Aviv Tamar, and Pieter Abbeel. Constrained policy optimization. In *International Conference on Machine Learning*, pages 22–31. PMLR, 2017.
- [26] Tsung-Yen Yang, Justinian Rosca, Karthik Narasimhan, and Peter J Ramadge. Projection-based constrained policy optimization. *International Conference on Learning Representations*, 2020.
- [27] John Schulman, Sergey Levine, Pieter Abbeel, Michael Jordan, and Philipp Moritz. Trust region policy optimization. In *International Conference on Machine Learning*, pages 1889–1897. PMLR, 2015.
- [28] Yinlam Chow, Ofir Nachum, Edgar Duenez-Guzman, and Mohammad Ghavamzadeh. A lyapunov-based approach to safe reinforcement learning. *Advances in Neural Information Processing Systems*, 2018.
- [29] Theodore J Perkins and Andrew G Barto. Lyapunov design for safe reinforcement learning. *Journal of Machine Learning Research*, 3(Dec):803–832, 2002.
- [30] Felix Berkenkamp, Matteo Turchetta, Angela P Schoellig, and Andreas Krause. Safe model-based reinforcement learning with stability guarantees. *Advances in Neural Information Processing Systems*, 2017.
- [31] Aleksandr Mikhailovich Lyapunov. The general problem of the stability of motion. *International journal of control*, 55(3):531–534, 1992.
- [32] Peter Giesl and Sigurdur Hafstein. Review on computational methods for lyapunov functions. *Discrete & Continuous Dynamical Systems-B*, 20(8):2291, 2015.
- [33] Matteo Turchetta, Felix Berkenkamp, and Andreas Krause. Safe exploration in finite markov decision processes with gaussian processes. *Advances in Neural Information Processing Systems*, 29:4312–4320, 2016.

- [34] Akifumi Wachi and Yanan Sui. Safe reinforcement learning in constrained markov decision processes. In *International Conference on Machine Learning*, pages 9797–9806. PMLR, 2020.
- [35] Somil Bansal, Mo Chen, Sylvia Herbert, and Claire J Tomlin. Hamilton-jacobi reachability: A brief overview and recent advances. In *IEEE Conference on Decision and Control*, pages 2242–2253, 2017.
- [36] Peter Wieland and Frank Allgöwer. Constructive safety using control barrier functions. *IFAC Proceedings Volumes*, 40(12):462–467, 2007.
- [37] Aaron D Ames, Xiangru Xu, Jessy W Grizzle, and Paulo Tabuada. Control barrier function based quadratic programs for safety critical systems. *IEEE Transactions on Automatic Control*, 62(8):3861–3876, 2016.
- [38] Jaime F Fisac, Anayo K Akametalu, Melanie N Zeilinger, Shahab Kaynama, Jeremy Gillula, and Claire J Tomlin. A general safety framework for learning-based control in uncertain robotic systems. *IEEE Transactions on Automatic Control*, 64(7):2737–2752, 2018.
- [39] Sylvia L Herbert, Mo Chen, SooJean Han, Somil Bansal, Jaime F Fisac, and Claire J Tomlin. Fastrack: A modular framework for fast and guaranteed safe motion planning. In *IEEE Conference on Decision and Control*, pages 1517–1522, 2017.
- [40] Mo Chen, Jaime F Fisac, Shankar Sastry, and Claire J Tomlin. Safe sequential path planning of multi-vehicle systems via double-obstacle hamilton-jacobi-isaacs variational inequality. In *European Control Conference*, pages 3304–3309, 2015.
- [41] Lawrence C Evans and Panagiotis E Souganidis. Differential games and representation formulas for solutions of hamilton-jacobi-isaacs equations. *Indiana University mathematics journal*, 33(5):773–797, 1984.
- [42] Aaron D Ames, Samuel Coogan, Magnus Egerstedt, Gennaro Notomista, Koushil Sreenath, and Paulo Tabuada. Control barrier functions: Theory and applications. In *European Control Conference*, pages 3420–3431, 2019.
- [43] Jason Choi, Fernando Castaneda, Claire J Tomlin, and Koushil Sreenath. Reinforcement learning for safety-critical control under model uncertainty, using control lyapunov functions and control barrier functions. *arXiv preprint arXiv:2004.07584*, 2020.
- [44] Richard Cheng, Gábor Orosz, Richard M Murray, and Joel W Burdick. End-to-end safe reinforcement learning through barrier functions for safety-critical continuous control tasks. In *AAAI Conference on Artificial Intelligence*, pages 3387–3395, 2019.
- [45] Alexander Robey, Haimin Hu, Lars Lindemann, Hanwen Zhang, Dimos V Dimarogonas, Stephen Tu, and Nikolai Matni. Learning control barrier functions from expert demonstrations. In *IEEE Conference on Decision and Control*, pages 3717–3724, 2020.
- [46] Alexander Robey, Lars Lindemann, Stephen Tu, and Nikolai Matni. Learning robust hybrid control barrier functions for uncertain systems. *arXiv preprint arXiv:2101.06492*, 2021.
- [47] Wanxin Jin, Zhaoran Wang, Zhuoran Yang, and Shaoshuai Mou. Neural certificates for safe control policies. *arXiv preprint arXiv:2006.08465*, 2020.
- [48] Anthony V Fiacco and Garth P McCormick. *Nonlinear programming: sequential unconstrained minimization techniques*. SIAM, 1990.
- [49] Yurii Nesterov and Arkadii Nemirovskii. *Interior-point polynomial algorithms in convex programming*. SIAM, 1994.
- [50] Anders Forsgren, Philip E Gill, and Margaret H Wright. Interior methods for nonlinear optimization. *SIAM review*, 44(4):525–597, 2002.
- [51] AEB Lim, JB Moore, and L Faybusovich. Linearly constrained lq and lqg optimal control. *IFAC Proceedings Volumes*, 29(1):1110–1115, 1996.

- [52] SJ Wright. Structured interior point methods for optimal control. In *IEEE Conference on Decision and Control*, pages 1711–1716, 1991.
- [53] Stephen J Wright. Interior point methods for optimal control of discrete time systems. *Journal of Optimization Theory and Applications*, 77(1):161–187, 1993.
- [54] Christopher V Rao, Stephen J Wright, and James B Rawlings. Application of interior-point methods to model predictive control. *Journal of optimization theory and applications*, 99(3):723–757, 1998.
- [55] Anders Hansson and S Boyd. Robust optimal control of linear discrete-time systems using primal-dual interior-point methods. In *American Control Conference*, volume 1, pages 183–187, 1998.
- [56] Anders Hansson. A primal-dual interior-point method for robust optimal control of linear discrete-time systems. *IEEE Transactions on Automatic Control*, 45(9):1639–1655, 2000.
- [57] Christian Feller and Christian Ebenbauer. Relaxed logarithmic barrier function based model predictive control of linear systems. *IEEE Transactions on Automatic Control*, 62(3):1223–1238, 2016.
- [58] Julien Laurent-Varin, J Frederic Bonnans, Nicolas Bérend, Mounir Haddou, and Christophe Talbot. Interior-point approach to trajectory optimization. *Journal of Guidance, Control, and Dynamics*, 30(5):1228–1238, 2007.
- [59] John Hauser and Alessandro Saccon. A barrier function method for the optimization of trajectory functionals with constraints. In *IEEE Conference on Decision and Control*, pages 864–869. IEEE, 2006.
- [60] Paul Malisani, François Chaplais, and Nicolas Petit. An interior penalty method for optimal control problems with state and input constraints of nonlinear systems. *Optimal Control Applications and Methods*, 37(1):3–33, 2016.
- [61] Alexander Domahidi, Aldo U Zraggen, Melanie N Zeilinger, Manfred Morari, and Colin N Jones. Efficient interior point methods for multistage problems arising in receding horizon control. In *IEEE conference on decision and control*, pages 668–674, 2012.
- [62] Andrei Pavlov, Iman Shames, and Chris Manzie. Interior point differential dynamic programming. *IEEE Transactions on Control Systems Technology*, 2021.
- [63] Ilnura Usmanova, Andreas Krause, and Maryam Kamgarpour. Safe non-smooth black-box optimization with application to policy search. In *Learning for Dynamics and Control*, pages 980–989. PMLR, 2020.
- [64] Yongshuai Liu, Jiabin Ding, and Xin Liu. Ipo: Interior-point policy optimization under constraints. In *AAAI Conference on Artificial Intelligence*, pages 4940–4947, 2020.
- [65] Priya L Donti, Melrose Roderick, Mahyar Fazlyab, and J Zico Kolter. Enforcing robust control guarantees within neural network policies. In *International Conference on Learning Representations*, 2020.
- [66] Bingqing Chen, Priya L. Donti, Kyri Baker, J. Zico Kolter, and Mario Bergés. Enforcing policy feasibility constraints through differentiable projection for energy optimization. In *ACM International Conference on Future Energy Systems*, page 199–210, New York, NY, USA, 2021. Association for Computing Machinery.
- [67] Tu-Hoa Pham, Giovanni De Magistris, and Ryuki Tachibana. Optlayer-practical constrained optimization for deep reinforcement learning in the real world. In *International Conference on Robotics and Automation*, pages 6236–6243. IEEE, 2018.
- [68] Brandon Amos, Ivan Dario Jimenez Rodriguez, Jacob Sacks, Byron Boots, and J Zico Kolter. Differentiable mpc for end-to-end planning and control. In *Advances in Neural Information Processing Systems*, 2018.

- [69] Brandon Amos and J Zico Kolter. Optnet: Differentiable optimization as a layer in neural networks. In *International Conference on Machine Learning*, pages 136–145. PMLR, 2017.
- [70] Joel AE Andersson and James B Rawlings. Sensitivity analysis for nonlinear programming in casadi. *IFAC-PapersOnLine*, 51(20):331–336, 2018.
- [71] Wanxin Jin, Zhaoran Wang, Zhuoran Yang, and Shaoshuai Mou. Pontryagin differentiable programming: An end-to-end learning and control framework. In *Advances in Neural Information Processing Systems*, 2020.
- [72] Ankur Sinha, Pekka Malo, and Kalyanmoy Deb. A review on bilevel optimization: from classical to evolutionary approaches and applications. *IEEE Transactions on Evolutionary Computation*, 22(2):276–295, 2017.
- [73] J Pearson and R Sridhar. A discrete optimal control problem. *IEEE Transactions on automatic control*, 11(2):171–174, 1966.
- [74] Anthony V Fiacco. Sensitivity analysis for nonlinear programming using penalty methods. *Mathematical programming*, 10(1):287–311, 1976.
- [75] Walter Rudin et al. *Principles of mathematical analysis*, volume 3. McGraw-hill New York, 1976.
- [76] Charles D Kolstad and Leon S Lasdon. Derivative evaluation and computational experience with large bilevel mathematical programs. *Journal of optimization theory and applications*, 65(3):485–499, 1990.
- [77] Joel AE Andersson, Joris Gillis, Greg Horn, James B Rawlings, and Moritz Diehl. Casadi: a software framework for nonlinear optimization and optimal control. *Mathematical Programming Computation*, 11(1):1–36, 2019.
- [78] Athanasios Sideris and Luis A Rodriguez. A riccati approach to equality constrained linear quadratic optimal control. In *American Control Conference*, pages 5167–5172, 2010.
- [79] Shuo Yang, Gerry Chen, Yetong Zhang, Frank Dellaert, and Howie Choset. Equality constrained linear optimal control with factor graphs. *arXiv preprint arXiv:2011.01360*, 2020.
- [80] Forrest Laine and Claire Tomlin. Efficient computation of feedback control for equality-constrained lqr. In *International Conference on Robotics and Automation*, pages 6748–6754. IEEE, 2019.
- [81] Weiwei Li and Emanuel Todorov. Iterative linear quadratic regulator design for nonlinear biological movement systems. In *International Conference on Informatics in Control, Automation and Robotics*, pages 222–229, 2004.
- [82] David H Jacobson and David Q Mayne. *Differential dynamic programming*. Number 24. Elsevier Publishing Company, 1970.
- [83] Milton Abramowitz and Irene A Stegun. *Handbook of mathematical functions with formulas, graphs, and mathematical tables*, volume 55. US Government printing office, 1964.
- [84] Felix Berkenkamp, Andreas Krause, and Angela P Schoellig. Bayesian optimization with safety constraints: safe and automatic parameter tuning in robotics. *Machine Learning*, pages 1–35, 2021.
- [85] Wanxin Jin, Todd D Murphey, Dana Kulić, Neta Ezer, and Shaoshuai Mou. Learning from sparse demonstrations. *arXiv preprint arXiv:2008.02159*, 2020.
- [86] Michael Athans. The matrix minimum principle. *Information and control*, 11(5-6):592–606, 1967.
- [87] Jean Dieudonné. *Foundations of modern analysis*. New York: Academic Press. Volume 1 of Treatise on Analysis, 2011.
- [88] Rolf Johansson. *System modeling and identification*. Prentice-hall, 1993.

- [89] Ricky TQ Chen, Yulia Rubanova, Jesse Bettencourt, and David Duvenaud. Neural ordinary differential equations. *Advances in Neural Information Processing Systems*, 2018.
- [90] Wanxin Jin, Dana Kulić, Shaoshuai Mou, and Sandra Hirche. Inverse optimal control from incomplete trajectory observations. *The International Journal of Robotics Research*, 40(6-7):848–865, 2021.
- [91] Wanxin Jin and Shaoshuai Mou. Distributed inverse optimal control. *Automatica*, 129, 2021.
- [92] Wanxin Jin, Dana Kulić, Jonathan Feng-Shun Lin, Shaoshuai Mou, and Sandra Hirche. Inverse optimal control for multiphase cost functions. *IEEE Transactions on Robotics*, 35(6):1387–1398, 2019.
- [93] Wanxin Jin, Todd D Murphey, and Shaoshuai Mou. Learning from incremental directional corrections. *arXiv preprint arXiv:2011.15014*, 2020.
- [94] Michael A Patterson and Anil V Rao. Gpops-ii: A matlab software for solving multiple-phase optimal control problems using hp-adaptive gaussian quadrature collocation methods and sparse nonlinear programming. *ACM Transactions on Mathematical Software (TOMS)*, 41(1):1–37, 2014.

## Checklist

1. For all authors...
  - (a) Do the main claims made in the abstract and introduction accurately reflect the paper’s contributions and scope? [Yes]
  - (b) Did you describe the limitations of your work? [Yes] Please see Sections 8 and Appendix G.5 in the paper.
  - (c) Did you discuss any potential negative societal impacts of your work? [N/A]
  - (d) Have you read the ethics review guidelines and ensured that your paper conforms to them? [Yes]
2. If you are including theoretical results...
  - (a) Did you state the full set of assumptions of all theoretical results? [Yes] Please find them in all theorems in the paper.
  - (b) Did you include complete proofs of all theoretical results? [Yes] Please find complete proofs for all theoretical results in the Appendix in the supplementary file.
3. If you ran experiments...
  - (a) Did you include the code, data, and instructions needed to reproduce the main experimental results (either in the supplemental material or as a URL)? [Yes] Please refer to the code at <https://github.com/wanxinjin/Safe-PDP>.
  - (b) Did you specify all the training details (e.g., data splits, hyperparameters, how they were chosen)? [Yes] Please see the Appendix F in the supplementary file.
  - (c) Did you report error bars (e.g., with respect to the random seed after running experiments multiple times)? [N/A]
  - (d) Did you include the total amount of compute and the type of resources used (e.g., type of GPUs, internal cluster, or cloud provider)? [Yes] Please see the Appendix F in the supplementary file.
4. If you are using existing assets (e.g., code, data, models) or curating/releasing new assets...
  - (a) If your work uses existing assets, did you cite the creators? [Yes] Please see the citation of the experimental environments in Table 1 in the paper.
  - (b) Did you mention the license of the assets? [N/A]
  - (c) Did you include any new assets either in the supplemental material or as a URL? [Yes] Some video demo links are included in Appendix F in the supplementary file.
  - (d) Did you discuss whether and how consent was obtained from people whose data you’re using/curating? [N/A]



- (e) Did you discuss whether the data you are using/curating contains personally identifiable information or offensive content? [N/A]
5. If you used crowdsourcing or conducted research with human subjects...
- (a) Did you include the full text of instructions given to participants and screenshots, if applicable? [N/A]
  - (b) Did you describe any potential participant risks, with links to Institutional Review Board (IRB) approvals, if applicable? [N/A]
  - (c) Did you include the estimated hourly wage paid to participants and the total amount spent on participant compensation? [N/A]

## A Second-order Sufficient Condition

Before presenting the second-order condition for the optimal control Problem  $\mathbf{B}(\theta)$ , we present the second-order condition for a general constrained nonlinear programming. The interested reader can find the details in Theorem 4 in [48].

**Lemma A.1** (Second-order sufficient condition [48]). *If all functions defining a constrained optimization*

$$\begin{aligned} \min_{\mathbf{x}} \quad & f(\mathbf{x}) \\ \text{subject to} \quad & g_i(\mathbf{x}) \leq 0 \quad i = 1, 2, \dots, m, \\ & h_j(\mathbf{x}) = 0 \quad j = 1, 2, \dots, p, \end{aligned} \quad (\text{S.1})$$

are twice-continuous differentiable, the second-order sufficient condition for  $\mathbf{x}^*$  to be a local isolated minimizing solution to (S.1) is that there exist vectors  $\mathbf{v}^*$  and  $\mathbf{w}^*$  such that  $(\mathbf{x}^*, \mathbf{v}^*, \mathbf{w}^*)$  satisfies

$$\begin{aligned} g_i(\mathbf{x}^*) &\leq 0, \quad i = 1, 2, \dots, m, \\ h_j(\mathbf{x}^*) &= 0, \quad j = 1, 2, \dots, p, \\ v_i g_i(\mathbf{x}^*) &= 0, \quad i = 1, 2, \dots, m, \\ u_i &\geq 0, \quad i = 1, 2, \dots, m, \\ \nabla L(\mathbf{x}^*, \mathbf{v}^*, \mathbf{w}^*) &= 0, \end{aligned} \quad (\text{S.2})$$

with

$$L(\mathbf{x}, \mathbf{v}, \mathbf{w}) = f(\mathbf{x}) + \sum_{i=1}^m v_i g_i(\mathbf{x}) + \sum_{i=1}^p w_i h_i(\mathbf{x}), \quad (\text{S.3})$$

and  $\nabla L$  being the derivative of  $L$  with respect to  $\mathbf{x}$ ; and further for any nonzero  $\mathbf{y} \neq \mathbf{0}$  satisfying  $\mathbf{y}' \nabla g_i(\mathbf{x}^*) = 0$  for all  $i$  with  $v_i^* > 0$ ,  $\mathbf{y}' \nabla g_i(\mathbf{x}^*) \leq 0$  for all  $i$  with  $v_i^* \geq 0$ , and  $\mathbf{y}' \nabla h_j(\mathbf{x}^*) = 0$  for all  $j = 1, 2, \dots, p$ , it follows that

$$\mathbf{y}' \nabla^2 L(\mathbf{x}^*, \mathbf{v}^*, \mathbf{w}^*) \mathbf{y} > 0. \quad (\text{S.4})$$

The above second-order sufficient condition for nonlinear programming is well-known. The proof for Lemma A.1 can be found in Theorem 4 in [48]. Similarly, we can establish the second-order sufficient condition for a general constrained optimal control system  $\Sigma(\theta)$  in (1), as below.

**Lemma A.2** (Second-order sufficient condition for  $\Sigma(\theta)$  to have a local isolated minimizing trajectory  $\xi_\theta$  [73]). *Given  $\theta$ , if all functions defining the constrained optimal control system  $\Sigma(\theta)$  are twice continuously differentiable in a neighborhood (tube) of  $\xi_\theta = \{\mathbf{x}_{0:T}^\theta, \mathbf{u}_{0:T-1}^\theta\}$ ,  $\xi_\theta$  is a local isolated minimizing trajectory to Problem  $\mathbf{B}(\theta)$  if there exist sequences  $\lambda_{1:T}^\theta$ ,  $\mathbf{v}_{0:T}^\theta$ , and  $\mathbf{w}_{0:T}^\theta$  such that the following Constrained Pontryagin Maximum/Minimum Principle (C-PMP) conditions hold,*

$$\begin{aligned} \mathbf{x}_{t+1}^\theta &= \mathbf{f}(\mathbf{x}_t^\theta, \mathbf{u}_t^\theta, \theta) \quad \text{and} \quad \mathbf{x}_0^\theta = \mathbf{x}_0(\theta), \\ \lambda_t^\theta &= L_t^x(\mathbf{x}_t^\theta, \mathbf{u}_t^\theta, \lambda_{t+1}^\theta, \mathbf{v}_t^\theta, \mathbf{w}_t^\theta, \theta) \quad \text{and} \quad \lambda_T^\theta = L_T^x(\mathbf{x}_T^\theta, \mathbf{v}_T^\theta, \mathbf{w}_T^\theta, \theta), \\ \mathbf{0} &= L_t^u(\mathbf{x}_t^\theta, \mathbf{u}_t^\theta, \lambda_{t+1}^\theta, \mathbf{v}_t^\theta, \mathbf{w}_t^\theta, \theta), \\ h_{t,j}(\mathbf{x}_t^\theta, \mathbf{u}_t^\theta, \theta) &= 0, \quad j = 1, 2, \dots, s_t, \\ h_{T,j}(\mathbf{x}_T^\theta, \theta) &= 0, \quad j = 1, 2, \dots, s_T, \\ g_{t,i}(\mathbf{x}_t^\theta, \mathbf{u}_t^\theta, \theta) &\leq 0, \quad v_{t,i} g_{t,i}(\mathbf{x}_t^\theta, \mathbf{u}_t^\theta, \theta) = 0, \quad v_{t,i} \geq 0, \quad i = 1, 2, \dots, q_t, \\ g_{T,i}(\mathbf{x}_T^\theta, \theta) &\leq 0, \quad v_{T,i} g_{T,i}(\mathbf{x}_T^\theta, \theta) = 0, \quad v_{T,i} \geq 0, \quad i = 1, 2, \dots, q_T, \end{aligned} \quad (\text{S.5})$$

and further if

$$\sum_{t=0}^{T-1} \begin{bmatrix} \mathbf{x}_t \\ \mathbf{u}_t \end{bmatrix}' \begin{bmatrix} L_t^{xx} & L_t^{xu} \\ L_t^{ux} & L_t^{uu} \end{bmatrix} \begin{bmatrix} \mathbf{x}_t \\ \mathbf{u}_t \end{bmatrix} + \mathbf{x}_T' L_T^{xx} \mathbf{x}_T > 0 \quad (\text{S.6})$$

for any non-zero trajectory  $\{\mathbf{x}_{0:T}, \mathbf{u}_{0:T-1}\} \neq \mathbf{0}$  satisfying

$$\begin{aligned} \mathbf{x}_{t+1} &= F_t^x \mathbf{x}_t + F_t^u \mathbf{u}_t & \mathbf{x}_0 &= \mathbf{0}, \\ H_t^x \mathbf{x}_t + H_t^u \mathbf{u}_t &= \mathbf{0} & \text{and} & \quad H_T^x \mathbf{x}_T = \mathbf{0}, \\ \check{G}_t^x \mathbf{x}_t + \check{G}_t^u \mathbf{u}_t &= \mathbf{0} & \text{and} & \quad \check{G}_T^x \mathbf{x}_T = \mathbf{0}, \\ \bar{G}_t^x \mathbf{x}_t + \bar{G}_t^u \mathbf{u}_t &\leq \mathbf{0} & \text{and} & \quad \bar{G}_T^x \mathbf{x}_T \leq \mathbf{0}. \end{aligned} \tag{S.7}$$

Here,  $t = 0, 1, \dots, T-1$ ;  $L_t^x$  is the first-order derivative of the Hamiltonian  $L_t$  in (2) with respect to  $\mathbf{x}$ , and  $L_t^{xx}$  is the second-derivative of  $L_t$  with respect to  $\mathbf{x}$ , and similar notation convention applies to  $L_T^x$ ,  $L_t^u$ ,  $L_t^{xu} = (L_t^{ux})'$ , and  $L_t^{uu}$ ;  $H_t^x$  is the first-order derivative of  $\mathbf{h}_t$  with respect to  $\mathbf{x}$  and the similar convention applies to  $H_T^x$ ,  $H_t^u$ ,  $F_t^x$  and  $F_t^u$  for  $\mathbf{f}$ ,  $\check{G}_t^x$  and  $\check{G}_t^u$  for  $\check{\mathbf{g}}_t$ ,  $\check{G}_T^x$  for  $\check{\mathbf{g}}_T$ ,  $\bar{G}_t^x$  and  $\bar{G}_t^u$  for  $\bar{\mathbf{g}}_t$ ,  $\bar{G}_T^x$  for  $\bar{\mathbf{g}}_T$ , where

$$\begin{aligned} \check{\mathbf{g}}_t(\mathbf{x}_t, \mathbf{u}_t, \boldsymbol{\theta}) &= \text{col}\{g_{t,i}(\mathbf{x}_t, \mathbf{u}_t, \boldsymbol{\theta}) \mid v_{t,i}^\theta > 0, i = 1, \dots, q_t\}, \\ \check{\mathbf{g}}_T(\mathbf{x}_T, \boldsymbol{\theta}) &= \text{col}\{g_{T,i}(\mathbf{x}_T, \boldsymbol{\theta}) \mid v_{T,i}^\theta > 0, i = 1, \dots, q_T\}, \\ \bar{\mathbf{g}}_t(\mathbf{x}_t, \mathbf{u}_t, \boldsymbol{\theta}) &= \text{col}\{g_{t,i}(\mathbf{x}_t, \mathbf{u}_t, \boldsymbol{\theta}) \mid g_{t,i}(\mathbf{x}_t, \mathbf{u}_t, \boldsymbol{\theta}) = 0, i = 1, \dots, q_t\} \in \mathbb{R}^{q_t}, \\ \bar{\mathbf{g}}_T(\mathbf{x}_T, \boldsymbol{\theta}) &= \text{col}\{g_{T,i}(\mathbf{x}_T, \boldsymbol{\theta}) \mid g_{T,i}(\mathbf{x}_T, \boldsymbol{\theta}) = 0, i = 1, \dots, q_T\} \in \mathbb{R}^{q_T}, \end{aligned} \tag{S.8}$$

i.e.,  $\bar{\mathbf{g}}_t$  and  $\bar{\mathbf{g}}_T$  are the vector functions formed by stacking all active inequality constraints at  $\boldsymbol{\xi}_\theta$ . All the above first- and second-order derivatives are evaluated at  $(\boldsymbol{\xi}_\theta, \boldsymbol{\lambda}_{1:T}^\theta, \mathbf{v}_{0:T}^\theta, \mathbf{w}_{0:T}^\theta)$ .

The above second-order sufficient condition for the constrained optimal control system  $\Sigma(\boldsymbol{\theta})$  is well-known and has been well-established since [73]. The conditions in (S.5) is referred to as discrete-time Constrained Pontryagin Maximum/Minimum Principle (C-PMP) [73]. Note that in the case of strict complementarity, one has  $\check{\mathbf{g}}_t(\mathbf{x}_t, \mathbf{u}_t, \boldsymbol{\theta}) = \bar{\mathbf{g}}_t(\mathbf{x}_t, \mathbf{u}_t, \boldsymbol{\theta})$  and  $\check{\mathbf{g}}_T(\mathbf{x}_T, \boldsymbol{\theta}) = \bar{\mathbf{g}}_T(\mathbf{x}_T, \boldsymbol{\theta})$  in (S.8).

## B Proof of Theorem 1

To prove Theorem 1, in the first part, we need to derive the Differential Constrained Pontryagin Maximum/Minimum Principle (Differential C-PMP), which  $\frac{\partial \boldsymbol{\xi}_\theta}{\partial \boldsymbol{\theta}} = \{X_{0:T}^\theta, U_{0:T}^\theta\}$  must satisfy. Then, in the second part, we formally present the proof for Theorem 1.

### B.1 Differential Constrained Pontryagin Maximum/Minimum Principle

From Lemma 1, for the constrained optimal control system  $\Sigma(\boldsymbol{\theta})$  with any  $\boldsymbol{\theta}$  in a neighborhood of  $\bar{\boldsymbol{\theta}}$ ,  $(\boldsymbol{\xi}_\theta, \boldsymbol{\lambda}_{1:T}^\theta, \mathbf{v}_{0:T}^\theta, \mathbf{w}_{0:T}^\theta)$  satisfies the C-PMP conditions in (S.5). Since  $(\boldsymbol{\xi}_\theta, \boldsymbol{\lambda}_{1:T}^\theta, \mathbf{v}_{0:T}^\theta, \mathbf{w}_{0:T}^\theta)$  is also once-continuously differentiable with respect to  $\boldsymbol{\theta}$  from Lemma 1, one can differentiate the C-PMP conditions in (S.5) on both sides with respect to  $\boldsymbol{\theta}$ , as below.

Differentiating the first five lines in (S.5) is straightforward, yielding

$$\begin{aligned} \frac{\partial \mathbf{x}_{t+1}^\theta}{\partial \boldsymbol{\theta}} &= F_t^x \frac{\partial \mathbf{x}_t^\theta}{\partial \boldsymbol{\theta}} + F_t^u \frac{\partial \mathbf{u}_t^\theta}{\partial \boldsymbol{\theta}} + F_t^\theta \quad \text{and} \quad X_0^\theta = \frac{\partial \mathbf{x}_0^\theta}{\partial \boldsymbol{\theta}} = \frac{\partial \mathbf{x}_0(\boldsymbol{\theta})}{\partial \boldsymbol{\theta}}, \\ \frac{\partial \boldsymbol{\lambda}_t^\theta}{\partial \boldsymbol{\theta}} &= L_t^{xx} \frac{\partial \mathbf{x}_t^\theta}{\partial \boldsymbol{\theta}} + L_t^{xu} \frac{\partial \mathbf{u}_t^\theta}{\partial \boldsymbol{\theta}} + (F_t^x)' \frac{\partial \boldsymbol{\lambda}_{t+1}^\theta}{\partial \boldsymbol{\theta}} + (G_t^x)' \frac{\partial \mathbf{v}_t^\theta}{\partial \boldsymbol{\theta}} + (H_t^x)' \frac{\partial \mathbf{w}_t^\theta}{\partial \boldsymbol{\theta}} + L_t^{x\theta} \quad \text{and} \\ \frac{\partial \boldsymbol{\lambda}_T^\theta}{\partial \boldsymbol{\theta}} &= L_T^{xx} \frac{\partial \mathbf{x}_T^\theta}{\partial \boldsymbol{\theta}} + (G_T^x)' \frac{\partial \mathbf{v}_T^\theta}{\partial \boldsymbol{\theta}} + (H_T^x)' \frac{\partial \mathbf{w}_T^\theta}{\partial \boldsymbol{\theta}} + L_T^{x\theta}, \\ \mathbf{0} &= L_t^{ux} \frac{\partial \mathbf{x}_t^\theta}{\partial \boldsymbol{\theta}} + L_t^{uu} \frac{\partial \mathbf{u}_t^\theta}{\partial \boldsymbol{\theta}} + (F_t^u)' \frac{\partial \boldsymbol{\lambda}_{t+1}^\theta}{\partial \boldsymbol{\theta}} + (G_t^u)' \frac{\partial \mathbf{v}_t^\theta}{\partial \boldsymbol{\theta}} + (H_t^u)' \frac{\partial \mathbf{w}_t^\theta}{\partial \boldsymbol{\theta}} + L_t^{u\theta}, \\ H_t^x \frac{\partial \mathbf{x}_t^\theta}{\partial \boldsymbol{\theta}} + H_t^u \frac{\partial \mathbf{u}_t^\theta}{\partial \boldsymbol{\theta}} + H_t^\theta &= \mathbf{0} \quad \text{and} \quad H_T^x \frac{\partial \mathbf{x}_T^\theta}{\partial \boldsymbol{\theta}} + H_T^\theta = \mathbf{0}. \end{aligned} \tag{S.9}$$

We now consider to differentiate the two last equations (i.e., complementarity conditions) in the last two lines in (S.5). We start with

$$v_{t,i}^\theta g_{t,i}(\mathbf{x}_t, \mathbf{u}_t, \boldsymbol{\theta}) = 0, \quad i = 1, 2, \dots, q_t. \tag{S.10}$$

Differentiating the above (S.10) on both sides with respect to  $\theta$  yields

$$\frac{\partial v_{t,i}^\theta}{\partial \theta} g_{t,i}(\mathbf{x}_t^\theta, \mathbf{u}_t^\theta, \theta) + \mu_{t,i}^\theta \frac{\partial g_{t,i}(\mathbf{x}_t^\theta, \mathbf{u}_t^\theta, \theta)}{\partial \theta} = \mathbf{0}, \quad i = 1, 2, \dots, q_t. \quad (\text{S.11})$$

In the above, we consider two following cases. If  $g_{t,i}(\mathbf{x}_t^\theta, \mathbf{u}_t^\theta, \theta) = 0$ , i.e.,  $g_{t,i}$  is an active inequality constraint, then,  $\mu_{t,i}^\theta > 0$  according to strict complementarity (condition (iii) in Lemma 1). From (S.11), one thus has

$$\frac{\partial g_{t,i}(\mathbf{x}_t^\theta, \mathbf{u}_t^\theta, \theta)}{\partial \theta} = \mathbf{0}. \quad (\text{S.12})$$

If  $g_{t,i}(\mathbf{x}_t^\theta, \mathbf{u}_t^\theta, \theta) < 0$ , i.e.,  $g_{t,i}$  is an inactive constraint, then  $v_{t,i}^\theta = 0$  and one has

$$\frac{\partial v_{t,i}^\theta}{\partial \theta} = \mathbf{0} \quad \text{for} \quad v_{t,i}^\theta = 0. \quad (\text{S.13})$$

Stacking (S.12) for all active inequality constraints defined in (S.8) will lead to

$$\mathbf{0} = \bar{G}_t^x \frac{\partial \mathbf{x}_t^\theta}{\partial \theta} + \bar{G}_t^u \frac{\partial \mathbf{u}_t^\theta}{\partial \theta} + \bar{G}_t^\theta. \quad (\text{S.14})$$

Similarly, we can show that differentiating  $v_{T,i} g_{T,i}(\mathbf{x}_T^\theta, \theta) = 0, i = 1, 2, \dots, q_T$ , will lead to

$$\bar{G}_T^x \frac{\partial \mathbf{x}_T^\theta}{\partial \theta} + \bar{G}_T^\theta = \mathbf{0}. \quad (\text{S.15})$$

If we further define

$$\bar{\mathbf{v}}_t^\theta = \text{col}\{v_{t,i}^\theta \mid v_{t,i}^\theta > 0, i = 1, \dots, q_t\} \in \mathbb{R}^{\bar{q}_t}, \quad (\text{S.16})$$

then, due to (S.13), the following terms in the second, third, and fourth lines in (S.9) can be written in an equivalent way:

$$(G_t^x)' \frac{\partial \mathbf{v}_t^\theta}{\partial \theta} = (\bar{G}_t^x)' \frac{\partial \bar{\mathbf{v}}_t^\theta}{\partial \theta} \quad \text{and} \quad (G_t^u)' \frac{\partial \mathbf{v}_t^\theta}{\partial \theta} = (\bar{G}_t^u)' \frac{\partial \bar{\mathbf{v}}_t^\theta}{\partial \theta}. \quad (\text{S.17})$$

In sum, combining (S.9), (S.14), (S.15), and (S.17), one can finally write the Differential C-PMP:

$$\begin{aligned} \frac{\partial \mathbf{x}_{t+1}^\theta}{\partial \theta} &= F_t^x \frac{\partial \mathbf{x}_t^\theta}{\partial \theta} + F_t^u \frac{\partial \mathbf{u}_t^\theta}{\partial \theta} + F_t^\theta \quad \text{and} \quad X_0^\theta = \frac{\partial \mathbf{x}_0^\theta}{\partial \theta}, \\ \frac{\partial \lambda_t^\theta}{\partial \theta} &= L_t^{xx} \frac{\partial \mathbf{x}_t^\theta}{\partial \theta} + L_t^{xu} \frac{\partial \mathbf{u}_t^\theta}{\partial \theta} + (F_t^x)' \frac{\partial \lambda_{t+1}^\theta}{\partial \theta} + (\bar{G}_t^x)' \frac{\partial \bar{\mathbf{v}}_t^\theta}{\partial \theta} + (H_t^x)' \frac{\partial \mathbf{w}_t^\theta}{\partial \theta} + L_t^{x\theta} \quad \text{and} \\ \frac{\partial \lambda_T^\theta}{\partial \theta} &= L_T^{xx} \frac{\partial \mathbf{x}_T^\theta}{\partial \theta} + (\bar{G}_T^x)' \frac{\partial \bar{\mathbf{v}}_T^\theta}{\partial \theta} + (H_T^x)' \frac{\partial \mathbf{w}_T^\theta}{\partial \theta} + L_T^{x\theta}, \\ \mathbf{0} &= L_t^{ux} \frac{\partial \mathbf{x}_t^\theta}{\partial \theta} + L_t^{uu} \frac{\partial \mathbf{u}_t^\theta}{\partial \theta} + (F_t^u)' \frac{\partial \lambda_{t+1}^\theta}{\partial \theta} + (\bar{G}_t^u)' \frac{\partial \bar{\mathbf{v}}_t^\theta}{\partial \theta} + (H_t^u)' \frac{\partial \mathbf{w}_t^\theta}{\partial \theta} + L_t^{u\theta}, \\ H_t^x \frac{\partial \mathbf{x}_t^\theta}{\partial \theta} + H_t^u \frac{\partial \mathbf{u}_t^\theta}{\partial \theta} + H_t^\theta &= \mathbf{0} \quad \text{and} \quad H_T^x \frac{\partial \mathbf{x}_T^\theta}{\partial \theta} + H_T^\theta = \mathbf{0}, \\ \bar{G}_t^x \frac{\partial \mathbf{x}_t^\theta}{\partial \theta} + \bar{G}_t^u \frac{\partial \mathbf{u}_t^\theta}{\partial \theta} + \bar{G}_t^\theta &= \mathbf{0} \quad \text{and} \quad \bar{G}_T^x \frac{\partial \mathbf{x}_T^\theta}{\partial \theta} + \bar{G}_T^\theta = \mathbf{0}. \end{aligned} \quad (\text{S.18})$$

With the above Differential C-PMP, we next prove the claims in Theorem 1.

## B.2 Proof of Theorem 1

We prove Theorem 1 by two steps. We first prove that the trajectory in (4), rewritten below,

$$\{X_{0:T}^\theta, U_{0:T-1}^\theta\} \quad \text{with} \quad X_t^\theta = \frac{\partial \mathbf{x}_t^\theta}{\partial \theta} \quad \text{and} \quad U_t^\theta = \frac{\partial \mathbf{u}_t^\theta}{\partial \theta},$$

is the *local isolated* minimizing trajectory to the auxiliary control system  $\bar{\Sigma}(\xi_\theta)$  in (3); and second, we prove that such a local minimizing trajectory is also a *global* minimizing trajectory.

First, we prove that  $\{X_{0:T}^\theta, U_{0:T-1}^\theta\}$  is a *local isolated* minimizing trajectory to  $\bar{\Sigma}(\xi_\theta)$ .

To show that  $\{X_{0:T}^\theta, U_{0:T-1}^\theta\}$  is a local isolated minimizing trajectory to  $\bar{\Sigma}(\xi_\theta)$ , we only need to check whether it satisfies the second-order sufficient condition for the constrained optimal control system  $\bar{\Sigma}(\xi_\theta)$ , as stated in Lemma A.2. To that end, we define the following Hamiltonian for  $\bar{\Sigma}(\xi_\theta)$ :

$$\begin{aligned}\bar{L}_t &= \text{Tr} \left( \frac{1}{2} \begin{bmatrix} X_t \\ U_t \end{bmatrix}' \begin{bmatrix} L_t^{xx} & L_t^{xu} \\ L_t^{ux} & L_t^{uu} \end{bmatrix} \begin{bmatrix} X_t \\ U_t \end{bmatrix} + \begin{bmatrix} L_t^{x\theta} \\ L_t^{u\theta} \end{bmatrix}' \begin{bmatrix} X_t \\ U_t \end{bmatrix} \right) + \text{Tr} \left( \Lambda_{t+1}' (F_t^x X_t + F_t^u U_t + F_t^\theta) \right) \\ &\quad + \text{Tr} \left( \bar{V}_t' (\bar{G}_t^x X_t + \bar{G}_t^u U_t + \bar{G}_t^\theta) \right) + \text{Tr} \left( W_t' (H_t^x X_t + H_t^u U_t + H_t^\theta) \right), \quad t = 0, \dots, T-1, \\ \bar{L}_T &= \text{Tr} \left( \frac{1}{2} X_T' L_T^{xx} X_T + (L_T^{x\theta})' X_T \right) + \text{Tr} \left( \bar{M}_T' (\bar{G}_T^x X_T + \bar{G}_T^\theta) \right) \\ &\quad + \text{Tr} \left( N_T' (H_T^x X_T + H_T^\theta) \right), \quad t = T.\end{aligned}\tag{S.19}$$

Here,  $\Lambda_t \in \mathbb{R}^{n \times r}$ ,  $t = 1, 2, \dots, T$ , denotes the costate (matrix) variables for  $\bar{\Sigma}(\xi_\theta)$ ;  $\bar{V}_t \in \mathbb{R}^{\bar{q}_t \times r}$  and  $W_t \in \mathbb{R}^{s_t \times r}$ ,  $t = 0, 1, \dots, T$ , are the multipliers for the constraints in  $\bar{\Sigma}(\xi_\theta)$ . Further define

$$\Lambda_t^\theta = \frac{\partial \lambda_t^\theta}{\partial \theta}, \quad W_t^\theta = \frac{\partial w_t^\theta}{\partial \theta}, \quad \bar{V}_t^\theta = \frac{\partial \bar{v}_t^\theta}{\partial \theta},\tag{S.20}$$

with  $\bar{v}_t^\theta$  in (S.16). Then, the Differential C-PMP in (S.18) is exactly the Constrained Pontryagin Minimal Principle (C-PMP) for the auxiliary control system  $\bar{\Sigma}(\xi_\theta)$  because

$$\begin{aligned}X_{t+1}^\theta &= \frac{\partial \bar{L}_t}{\partial \Lambda_{t+1}^\theta} = F_t^x X_t^\theta + F_t^u U_t^\theta + F_t^\theta \quad \text{and} \quad X_0 = X_0^\theta, \\ \Lambda_t^\theta &= \frac{\partial \bar{L}_t}{\partial X_t^\theta} = L_t^{xx} X_t^\theta + L_t^{xu} U_t^\theta + L_t^{x\theta} + (F_t^x)' \Lambda_{t+1}^\theta + (\bar{G}_t^x)' \bar{V}_t^\theta + (H_t^x)' W_t^\theta \quad \text{and} \\ \Lambda_T^\theta &= \frac{\partial \bar{L}_T}{\partial X_T^\theta} = H_T^{xx} X_T^\theta + H_T^{x\theta} + (\bar{G}_T^x)' \bar{V}_T^\theta + (H_T^x)' W_T^\theta, \\ \mathbf{0} &= \frac{\partial \bar{L}_t}{\partial U_t^\theta} = L_t^{uu} U_t^\theta + L_t^{ux} X_t^\theta + L_t^{u\theta} + (F_t^u)' \Lambda_{t+1}^\theta + (\bar{G}_t^u)' \bar{V}_t^\theta + (H_t^u)' W_t^\theta, \\ H_t^x X_t^\theta + H_t^u U_t^\theta + H_t^\theta &= \mathbf{0} \quad \text{and} \quad H_T^x X_T^\theta + H_T^\theta = \mathbf{0}, \\ \bar{G}_t^x X_t^\theta + \bar{G}_t^u U_t^\theta + \bar{G}_t^\theta &= \mathbf{0} \quad \text{and} \quad \bar{G}_T^x X_T^\theta + \bar{G}_T^\theta = \mathbf{0}.\end{aligned}\tag{S.21}$$

Note that in (S.21), we have used the following matrix calculus [86] and trace properties:

$$\begin{aligned}\frac{\partial \text{Tr}(AB)}{\partial A} &= B', \quad \frac{\partial f(A)}{\partial A'} = \left[ \frac{\partial f(A)}{\partial A} \right]', \quad \frac{\partial \text{Tr}(X'HX)}{\partial X} = HX + H'X, \\ \text{Tr}(A) &= \text{Tr}(A'), \quad \text{Tr}(ABC) = \text{Tr}(BCA) = \text{Tr}(CAB), \quad \text{Tr}(A+B) = \text{Tr}(A) + \text{Tr}(B).\end{aligned}$$

Next, we need to show that the second-order condition

$$\sum_{t=0}^{T-1} \text{Tr} \left( \begin{bmatrix} \Delta X_t \\ \Delta U_t \end{bmatrix}' \underbrace{\begin{bmatrix} \frac{\partial \bar{L}_t^2}{\partial X_t^\theta \partial X_t^\theta} & \frac{\partial \bar{L}_t^2}{\partial X_t^\theta \partial U_t^\theta} \\ \frac{\partial \bar{L}_t^2}{\partial U_t^\theta \partial X_t^\theta} & \frac{\partial \bar{L}_t^2}{\partial U_t^\theta \partial U_t^\theta} \end{bmatrix}}_{\begin{bmatrix} L_t^{xx} & L_t^{xu} \\ L_t^{ux} & L_t^{uu} \end{bmatrix}} \begin{bmatrix} \Delta X_t \\ \Delta U_t \end{bmatrix} \right) + \text{Tr} \left( \Delta X_T' \underbrace{\begin{bmatrix} \frac{\partial \bar{L}_T^2}{\partial X_T^\theta \partial X_T^\theta} \end{bmatrix}}_{L_T^{xx}} \Delta X_T \right) > 0,\tag{S.22}$$

hold for any trajectory  $\{\Delta X_{0:T}, \Delta U_{0:T-1}\} \neq \mathbf{0}$  satisfying

$$\begin{aligned} \Delta X_{t+1} &= F_t^x \Delta X_t + F_t^u \Delta U_t \quad \text{and} \quad \Delta X_0 = \mathbf{0}, \\ \bar{G}_t^x \Delta X_t + \bar{G}_t^u \Delta U_t &= \mathbf{0} \quad \text{and} \quad \bar{G}_T^x \Delta X_T = \mathbf{0}, \\ H_t^x \Delta X_t + H_t^u \Delta U_t &= \mathbf{0} \quad \text{and} \quad H_T^x \Delta X_T = \mathbf{0}, \end{aligned} \quad (\text{S.23})$$

In fact, this is true directly due to (S.6) and (S.7) in Lemma A.2 and the strict complementarity in condition (iii) in Lemma 1 (note that  $\check{g}_t(\mathbf{x}_t, \mathbf{u}_t, \boldsymbol{\theta}) = \bar{g}_t(\mathbf{x}_t, \mathbf{u}_t, \boldsymbol{\theta})$  and  $\check{g}_T(\mathbf{x}_T, \boldsymbol{\theta}) = \bar{g}_T(\mathbf{x}_T, \boldsymbol{\theta})$  because of the strict complementarity). Therefore, with the C-PMP (S.21) and (S.22)-(S.23) holding for  $\{X_{0:T}^\theta, U_{0:T-1}^\theta\}$ , we can conclude that  $\{X_{0:T}^\theta, U_{0:T-1}^\theta\}$  is a local unique minimizing trajectory to the auxiliary control system  $\bar{\Sigma}(\boldsymbol{\xi}_\theta)$  according to Lemma A.2.

Second, we prove that the local unique minimizing trajectory  $\{X_{0:T}^\theta, U_{0:T-1}^\theta\}$  is also a *global* one.

We note that any feasible trajectory  $\{X_{0:T}, U_{0:T-1}\}$  that satisfies all constraints (dynamics, path and final constraints) in the auxiliary control system  $\bar{\Sigma}(\boldsymbol{\xi}_\theta)$  can be written as

$$\{X_{0:T}, U_{0:T-1}\} = \{X_{0:T}^\theta, U_{0:T-1}^\theta\} + \{\Delta X_{0:T}, \Delta U_{0:T-1}\}, \quad (\text{S.24})$$

with  $\{\Delta X_{0:T}, \Delta U_{0:T-1}\}$  satisfying the conditions in (S.23). Let

$$\begin{aligned} & \bar{J}(X_{0:T}, U_{0:T-1}) - \bar{J}(X_{0:T}^\theta, U_{0:T-1}^\theta) \\ &= \text{Tr} \sum_{t=0}^{T-1} \left( \frac{1}{2} \begin{bmatrix} \Delta X_t \\ \Delta U_t \end{bmatrix}' \begin{bmatrix} L_t^{xx} & L_t^{xu} \\ L_t^{ux} & L_t^{uu} \end{bmatrix} \begin{bmatrix} \Delta X_t \\ \Delta U_t \end{bmatrix} + \begin{bmatrix} X_t^\theta \\ U_t^\theta \end{bmatrix}' \begin{bmatrix} L_t^{xx} & L_t^{xu} \\ L_t^{ux} & L_t^{uu} \end{bmatrix} \begin{bmatrix} \Delta X_t \\ \Delta U_t \end{bmatrix} + \begin{bmatrix} L_t^{x\theta} \\ L_t^{u\theta} \end{bmatrix}' \begin{bmatrix} \Delta X_t \\ \Delta U_t \end{bmatrix} \right) \\ & \quad + \text{Tr} \left( \frac{1}{2} \Delta X_T' L_T^{xx} \Delta X_T + (X_T^\theta)' L_T^{xx} \Delta X_T + (L_T^{x\theta})' \Delta X_T \right). \end{aligned} \quad (\text{S.25})$$

Based on (S.21), the following term in (S.25) can be simplified to

$$\begin{aligned} & \begin{bmatrix} \Delta X_t \\ \Delta U_t \end{bmatrix}' \left( \begin{bmatrix} L_t^{xx} & L_t^{xu} \\ L_t^{ux} & L_t^{uu} \end{bmatrix} \begin{bmatrix} X_t^\theta \\ U_t^\theta \end{bmatrix} + \begin{bmatrix} L_t^{x\theta} \\ L_t^{u\theta} \end{bmatrix} \right) \\ &= \begin{bmatrix} \Delta X_t \\ \Delta U_t \end{bmatrix}' \begin{bmatrix} -(F_t^x)' \Lambda_{t+1}^\theta - (\bar{G}_t^x)' \bar{V}_t^\theta - (H_t^x)' W_t^\theta + \Lambda_t^\theta \\ -(F_t^u)' \Lambda_{t+1}^\theta - (\bar{G}_t^u)' \bar{V}_t^\theta - (H_t^u)' W_t^\theta \end{bmatrix} \\ &= -(\Lambda_{t+1}^\theta)' F_t^x \Delta X_t - \underbrace{(\bar{V}_t^\theta)' \bar{G}_t^x \Delta X_t}_{-(\Lambda_{t+1}^\theta)' \Delta X_{t+1}} - \underbrace{(W_t^\theta)' H_t^x \Delta X_t}_{-(\Lambda_{t+1}^\theta)' \Delta X_{t+1}} + (\Lambda_t^\theta)' \Delta X_t \\ & \quad - (\Lambda_{t+1}^\theta)' F_t^u \Delta U_t - \underbrace{(\bar{V}_t^\theta)' \bar{G}_t^u \Delta U_t}_{-(\Lambda_{t+1}^\theta)' \Delta X_{t+1}} - \underbrace{(W_t^\theta)' H_t^u \Delta U_t}_{-(\Lambda_{t+1}^\theta)' \Delta X_{t+1}} \\ &= \underbrace{-(\Lambda_{t+1}^\theta)' F_t^x \Delta X_t - (\Lambda_{t+1}^\theta)' F_t^u \Delta U_t}_{-(\Lambda_{t+1}^\theta)' \Delta X_{t+1}} + (\Lambda_t^\theta)' \Delta X_t = -(\Lambda_{t+1}^\theta)' \Delta X_{t+1} + (\Lambda_t^\theta)' \Delta X_t \end{aligned} \quad (\text{S.26})$$

where the cancellations in the last three lines are due to (S.23). Also based on (S.21), the following term in (S.25) can be simplified to

$$\begin{aligned} & ((X_T^\theta)' L_T^{xx} + (L_T^{x\theta})') \Delta X_T \\ &= - \underbrace{(\bar{V}_T^\theta)' \bar{G}_T \Delta X_T}_{-(\Lambda_T^\theta)' \Delta X_T} - \underbrace{(W_T^\theta)' H_T^x \Delta X_T}_{-(\Lambda_T^\theta)' \Delta X_T} + (\Lambda_T^\theta)' \Delta X_T \\ &= (\Lambda_T^\theta)' \Delta X_T \end{aligned} \quad (\text{S.27})$$

where the cancellation here is due to (S.23).

Then, based on (S.26) and (S.27), (S.25) is simplified to

$$\begin{aligned}
& \bar{J}(X_{0:T}, U_{0:T-1}) - \bar{J}(X_{0:T}^\theta, U_{0:T-1}^\theta) \\
&= \text{Tr} \sum_{t=0}^{T-1} \left( \frac{1}{2} \begin{bmatrix} \Delta X_t \\ \Delta U_t \end{bmatrix}' \begin{bmatrix} L_t^{xx} & L_t^{xu} \\ L_t^{ux} & L_t^{uu} \end{bmatrix} \begin{bmatrix} \Delta X_t \\ \Delta U_t \end{bmatrix} + \begin{bmatrix} X_t^\theta \\ U_t^\theta \end{bmatrix}' \begin{bmatrix} L_t^{xx} & L_t^{xu} \\ L_t^{ux} & L_t^{uu} \end{bmatrix} \begin{bmatrix} \Delta X_t \\ \Delta U_t \end{bmatrix} + \begin{bmatrix} L_t^{x\theta} \\ L_t^{u\theta} \end{bmatrix}' \begin{bmatrix} \Delta X_t \\ \Delta U_t \end{bmatrix} \right) \\
&+ \text{Tr} \left( \frac{1}{2} \Delta X_T' L_T^{xx} \Delta X_T + (X_T^\theta)' L_T^{xx} \Delta X_T + (L_T^{x\theta})' \Delta X_T \right) \\
&= \text{Tr} \sum_{t=0}^{T-1} \left( \frac{1}{2} \begin{bmatrix} \Delta X_t \\ \Delta U_t \end{bmatrix}' \begin{bmatrix} L_t^{xx} & L_t^{xu} \\ L_t^{ux} & L_t^{uu} \end{bmatrix} \begin{bmatrix} \Delta X_t \\ \Delta U_t \end{bmatrix} - (\Lambda_{t+1}^\theta)' \Delta X_{t+1} + (\Lambda_t^\theta)' \Delta X_t \right) \\
&+ \text{Tr} \left( \frac{1}{2} \Delta X_T' L_T^{xx} \Delta X_T + (\Lambda_T^\theta)' \Delta X_T \right) \\
&= \text{Tr} \sum_{t=0}^{T-1} \left( \frac{1}{2} \begin{bmatrix} \Delta X_t \\ \Delta U_t \end{bmatrix}' \begin{bmatrix} L_t^{xx} & L_t^{xu} \\ L_t^{ux} & L_t^{uu} \end{bmatrix} \begin{bmatrix} \Delta X_t \\ \Delta U_t \end{bmatrix} \right) + \text{Tr} \left( \frac{1}{2} \Delta X_T' L_T^{xx} \Delta X_T \right), \tag{S.28}
\end{aligned}$$

where the last line is because (note  $\Delta X_0 = \mathbf{0}$  in (S.23))

$$\text{Tr} \sum_{t=0}^{T-1} \left( -(\Lambda_{t+1}^\theta)' \Delta X_{t+1} + (\Lambda_t^\theta)' \Delta X_t \right) + \text{Tr} \left( (\Lambda_T^\theta)' \Delta X_T \right) = \text{Tr} \left( (\Lambda_0^\theta)' \Delta X_0 \right) = 0.$$

Since

$$\text{Tr} \sum_{t=0}^{T-1} \left( \frac{1}{2} \begin{bmatrix} \Delta X_t \\ \Delta U_t \end{bmatrix}' \begin{bmatrix} L_t^{xx} & L_t^{xu} \\ L_t^{ux} & L_t^{uu} \end{bmatrix} \begin{bmatrix} \Delta X_t \\ \Delta U_t \end{bmatrix} \right) + \text{Tr} \left( \frac{1}{2} \Delta X_T' L_T^{xx} \Delta X_T \right) \geq 0 \tag{S.29}$$

due to (S.22) for all  $\{\Delta X_{0:T}, \Delta U_{0:T-1}\}$  satisfying (S.23), therefore

$$\bar{J}(X_{0:T}, U_{0:T-1}) - \bar{J}(X_{0:T}^\theta, U_{0:T-1}^\theta) \geq 0. \tag{S.30}$$

for any feasible trajectory  $\{X_{0:T}, U_{0:T-1}\}$  in (S.24). This concludes that the local unique minimizing trajectory  $\{X_{0:T}^\theta, U_{0:T-1}^\theta\}$  is also a *global* one.

In sum of the two proof steps, the assertion that the trajectory in (4), i.e.,

$$\frac{\partial \xi_\theta}{\partial \theta} = \{X_{0:T}^\theta, U_{0:T-1}^\theta\},$$

is a globally unique minimizing trajectory to the auxiliary control system  $\bar{\Sigma}(\xi_\theta)$  in (3) follows. This completes the proof of Theorem 1. □

## C Proof of Theorem 2

For the unconstrained optimal control system  $\Sigma(\theta, \gamma)$  in (5), we define its Hamiltonian below:

$$\begin{aligned}
\hat{L}_t &= c_t(\mathbf{x}_t, \mathbf{u}_t, \theta) + \lambda'_{t+1} \mathbf{f}(\mathbf{x}_t, \mathbf{u}_t, \theta) - \gamma \sum_{i=1}^{q_t} \ln(-g_{t,i}(\mathbf{x}_t, \mathbf{u}_t, \theta)) + \frac{1}{2\gamma} \sum_{i=1}^{s_t} (h_{t,i}(\mathbf{x}_t, \mathbf{u}_t, \theta))^2 \\
\hat{L}_T &= c_T(\mathbf{x}_T, \theta) - \gamma \sum_{i=1}^{q_T} \ln(-g_{T,i}(\mathbf{x}_T, \theta)) + \frac{1}{2\gamma} \sum_{i=1}^{s_T} (h_{T,i}(\mathbf{x}_T, \theta))^2. \tag{S.31}
\end{aligned}$$

with  $t = 0, 1, \dots, T-1$ .

### C.1 Proof of Claim (a)

We first modify the C-PMP condition (S.5) for the constrained optimal control system  $\Sigma(\theta)$  into the following set of equations:

$$\begin{aligned}
x_{t+1} &= f(x_t, u_t, \theta) \quad \text{and} \quad x_0 = x_0(\theta), \\
\lambda_t &= L_t^x(x_t, u_t, \lambda_{t+1}, v_t, w_t, \theta) \quad \text{and} \quad \lambda_T = L_T^x(x_T, v_T, w_T, \theta), \\
0 &= L_t^u(x_t, u_t, \lambda_{t+1}, v_t, w_t, \theta), \\
h_{t,i}(x_t, u_t, \theta) &= w_{t,i}\gamma, \quad i = 1, 2, \dots, s_t, \\
h_{T,i}(x_T, \theta) &= w_{T,i}\gamma, \quad i = 1, 2, \dots, s_T, \\
v_{t,i} g_{t,i}(x_t, u_t, \theta) &= -\gamma, \quad i = 1, 2, \dots, q_t, \\
v_{T,i} g_{T,i}(x_T, \theta) &= -\gamma, \quad i = 1, 2, \dots, q_T,
\end{aligned} \tag{S.32}$$

where the first three equations are the same with the those in (S.5) and only the last two lines of equations are modified by adding some perturbation terms related to  $\gamma$ .

Now, one can view that the parameters  $(\theta, \gamma)$  jointly determine  $\xi = \{x_{0:T}, u_{0:T-1}\}$ ,  $\lambda_{1:T}$ ,  $v_{0:T}$ , and  $w_{0:T}$  through the implicit equations in (S.32). Also, one can note that by letting  $\gamma = 0$  and  $\theta = \bar{\theta}$ , the above equations in (S.32) coincide with the C-PMP condition (S.5) for  $\Sigma(\bar{\theta})$ . Thus, given that the conditions (i)-(iii) in Lemma 1 hold for  $\Sigma(\bar{\theta})$ , one can readily apply the implicit function theorem [75] to (S.32) in a neighborhood of  $(\bar{\theta}, 0)$  and make the following assertion (its proof can directly follow the proof for Lemma 1 (i.e., the first-order sensitivity result) with little change):

*For any  $(\theta, \gamma)$  within a neighborhood of  $(\bar{\theta}, 0)$ , there exists a unique once-continuously differentiable function  $(\xi_{(\theta,\gamma)}, \lambda_{0:T}^{(\theta,\gamma)}, v_{0:T}^{(\theta,\gamma)}, w_{0:T}^{(\theta,\gamma)})$ , which satisfies (S.32) and*

$$(\xi_{(\theta,\gamma)}, \lambda_{0:T}^{(\theta,\gamma)}, v_{0:T}^{(\theta,\gamma)}, w_{0:T}^{(\theta,\gamma)}) = (\xi_{\bar{\theta}}, \lambda_{1:T}^{\bar{\theta}}, v_{0:T}^{\bar{\theta}}, w_{0:T}^{\bar{\theta}}) \quad \text{when} \quad (\theta, \gamma) = (\bar{\theta}, 0). \tag{S.33}$$

With the above claim, in what follows, we will prove that for any  $(\theta, \gamma)$  near  $(\bar{\theta}, 0)$  additionally with  $\gamma > 0$ ,  $\xi_{(\theta,\gamma)}$  is a local isolated minimizing trajectory to the unconstrained optimal control system  $\Sigma(\theta, \gamma)$  in (5). First, we need to show that such  $\xi_{(\theta,\gamma)}$  will make  $\Sigma(\theta, \gamma)$  well-defined, which is the second part of Claim (a), rewritten below

$$\begin{aligned}
g_{t,i}(x_t^{(\theta,\gamma)}, u_t^{(\theta,\gamma)}, \theta) &< 0, \quad i = 1, 2, \dots, q_t, \quad \text{and} \\
g_{T,i}(x_T^{(\theta,\gamma)}, \theta) &< 0, \quad i = 1, 2, \dots, q_T.
\end{aligned} \tag{S.34}$$

In fact, such an assertion always holds because the strict complementary for  $\Sigma(\bar{\theta})$  from Lemma 1. Specifically, for any  $i = 1, 2, \dots, q_t$ , if  $g_{t,i}(x_t^{\bar{\theta}}, u_t^{\bar{\theta}}, \bar{\theta}) < 0$ , from continuity of  $g_{t,i}$  and  $\xi_{(\theta,\gamma)}$

$$g_{t,i}(x_t^{(\theta,\gamma)}, u_t^{(\theta,\gamma)}, \theta) \rightarrow g_{t,i}(x_t^{\bar{\theta}}, u_t^{\bar{\theta}}, \bar{\theta}) < 0 \quad \text{as} \quad (\theta, \gamma) \rightarrow (\bar{\theta}, 0),$$

thus  $g_{t,i}(x_t^{(\theta,\gamma)}, u_t^{(\theta,\gamma)}, \theta) < 0$  for any  $(\theta, \gamma)$  near  $(\bar{\theta}, 0)$  with  $\gamma > 0$ ; if  $g_{t,i}(x_t^{\bar{\theta}}, u_t^{\bar{\theta}}, \bar{\theta}) = 0$  and  $v_{t,i}^{\bar{\theta}} > 0$  (due to strict complementarity), from continuity of  $v_{t,i}^{(\theta,\gamma)}$ ,

$$v_{t,i}^{(\theta,\gamma)} \rightarrow v_{t,i}^{\bar{\theta}} > 0 \quad \text{as} \quad (\theta, \gamma) \rightarrow (\bar{\theta}, 0), \tag{S.35}$$

thus  $v_{t,i}^{(\theta,\gamma)} > 0$  for  $(\theta, \gamma)$  near  $(\bar{\theta}, 0)$  with  $\gamma > 0$ , and also due to (S.32),  $g_{t,i}(x_t^{(\theta,\gamma)}, u_t^{(\theta,\gamma)}, \theta) = -\frac{\gamma}{v_{t,i}^{(\theta,\gamma)}} < 0$  for  $(\theta, \gamma)$  near  $(\bar{\theta}, 0)$  with  $\gamma > 0$ . So, for either case, the first inequality in (S.34) always holds. Similar proof procedure also applies to prove the second inequality in (S.34). In sum, we conclude that  $\xi_{(\theta,\gamma)}$  satisfies (S.34) and thus makes the  $\Sigma(\theta, \gamma)$  well-defined for any  $(\theta, \gamma)$  near  $(\bar{\theta}, 0)$  with  $\gamma > 0$ . This completes the second part of Claim (a).



From now on, we prove that for any  $(\boldsymbol{\theta}, \gamma)$  near  $(\bar{\boldsymbol{\theta}}, 0)$  with  $\gamma > 0$ ,  $\boldsymbol{\xi}_{(\boldsymbol{\theta}, \gamma)}$  is a local isolated minimizing trajectory to the unconstrained optimal control system  $\Sigma(\boldsymbol{\theta}, \gamma)$  in (5). From the last four equations in (S.32), we solve

$$\begin{aligned} w_{t,i}^{(\boldsymbol{\theta}, \gamma)} &= \frac{h_{t,i}(\mathbf{x}_t^{(\boldsymbol{\theta}, \gamma)}, \mathbf{u}_t^{(\boldsymbol{\theta}, \gamma)}, \boldsymbol{\theta})}{\gamma}, & w_{T,i}^{(\boldsymbol{\theta}, \gamma)} &= \frac{h_{T,i}(\mathbf{x}_T^{(\boldsymbol{\theta}, \gamma)}, \boldsymbol{\theta})}{\gamma}, \\ v_{t,i}^{(\boldsymbol{\theta}, \gamma)} &= -\frac{\gamma}{g_{t,i}(\mathbf{x}_t^{(\boldsymbol{\theta}, \gamma)}, \mathbf{u}_t^{(\boldsymbol{\theta}, \gamma)}, \boldsymbol{\theta})}, & v_{T,i}^{(\boldsymbol{\theta}, \gamma)} &= -\frac{\gamma}{g_{T,i}(\mathbf{x}_T^{(\boldsymbol{\theta}, \gamma)}, \boldsymbol{\theta})}, \end{aligned} \quad (\text{S.36})$$

and plug them into the first three equations in (S.32), then one will find that the obtained equations are exactly the Pontryagin Maximum/Minimum Principle (PMP) for the unconstrained optimal control system  $\Sigma(\boldsymbol{\theta}, \gamma)$  with its Hamiltonian already defined in (S.31), that is to say,

$$\begin{aligned} \mathbf{x}_{t+1}^{(\boldsymbol{\theta}, \gamma)} &= \mathbf{f}(\mathbf{x}_t^{(\boldsymbol{\theta}, \gamma)}, \mathbf{u}_t^{(\boldsymbol{\theta}, \gamma)}, \boldsymbol{\theta}) \quad \text{and} \quad \mathbf{x}_0^{(\boldsymbol{\theta}, \gamma)} = \mathbf{x}_0(\boldsymbol{\theta}), \\ \boldsymbol{\lambda}_t^{(\boldsymbol{\theta}, \gamma)} &= \hat{L}_t^x(\mathbf{x}_t^{(\boldsymbol{\theta}, \gamma)}, \mathbf{u}_t^{(\boldsymbol{\theta}, \gamma)}, \boldsymbol{\lambda}_{t+1}^{(\boldsymbol{\theta}, \gamma)}, (\boldsymbol{\theta}, \gamma)), \\ \boldsymbol{\lambda}_T^{(\boldsymbol{\theta}, \gamma)} &= \hat{L}_T^x(\mathbf{x}_T^{(\boldsymbol{\theta}, \gamma)}, (\boldsymbol{\theta}, \gamma)), \\ 0 &= \hat{L}_t^u(\mathbf{x}_t^{(\boldsymbol{\theta}, \gamma)}, \mathbf{u}_t^{(\boldsymbol{\theta}, \gamma)}, \boldsymbol{\lambda}_{t+1}^{(\boldsymbol{\theta}, \gamma)}, (\boldsymbol{\theta}, \gamma)), \end{aligned} \quad (\text{S.37})$$

indicating that  $\boldsymbol{\xi}_{(\boldsymbol{\theta}, \gamma)} = \{\mathbf{x}_{0:T}^{(\boldsymbol{\theta}, \gamma)}, \mathbf{u}_{0:T-1}^{(\boldsymbol{\theta}, \gamma)}\}$  already satisfies the PMP condition for unconstrained optimal control system  $\Sigma(\boldsymbol{\theta}, \gamma)$ . To show  $\boldsymbol{\xi}_{(\boldsymbol{\theta}, \gamma)} = \{\mathbf{x}_{0:T}^{(\boldsymbol{\theta}, \gamma)}, \mathbf{u}_{0:T-1}^{(\boldsymbol{\theta}, \gamma)}\}$  is a local isolated minimizing trajectory to  $\Sigma(\boldsymbol{\theta}, \gamma)$  for any  $(\boldsymbol{\theta}, \gamma)$  near  $(\bar{\boldsymbol{\theta}}, 0)$  with  $\gamma > 0$ , we only need to verify its second-order condition as stated in (S.6)-(S.7) in Lemma A.2, which is presented next. In the remainder of proof, for convenience of notation, all derivatives are evaluated at  $(\boldsymbol{\theta}, \gamma)$  (or  $\boldsymbol{\xi}_{(\boldsymbol{\theta}, \gamma)}$ ) unless otherwise stated.

Before proceeding, we show two facts (easy to prove) about the second-order derivatives of Hamiltonian  $\hat{L}_t$  and  $\hat{L}_T$  in (S.31). First,

$$\begin{aligned} \begin{bmatrix} \hat{L}_t^{xx} & \hat{L}_t^{xu} \\ \hat{L}_t^{ux} & \hat{L}_t^{uu} \end{bmatrix} &= \begin{bmatrix} L_t^{xx} & L_t^{xu} \\ L_t^{ux} & L_t^{uu} \end{bmatrix} + \\ &\begin{bmatrix} \sum_{i=1}^{q_t} \frac{\gamma}{g_{t,i}^2} \frac{\partial g'_{t,i}}{\partial \mathbf{x}_t} \frac{\partial g_{t,i}}{\partial \mathbf{x}_t} + \sum_{i=1}^{s_t} \frac{1}{\gamma} \frac{\partial h'_{t,i}}{\partial \mathbf{x}_t} \frac{\partial h_{t,i}}{\partial \mathbf{x}_t} & \sum_{i=1}^{q_t} \frac{\gamma}{g_{t,i}^2} \frac{\partial g'_{t,i}}{\partial \mathbf{x}_t} \frac{\partial g_{t,i}}{\partial \mathbf{u}_t} + \sum_{i=1}^{s_t} \frac{1}{\gamma} \frac{\partial h'_{t,i}}{\partial \mathbf{x}_t} \frac{\partial h_{t,i}}{\partial \mathbf{u}_t} \\ \sum_{i=1}^{q_t} \frac{\gamma}{g_{t,i}^2} \frac{\partial g'_{t,i}}{\partial \mathbf{u}_t} \frac{\partial g_{t,i}}{\partial \mathbf{x}_t} + \sum_{i=1}^{s_t} \frac{1}{\gamma} \frac{\partial h'_{t,i}}{\partial \mathbf{u}_t} \frac{\partial h_{t,i}}{\partial \mathbf{x}_t} & \sum_{i=1}^{q_t} \frac{\gamma}{g_{t,i}^2} \frac{\partial g'_{t,i}}{\partial \mathbf{u}_t} \frac{\partial g_{t,i}}{\partial \mathbf{u}_t} + \sum_{i=1}^{s_t} \frac{1}{\gamma} \frac{\partial h'_{t,i}}{\partial \mathbf{u}_t} \frac{\partial h_{t,i}}{\partial \mathbf{u}_t} \end{bmatrix}, \end{aligned} \quad (\text{S.38})$$

and

$$\hat{L}_T^{xx} = L_T^{xx} + \sum_{i=1}^{q_T} \frac{\gamma}{g_{T,i}^2} \frac{\partial g'_{T,i}}{\partial \mathbf{x}_T} \frac{\partial g_{T,i}}{\partial \mathbf{x}_T} + \sum_{i=1}^{s_T} \frac{1}{\gamma} \frac{\partial h'_{T,i}}{\partial \mathbf{x}_T} \frac{\partial h_{T,i}}{\partial \mathbf{x}_T}, \quad (\text{S.39})$$

respectively. Second, given any  $\mathbf{x}$  and  $\mathbf{u}$  with appropriate dimensions, one has

$$\begin{aligned} \begin{bmatrix} \mathbf{x} \\ \mathbf{u} \end{bmatrix}' \begin{bmatrix} \hat{L}_t^{xx} & \hat{L}_t^{xu} \\ \hat{L}_t^{ux} & \hat{L}_t^{uu} \end{bmatrix} \begin{bmatrix} \mathbf{x} \\ \mathbf{u} \end{bmatrix} &= \begin{bmatrix} \mathbf{x} \\ \mathbf{u} \end{bmatrix}' \begin{bmatrix} L_t^{xx} & L_t^{xu} \\ L_t^{ux} & L_t^{uu} \end{bmatrix} \begin{bmatrix} \mathbf{x} \\ \mathbf{u} \end{bmatrix} + \\ &\begin{bmatrix} \mathbf{x} \\ \mathbf{u} \end{bmatrix}' \begin{bmatrix} \sum_{i=1}^{q_t} \frac{\gamma}{g_{t,i}^2} \frac{\partial g'_{t,i}}{\partial \mathbf{x}_t} \frac{\partial g_{t,i}}{\partial \mathbf{x}_t} + \sum_{i=1}^{s_t} \frac{1}{\gamma} \frac{\partial h'_{t,i}}{\partial \mathbf{x}_t} \frac{\partial h_{t,i}}{\partial \mathbf{x}_t} & \sum_{i=1}^{q_t} \frac{\gamma}{g_{t,i}^2} \frac{\partial g'_{t,i}}{\partial \mathbf{x}_t} \frac{\partial g_{t,i}}{\partial \mathbf{u}_t} + \sum_{i=1}^{s_t} \frac{1}{\gamma} \frac{\partial h'_{t,i}}{\partial \mathbf{x}_t} \frac{\partial h_{t,i}}{\partial \mathbf{u}_t} \\ \sum_{i=1}^{q_t} \frac{\gamma}{g_{t,i}^2} \frac{\partial g'_{t,i}}{\partial \mathbf{u}_t} \frac{\partial g_{t,i}}{\partial \mathbf{x}_t} + \sum_{i=1}^{s_t} \frac{1}{\gamma} \frac{\partial h'_{t,i}}{\partial \mathbf{u}_t} \frac{\partial h_{t,i}}{\partial \mathbf{x}_t} & \sum_{i=1}^{q_t} \frac{\gamma}{g_{t,i}^2} \frac{\partial g'_{t,i}}{\partial \mathbf{u}_t} \frac{\partial g_{t,i}}{\partial \mathbf{u}_t} + \sum_{i=1}^{s_t} \frac{1}{\gamma} \frac{\partial h'_{t,i}}{\partial \mathbf{u}_t} \frac{\partial h_{t,i}}{\partial \mathbf{u}_t} \end{bmatrix} \begin{bmatrix} \mathbf{x} \\ \mathbf{u} \end{bmatrix} \\ &= \begin{bmatrix} \mathbf{x} \\ \mathbf{u} \end{bmatrix}' \begin{bmatrix} L_t^{xx} & L_t^{xu} \\ L_t^{ux} & L_t^{uu} \end{bmatrix} \begin{bmatrix} \mathbf{x} \\ \mathbf{u} \end{bmatrix} + \sum_{i=1}^{q_t} \frac{\gamma}{g_{t,i}^2} \left( \frac{\partial g_{t,i}}{\partial \mathbf{x}_t} \mathbf{x} + \frac{\partial g_{t,i}}{\partial \mathbf{u}_t} \mathbf{u} \right)^2 + \sum_{i=1}^{s_t} \frac{1}{\gamma} \left( \frac{\partial h_{t,i}}{\partial \mathbf{x}_t} \mathbf{x} + \frac{\partial h_{t,i}}{\partial \mathbf{u}_t} \mathbf{u} \right)^2, \end{aligned} \quad (\text{S.40})$$

and

$$\begin{aligned} \mathbf{x}' \hat{L}_T^{xx} \mathbf{x} &= \mathbf{x}' L_T^{xx} \mathbf{x} + \mathbf{x}' \left( \sum_{i=1}^{q_T} \frac{\gamma}{g_{T,i}^2} \frac{\partial g'_{T,i}}{\partial \mathbf{x}_T} \frac{\partial g_{T,i}}{\partial \mathbf{x}_T} + \sum_{i=1}^{s_T} \frac{1}{\gamma} \frac{\partial h'_{T,i}}{\partial \mathbf{x}_T} \frac{\partial h_{T,i}}{\partial \mathbf{x}_T} \right) \mathbf{x} \\ &= \mathbf{x}' L_T^{xx} \mathbf{x} + \sum_{i=1}^{q_T} \frac{\gamma}{g_{T,i}^2} \left( \frac{\partial g_{T,i}}{\partial \mathbf{x}_T} \mathbf{x} \right)^2 + \sum_{i=1}^{s_T} \frac{1}{\gamma} \left( \frac{\partial h_{T,i}}{\partial \mathbf{x}_T} \mathbf{x} \right)^2. \end{aligned} \quad (\text{S.41})$$

For the second-order condition of the unconstrained optimal control system  $\Sigma(\boldsymbol{\theta}, \gamma)$  with any  $(\boldsymbol{\theta}, \gamma)$  near  $(\bar{\boldsymbol{\theta}}, 0)$  with  $\gamma > 0$ , we need to prove that

$$\sum_{t=0}^{T-1} \begin{bmatrix} \mathbf{x}_t \\ \mathbf{u}_t \end{bmatrix}' \begin{bmatrix} \hat{L}_t^{xx}(\boldsymbol{\theta}, \gamma) & \hat{L}_t^{xu}(\boldsymbol{\theta}, \gamma) \\ \hat{L}_t^{ux}(\boldsymbol{\theta}, \gamma) & \hat{L}_t^{uu}(\boldsymbol{\theta}, \gamma) \end{bmatrix} \begin{bmatrix} \mathbf{x}_t \\ \mathbf{u}_t \end{bmatrix} + \mathbf{x}_T' \hat{L}_T^{xx}(\boldsymbol{\theta}, \gamma) \mathbf{x}_T > 0, \quad (\text{S.42})$$

for any  $\{\mathbf{x}_{0:T}, \mathbf{u}_{0:T-1}\} \neq \mathbf{0}$  satisfying

$$\mathbf{x}_{t+1} = F_t^x(\boldsymbol{\theta}, \gamma) \mathbf{x}_t + F_t^u(\boldsymbol{\theta}, \gamma) \mathbf{u}_t \quad \text{and} \quad \mathbf{x}_0 = \mathbf{0}. \quad (\text{S.43})$$

Here, for convenience, the dependence in  $F_t^x(\boldsymbol{\theta}, \gamma)$ ,  $F_t^u(\boldsymbol{\theta}, \gamma)$ ,  $H_t^{xx}(\boldsymbol{\theta}, \gamma)$ ,  $H_t^{xu}(\boldsymbol{\theta}, \gamma)$ ,  $H_t^{uu}(\boldsymbol{\theta}, \gamma)$ , and  $H_T^{xx}(\boldsymbol{\theta}, \gamma)$  means that these first- and second-order derivatives are evaluated at trajectory  $\boldsymbol{\xi}_{(\boldsymbol{\theta}, \gamma)}$  (the same notation convention applies below).

Proof by contradiction: suppose that the above second-order condition in (S.42)-(S.43) is false. Then, there must exist a sequence of parameters  $(\boldsymbol{\theta}^k, \gamma^k)$  with  $\gamma^k > 0$  and a sequence of trajectories  $\{\mathbf{x}_{0:T}^k, \mathbf{u}_{0:T-1}^k\} \neq \mathbf{0}$  such that  $(\boldsymbol{\theta}^k, \gamma^k) \rightarrow (\bar{\boldsymbol{\theta}}, 0)$ ,  $\mathbf{x}_{t+1}^k = F_t^x(\boldsymbol{\theta}^k, \gamma^k) \mathbf{x}_t^k + F_t^u(\boldsymbol{\theta}^k, \gamma^k) \mathbf{u}_t^k$  with  $\mathbf{x}_0^k = \mathbf{0}$ , and

$$\sum_{t=0}^{T-1} \begin{bmatrix} \mathbf{x}_t^k \\ \mathbf{u}_t^k \end{bmatrix}' \begin{bmatrix} \hat{L}_t^{xx}(\boldsymbol{\theta}^k, \gamma^k) & \hat{L}_t^{xu}(\boldsymbol{\theta}^k, \gamma^k) \\ \hat{L}_t^{ux}(\boldsymbol{\theta}^k, \gamma^k) & \hat{L}_t^{uu}(\boldsymbol{\theta}^k, \gamma^k) \end{bmatrix} \begin{bmatrix} \mathbf{x}_t^k \\ \mathbf{u}_t^k \end{bmatrix} + \mathbf{x}_T^k' \hat{L}_T^{xx}(\boldsymbol{\theta}^k, \gamma^k) \mathbf{x}_T^k \leq 0, \quad (\text{S.44})$$

for  $k = 1, 2, 3, \dots$ . Here, the dependence  $(\boldsymbol{\theta}^k, \gamma^k)$  means that these first- and second-order derivatives are evaluated at trajectory  $\boldsymbol{\xi}_{(\boldsymbol{\theta}^k, \gamma^k)}$  for notation convenience. Without loss of generality, assume  $\|\text{col}\{\mathbf{x}_{0:T}^k, \mathbf{u}_{0:T-1}^k\}\| = 1$  for all  $k$ . Select a convergent sub-sequence  $\{\mathbf{x}_{0:T}^k, \mathbf{u}_{0:T-1}^k\}$ , relabel the sequence  $\{\mathbf{x}_{0:T}^k, \mathbf{u}_{0:T-1}^k\}$  for convenience, and call its limit  $\{\mathbf{x}_{0:T}^*, \mathbf{u}_{0:T-1}^*\}$ , that is,  $\{\mathbf{x}_{0:T}^k, \mathbf{u}_{0:T-1}^k\} \rightarrow \{\mathbf{x}_{0:T}^*, \mathbf{u}_{0:T-1}^*\}$  and  $(\boldsymbol{\theta}^k, \gamma^k) \rightarrow (\bar{\boldsymbol{\theta}}, 0)$  as  $k \rightarrow +\infty$  and  $\mathbf{x}_{t+1}^* = F_t^x(\bar{\boldsymbol{\theta}}, 0) \mathbf{x}_t^* + F_t^u(\bar{\boldsymbol{\theta}}, 0) \mathbf{u}_t^*$  with  $\mathbf{x}_0^* = \mathbf{0}$ . Then, the limit  $\{\mathbf{x}_{0:T}^*, \mathbf{u}_{0:T-1}^*\}$  must fall into either of two cases discussed below.

Case 1:  $\|\text{col}\{\mathbf{x}_{0:T}^*, \mathbf{u}_{0:T-1}^*\}\| = 1$  and at least one of the following holds:

$$\begin{aligned} \bar{G}_t^x(\bar{\boldsymbol{\theta}}, 0) \mathbf{x}_t^* + \bar{G}_t^u(\bar{\boldsymbol{\theta}}, 0) \mathbf{u}_t^* \neq \mathbf{0} \quad \exists t \quad \text{or} \quad H_t^x(\bar{\boldsymbol{\theta}}, 0) \mathbf{x}_t^* + H_t^u(\bar{\boldsymbol{\theta}}, 0) \mathbf{u}_t^* \neq \mathbf{0} \quad \exists t \\ \text{or} \quad \bar{G}_T^x(\bar{\boldsymbol{\theta}}, 0) \mathbf{x}_T^* \neq \mathbf{0} \quad \text{or} \quad H_T^x(\bar{\boldsymbol{\theta}}, 0) \mathbf{x}_T^* \neq \mathbf{0}. \end{aligned} \quad (\text{S.45})$$

In this case, as  $k \rightarrow 0$ ,  $\{\mathbf{x}_{0:T}^k, \mathbf{u}_{0:T-1}^k\} \rightarrow \{\mathbf{x}_{0:T}^*, \mathbf{u}_{0:T-1}^*\}$ ,  $(\boldsymbol{\theta}^k, \gamma^k) \rightarrow (\bar{\boldsymbol{\theta}}, 0)$ , we will have

$$\begin{aligned} \sum_{t=0}^{T-1} \left( \sum_{i=1}^{q_t} \frac{\gamma^k}{(g_{t,i}^k)^2} \left( \frac{\partial g_{t,i}^k}{\partial \mathbf{x}_t} \mathbf{x}_t^k + \frac{\partial g_{t,i}^k}{\partial \mathbf{u}_t^k} \mathbf{u}_t^k \right)^2 + \sum_{i=1}^{s_t} \frac{1}{\gamma^k} \left( \frac{\partial h_{t,i}^k}{\partial \mathbf{x}_t^k} \mathbf{x}_t^k + \frac{\partial h_{t,i}^k}{\partial \mathbf{u}_t^k} \mathbf{u}_t^k \right)^2 \right) \\ + \sum_{i=1}^{q_T} \frac{\gamma^k}{(g_{T,i}^k)^2} \left( \frac{\partial g_{T,i}^k}{\partial \mathbf{x}_T} \mathbf{x}_T^k \right)^2 + \sum_{i=1}^{s_T} \frac{1}{\gamma^k} \left( \frac{\partial h_{T,i}^k}{\partial \mathbf{x}_T} \mathbf{x}_T^k \right)^2 \rightarrow +\infty, \end{aligned} \quad (\text{S.46})$$

where  $\frac{\partial g_{t,i}^k}{\partial \mathbf{x}_t}$ ,  $\frac{\partial g_{T,i}^k}{\partial \mathbf{x}_T}$ ,  $g_{t,i}^k$ ,  $g_{T,i}^k$ ,  $\frac{\partial h_{t,i}^k}{\partial \mathbf{x}_t}$ ,  $\frac{\partial h_{T,i}^k}{\partial \mathbf{x}_T}$  are with superscript  $k$  to denote their values are evaluated at  $\boldsymbol{\xi}_{(\boldsymbol{\theta}^k, \gamma^k)}$  for notation convenience. (S.46) is because at least one of the terms in the summation is  $+\infty$ . Here, we have used the following facts from the last two equations in (S.32):

$$\frac{\gamma}{(g_{t,i}(\mathbf{x}_t^{(\boldsymbol{\theta}, \gamma)}, \mathbf{u}_t^{(\boldsymbol{\theta}, \gamma)}, \boldsymbol{\theta}))^2} = -\frac{v_{t,i}^{(\boldsymbol{\theta}, \gamma)}}{g_{t,i}(\mathbf{x}_t^{(\boldsymbol{\theta}, \gamma)}, \mathbf{u}_t^{(\boldsymbol{\theta}, \gamma)}, \boldsymbol{\theta})} \rightarrow 0 \quad \text{or} \quad \rightarrow +\infty \quad \text{as} \quad (\boldsymbol{\theta}, \gamma) \rightarrow (\bar{\boldsymbol{\theta}}, 0),$$

where  $\rightarrow 0$  corresponds to the inactive inequalities  $g_{t,i}(\mathbf{x}_t^{\bar{\boldsymbol{\theta}}}, \mathbf{u}_t^{\bar{\boldsymbol{\theta}}}, \bar{\boldsymbol{\theta}}) < 0$  and  $\rightarrow +\infty$  corresponds to the active inequalities  $g_{t,i}(\mathbf{x}_t^{\bar{\boldsymbol{\theta}}}, \mathbf{u}_t^{\bar{\boldsymbol{\theta}}}, \bar{\boldsymbol{\theta}}) = 0$  ( $v_{t,i}^{\bar{\boldsymbol{\theta}}} > 0$  due to strict complementarity); and also

$$\frac{\gamma}{(g_{T,i}(\mathbf{x}_T^{(\boldsymbol{\theta}, \gamma)}, \boldsymbol{\theta}))^2} = -\frac{v_{T,i}^{(\boldsymbol{\theta}, \gamma)}}{g_{T,i}(\mathbf{x}_T^{(\boldsymbol{\theta}, \gamma)}, \boldsymbol{\theta})} \rightarrow 0 \quad \text{or} \quad \rightarrow +\infty \quad \text{as} \quad (\boldsymbol{\theta}, \gamma) \rightarrow (\bar{\boldsymbol{\theta}}, 0).$$

where  $\rightarrow 0$  corresponds to the inactive inequalities  $g_{T,i}(\mathbf{x}_T^{\bar{\boldsymbol{\theta}}}, \bar{\boldsymbol{\theta}}) < 0$  and  $\rightarrow +\infty$  corresponds to the active inequalities  $g_{T,i}(\mathbf{x}_T^{\bar{\boldsymbol{\theta}}}, \bar{\boldsymbol{\theta}}) = 0$  ( $v_{T,i}^{\bar{\boldsymbol{\theta}}} > 0$  due to strict complementarity).

By extending the left side of (S.44) based on the facts (S.40) and (S.41), (S.46) immediately leads to

$$\lim_{k \rightarrow +\infty} \left( \sum_{t=0}^{T-1} \begin{bmatrix} \mathbf{x}_t^k \\ \mathbf{u}_t^k \end{bmatrix}' \begin{bmatrix} \hat{L}_t^{xx}(\boldsymbol{\theta}^k, \gamma^k) & \hat{L}_t^{xu}(\boldsymbol{\theta}^k, \gamma^k) \\ \hat{L}_t^{ux}(\boldsymbol{\theta}^k, \gamma^k) & \hat{L}_t^{uu}(\boldsymbol{\theta}^k, \gamma^k) \end{bmatrix} \begin{bmatrix} \mathbf{x}_t^k \\ \mathbf{u}_t^k \end{bmatrix} + \mathbf{x}_T^k{}' \hat{L}_T^{xx}(\boldsymbol{\theta}^k, \gamma^k) \mathbf{x}_T^k \right) \rightarrow +\infty, \quad (\text{S.47})$$

which obviously contradicts (S.44).

Case 2:  $\|\text{col}\{\mathbf{x}_{0:T}^*, \mathbf{u}_{0:T-1}^*\}\| = 1$  and all of the following holds:

$$\begin{aligned} \bar{G}_t^x(\bar{\boldsymbol{\theta}}, 0) \mathbf{x}_t^* + \bar{G}_t^u(\bar{\boldsymbol{\theta}}, 0) \mathbf{u}_t^* &= \mathbf{0} \quad \forall t \quad \text{and} \quad H_t^x(\bar{\boldsymbol{\theta}}, 0) \mathbf{x}_t^* + H_t^u(\bar{\boldsymbol{\theta}}, 0) \mathbf{u}_t^* = \mathbf{0} \quad \forall t \\ \text{and} \quad \bar{G}_T^x(\bar{\boldsymbol{\theta}}, 0) \mathbf{x}_T^* &= \mathbf{0} \quad \text{and} \quad H_T^x(\bar{\boldsymbol{\theta}}, 0) \mathbf{x}_T^* = \mathbf{0}. \end{aligned} \quad (\text{S.48})$$

In this case, we have

$$\begin{aligned} &\lim_{k \rightarrow +\infty} \left( \sum_{t=0}^{T-1} \begin{bmatrix} \mathbf{x}_t^k \\ \mathbf{u}_t^k \end{bmatrix}' \begin{bmatrix} \hat{L}_t^{xx}(\boldsymbol{\theta}^k, \gamma^k) & \hat{L}_t^{xu}(\boldsymbol{\theta}^k, \gamma^k) \\ \hat{L}_t^{ux}(\boldsymbol{\theta}^k, \gamma^k) & \hat{L}_t^{uu}(\boldsymbol{\theta}^k, \gamma^k) \end{bmatrix} \begin{bmatrix} \mathbf{x}_t^k \\ \mathbf{u}_t^k \end{bmatrix} + \mathbf{x}_T^k{}' \hat{L}_T^{xx}(\boldsymbol{\theta}^k, \gamma^k) \mathbf{x}_T^k \right) \\ &\geq \lim_{k \rightarrow +\infty} \left( \sum_{t=0}^{T-1} \begin{bmatrix} \mathbf{x}_t^k \\ \mathbf{u}_t^k \end{bmatrix}' \begin{bmatrix} L_t^{xx}(\boldsymbol{\theta}^k, \gamma^k) & L_t^{xu}(\boldsymbol{\theta}^k, \gamma^k) \\ L_t^{ux}(\boldsymbol{\theta}^k, \gamma^k) & L_t^{uu}(\boldsymbol{\theta}^k, \gamma^k) \end{bmatrix} \begin{bmatrix} \mathbf{x}_t^k \\ \mathbf{u}_t^k \end{bmatrix} + \mathbf{x}_T^k{}' L_T^{xx}(\boldsymbol{\theta}^k, \gamma^k) \mathbf{x}_T^k \right) \\ &= \sum_{t=0}^{T-1} \begin{bmatrix} \mathbf{x}_t^* \\ \mathbf{u}_t^* \end{bmatrix}' \begin{bmatrix} L_t^{xx}(\bar{\boldsymbol{\theta}}, 0) & L_t^{xu}(\bar{\boldsymbol{\theta}}, 0) \\ L_t^{ux}(\bar{\boldsymbol{\theta}}, 0) & L_t^{uu}(\bar{\boldsymbol{\theta}}, 0) \end{bmatrix} \begin{bmatrix} \mathbf{x}_t^* \\ \mathbf{u}_t^* \end{bmatrix} + \mathbf{x}_T^*{}' L_T^{xx}(\bar{\boldsymbol{\theta}}, 0) \mathbf{x}_T^* > 0. \end{aligned} \quad (\text{S.49})$$

Here, the first inequality is based on the fact that the residual term is always non-negative, i.e.,

$$\begin{aligned} &\sum_{t=0}^{T-1} \left( \sum_{i=1}^{q_t} \frac{\gamma^k}{(g_{t,i}^k)^2} \left( \frac{\partial g_{t,i}^k}{\partial \mathbf{x}_t} \mathbf{x}_t^k + \frac{\partial g_{t,i}^k}{\partial \mathbf{u}_t^k} \mathbf{u}_t^k \right)^2 + \sum_{i=1}^{s_t} \frac{1}{\gamma^k} \left( \frac{\partial h_{t,i}^k}{\partial \mathbf{x}_t^k} \mathbf{x}_t^k + \frac{\partial h_{t,i}^k}{\partial \mathbf{u}_t^k} \mathbf{u}_t^k \right)^2 \right) \\ &\quad + \sum_{i=1}^{q_T} \frac{\gamma^k}{(g_{T,i}^k)^2} \left( \frac{\partial g_{T,i}^k}{\partial \mathbf{x}_T} \mathbf{x}_T^k \right)^2 + \sum_{i=1}^{s_T} \frac{1}{\gamma^k} \left( \frac{\partial h_{T,i}^k}{\partial \mathbf{x}_T} \mathbf{x}_T^k \right)^2 \geq 0, \end{aligned} \quad (\text{S.50})$$

the last inequality is directly from the second-order condition in (S.6)-(S.7) in Lemma A.2. Obviously, (S.49) also contracts (S.44).

Combining the above two cases, we can conclude that for any  $(\boldsymbol{\theta}, \gamma)$  near  $(\bar{\boldsymbol{\theta}}, 0)$  with  $\gamma > 0$ , the trajectory  $\boldsymbol{\xi}_{(\boldsymbol{\theta}, \gamma)}$  to the unconstrained optimal control system  $\Sigma(\boldsymbol{\theta}, \gamma)$  satisfies both its PMP condition in (S.31) and the second-order condition in (S.42)-(S.43). Thus, one can assert that  $\boldsymbol{\xi}_{(\boldsymbol{\theta}, \gamma)}$  is a local isolated minimizing trajectory to  $\Sigma(\boldsymbol{\theta}, \gamma)$ . This completes the proof of Claim (a) in Theorem 2.

## C.2 Proof of Claim (b)

Given that the conditions (i)-(iii) in Lemma 1 hold for  $\Sigma(\bar{\boldsymbol{\theta}})$ , we have the following conclusions:

(1) From Claim (a) and its proof, we know that for any  $(\boldsymbol{\theta}, \gamma)$  in the neighborhood of  $(\bar{\boldsymbol{\theta}}, 0)$ , there exists a unique once-continuously differentiable function  $(\boldsymbol{\xi}_{(\boldsymbol{\theta}, \gamma)}, \boldsymbol{\lambda}_{0:T}^{(\boldsymbol{\theta}, \gamma)}, \mathbf{v}_{0:T}^{(\boldsymbol{\theta}, \gamma)}, \mathbf{w}_{0:T}^{(\boldsymbol{\theta}, \gamma)})$ , which satisfies (S.32). Additionally provided  $\gamma > 0$ , such  $\boldsymbol{\xi}_{(\boldsymbol{\theta}, \gamma)}$  is also a local isolated minimizing trajectory for the well-defined unconstrained optimal control system  $\Sigma(\boldsymbol{\theta}, \gamma)$ .

(2) Additionally let  $\gamma = 0$  in (S.32), and (S.32) becomes the C-PMP condition for the constrained optimal control system  $\Sigma(\boldsymbol{\theta})$ . From Lemma 1, for any  $\boldsymbol{\theta}$  near  $\bar{\boldsymbol{\theta}}$ ,  $\boldsymbol{\xi}_{\boldsymbol{\theta}} = \boldsymbol{\xi}_{(\boldsymbol{\theta}, \gamma=0)}$  is a differentiable local isolated minimizing trajectory for  $\Sigma(\boldsymbol{\theta})$ , associated with the unique once-continuously differentiable function  $(\boldsymbol{\lambda}_{1:T}^{(\boldsymbol{\theta}, \gamma=0)}, \mathbf{v}_{0:T}^{(\boldsymbol{\theta}, \gamma=0)}, \mathbf{w}_{0:T}^{(\boldsymbol{\theta}, \gamma=0)})$ .

Therefore, due to the uniqueness and once-continuous differentiability of  $\boldsymbol{\xi}_{(\boldsymbol{\theta}, \gamma)}$  with respect to  $(\boldsymbol{\theta}, \gamma)$  near  $(\bar{\boldsymbol{\theta}}, 0)$ , one can obtain

$$\boldsymbol{\xi}_{(\boldsymbol{\theta}, \gamma)} \rightarrow \boldsymbol{\xi}_{(\boldsymbol{\theta}, 0)} = \boldsymbol{\xi}_{\boldsymbol{\theta}} \quad \text{as} \quad \gamma \rightarrow 0, \quad (\text{S.51})$$

and

$$\frac{\partial \boldsymbol{\xi}_{(\boldsymbol{\theta}, \gamma)}}{\partial \boldsymbol{\theta}} \rightarrow \frac{\partial \boldsymbol{\xi}_{(\boldsymbol{\theta}, 0)}}{\partial \boldsymbol{\theta}} = \frac{\boldsymbol{\xi}_{\boldsymbol{\theta}}}{\partial \boldsymbol{\theta}} \quad \text{as } \gamma \rightarrow 0. \quad (\text{S.52})$$

Here (S.51) is due to that  $\boldsymbol{\xi}_{(\boldsymbol{\theta}, \gamma)}$  is unique and continuous at  $(\boldsymbol{\theta}, \gamma = 0)$ , and (S.51) is because  $\boldsymbol{\xi}_{(\boldsymbol{\theta}, \gamma)}$  is unique and once-continuously differentiable at  $(\boldsymbol{\theta}, \gamma = 0)$ . This completes the proof of Claim (b) in Theorem 2.

### C.3 Proof of Claim (c)

For the unconstrained optimal control system  $\boldsymbol{\Sigma}(\boldsymbol{\theta}, \gamma)$  with any  $(\boldsymbol{\theta}, \gamma)$  near  $(\bar{\boldsymbol{\theta}}, 0)$ ,  $\gamma > 0$ , in order to show that its trajectory derivative  $\frac{\partial \boldsymbol{\xi}_{(\boldsymbol{\theta}, \gamma)}}{\partial \boldsymbol{\theta}}$  is a globally unique minimizing trajectory to its corresponding auxiliary control system  $\bar{\boldsymbol{\Sigma}}(\boldsymbol{\xi}_{(\boldsymbol{\theta}, \gamma)})$ , similarly to the claim of Theorem 1, we need to verify if the following three conditions hold for  $\boldsymbol{\Sigma}(\boldsymbol{\theta}, \gamma)$  at  $(\boldsymbol{\theta}, \gamma)$ .

- (i) The second-order condition holds for  $\boldsymbol{\xi}_{(\boldsymbol{\theta}, \gamma)}$  to be a local isolated minimizing trajectory for  $\boldsymbol{\Sigma}(\boldsymbol{\theta}, \gamma)$ . In fact, this has been proved in the proof of Claim (a).
- (ii) The gradients of all binding constraints (i.e., all equality and active inequality constraints) are linearly independent at  $\boldsymbol{\xi}_{(\boldsymbol{\theta}, \gamma)}$ . Since we do not have inequality constraints in  $\boldsymbol{\Sigma}(\boldsymbol{\theta}, \gamma)$ , we only need to show the gradients of the dynamics constraint are linearly independent at  $\boldsymbol{\xi}_{(\boldsymbol{\theta}, \gamma)}$ . Specifically, we need to show that the following linear equations are independent

$$\boldsymbol{x}_{t+1} = F_t^x(\boldsymbol{\theta}, \gamma)\boldsymbol{x}_t + F_t^u(\boldsymbol{\theta}, \gamma)\boldsymbol{u}_t, \quad \text{and} \quad \boldsymbol{x}_0 = \mathbf{0}, \quad t = 0, 1, \dots, T. \quad (\text{S.53})$$

where the dependence  $(\boldsymbol{\theta}, \gamma)$  means that the derivative matrices are evaluated at trajectory  $\boldsymbol{\xi}_{(\boldsymbol{\theta}, \gamma)}$ ,  $\boldsymbol{x}_{0:T}$  and  $\boldsymbol{u}_{0:T-1}$  here are variables. In fact, the above linear equations in (S.53) can be equivalently written as

$$\boldsymbol{F}_x \boldsymbol{x}_{1:T} + \boldsymbol{F}_u \boldsymbol{u}_{0:T-1} = \mathbf{0}, \quad (\text{S.54})$$

with

$$\boldsymbol{F}_u = \begin{bmatrix} -F_0^u(\boldsymbol{\theta}, \gamma) & 0 & \cdots & 0 \\ 0 & -F_1^u(\boldsymbol{\theta}, \gamma) & \cdots & 0 \\ \vdots & \vdots & \ddots & \vdots \\ 0 & 0 & \cdots & -F_{T-1}^x(\boldsymbol{\theta}, \gamma) \end{bmatrix}, \quad (\text{S.55})$$

and

$$\boldsymbol{F}_x = \begin{bmatrix} I & 0 & \cdots & 0 & 0 \\ -F_1^x(\boldsymbol{\theta}, \gamma) & I & \cdots & 0 & 0 \\ \vdots & \vdots & \ddots & \vdots & \vdots \\ 0 & 0 & \cdots & I & 0 \\ 0 & 0 & \cdots & -F_{T-1}^x(\boldsymbol{\theta}, \gamma) & I \end{bmatrix}. \quad (\text{S.56})$$

Obviously, all rows in the concatenation matrix  $[\boldsymbol{F}_u, \boldsymbol{F}_x]$  are linear-independent because  $[\boldsymbol{F}_u, \boldsymbol{F}_x]$  is already in its the reduced echelon form and has full row rank. Thus, one can conclude that the linear equations in (S.53) are linearly independent.

- (iii) Strict complementarity does not apply because there are no inequality constraints in  $\boldsymbol{\Sigma}(\boldsymbol{\theta}, \gamma)$  at  $(\boldsymbol{\theta}, \gamma)$ .

With the above three conditions satisfied, by applying Theorem 1, we can conclude that  $\frac{\partial \boldsymbol{\xi}_{(\boldsymbol{\theta}, \gamma)}}{\partial \boldsymbol{\theta}}$  is a globally unique minimizing trajectory to the auxiliary control system  $\bar{\boldsymbol{\Sigma}}(\boldsymbol{\xi}_{(\boldsymbol{\theta}, \gamma)})$ . This completes the Claim (c) in Theorem 2.

With the Claims (a), (b), and (c) proved, we have completed the proof of Theorem 2.  $\square$

## D Proof of Theorem 3

We know from the proof of Claim (a) of Theorem 2 in Appendix C.1 that given the conditions in Theorem 3,

- for any  $(\theta, \gamma)$  in the neighborhood of  $(\theta^*, 0)$ , there exists a unique once-continuously differentiable function  $(\xi_{(\theta, \gamma)}, \lambda_{0:T}^{(\theta, \gamma)}, v_{0:T}^{(\theta, \gamma)}, w_{0:T}^{(\theta, \gamma)})$ , which satisfies (S.32), and

$$\left( \xi_{(\theta, \gamma)}, \lambda_{0:T}^{(\theta, \gamma)}, v_{0:T}^{(\theta, \gamma)}, w_{0:T}^{(\theta, \gamma)} \right) = \left( \xi_{\theta^*}, \lambda_{1:T}^{\theta^*}, v_{0:T}^{\theta^*}, w_{0:T}^{\theta^*} \right) \text{ when } (\theta, \gamma) = (\theta^*, 0);$$

- additionally, if all functions defining  $\Sigma(\theta)$  are *three-times* continuously differentiable, it immediately follows that  $\xi_{(\theta, \gamma)}$  is then *twice* continuously differentiable near  $(\theta^*, 0)$ . This is a direct result by applying the  $C^k$  implicit function theorem [87], to the C-PMP condition (S.32) in the neighborhood of  $(\theta^*, 0)$ .
- additionally provided  $\gamma > 0$ , such  $\xi_{(\theta, \gamma)}$  is also a local isolated minimizing trajectory for the well-defined unconstrained optimal control system  $\Sigma(\theta, \gamma)$  in Problem SB( $\theta, \gamma$ ).

Thus, in the following, we will ignore the computation process for obtaining  $\xi_{(\theta, \gamma)}$  and simply view that  $\xi_{(\theta, \gamma)}$  is the twice continuously differentiable function of  $(\theta, \gamma)$  near  $(\theta^*, 0)$  and  $\xi_{\theta^*} = \xi_{(\theta=\theta^*, \gamma=0)}$ . The following proof of Theorem 3 follows the procedure of the general interior-point minimization methods, which are systematically studied in [48] (see Theorem 14, p. 80).

Recall the optimization in Problem SP( $\epsilon, \gamma$ ), re-write it below for easy reference,

$$\theta^*(\epsilon, \gamma) = \arg \min_{\theta} W(\theta, \epsilon, \gamma) \quad (\text{S.57})$$

with

$$W(\theta, \epsilon, \gamma) = \ell(\xi_{(\theta, \gamma)}, \theta) - \epsilon \sum_{i=1}^l \ln \left( -R_i(\xi_{(\theta, \gamma)}, \theta) \right) \quad (\text{S.58})$$

Given in Theorem 3 that  $\theta^*$  satisfies the second-order sufficient condition for a local isolated minimizer to Problem P (recall the general second-order sufficient condition in Lemma A.1), one can say that there exists a multiplier  $u^* \in \mathbb{R}^l$  such that

$$\begin{aligned} \nabla L(\theta^*, u^*) &= \nabla \ell(\xi_{\theta^*}, \theta^*) + \sum_{i=1}^l u_i^* \nabla R_i(\xi_{\theta^*}, \theta^*) = \mathbf{0}, \\ u_i^* R_i(\xi_{\theta^*}, \theta^*) &= 0, \quad i = 1, 2, \dots, l, \\ R_i(\xi_{\theta^*}, \theta^*) &\leq 0, \quad u_i^* \geq 0, \quad i = 1, 2, \dots, l, \end{aligned} \quad (\text{S.59})$$

with the Lagrangian defined as

$$L(\theta, u) = \ell(\xi_{\theta}, \theta) + \sum_{i=1}^l u_i R_i(\xi_{\theta}, \theta), \quad (\text{S.60})$$

and further for any  $\theta \neq \mathbf{0}$  satisfying  $\theta' \nabla R_i(\xi_{\theta^*}, \theta^*) = 0$  with  $u_i^* > 0$  and  $\theta' \nabla R_i(\xi_{\theta^*}, \theta^*) \leq 0$  with  $u_i^* \geq 0$ , it follows

$$\theta' \nabla^2 L(\theta^*, u^*) \theta > 0. \quad (\text{S.61})$$

Here,  $\nabla L$  and  $\nabla^2 L$  denote the first- and second-order derivatives of  $L$  with respect to  $\theta$ , respectively; and  $\xi_{\theta^*} = \xi_{(\theta=\theta^*, \gamma=0)}$ .

### D.1 Proof of Claim (a)

We modify the first two equations in (S.59) into

$$\begin{aligned} \nabla \ell(\xi_{(\theta^*(\epsilon, \gamma), \gamma)}, \theta^*(\epsilon, \gamma)) + \sum_{i=1}^l u_i^*(\epsilon, \gamma) \nabla R_i(\xi_{(\theta^*(\epsilon, \gamma), \gamma)}, \theta^*(\epsilon, \gamma)) &= \mathbf{0}, \\ u_i^*(\epsilon, \gamma) R_i(\xi_{(\theta^*(\epsilon, \gamma), \gamma)}, \theta^*(\epsilon, \gamma)) &= -\epsilon, \quad i = 1, 2, \dots, l, \end{aligned} \quad (\text{S.62})$$

respectively, and consider both  $\theta^*(\epsilon, \gamma)$  and  $\mathbf{u}^*(\epsilon, \gamma)$  are implicitly determined by  $\epsilon$  and  $\gamma$  through the above equations.

Look at (S.62) and note that when  $\epsilon = 0$  and  $\gamma = 0$ , (S.62) is identical to the first two equations in (S.59). Given in Theorem 3 that all binding constraint gradients  $\nabla R_i(\xi_{\theta^*}, \theta^*)$  are linearly independent at  $\theta^*$  and the strict complementary holds at  $\theta^*$ , similar to the proof of Theorem 2, one can apply the well-known implicit function theorem [75] to (S.62) in a neighborhood of  $(\epsilon, \gamma) = (0, 0)$ , leading to the following claim (i.e., the first-order sensitivity result in Theorem 14 in [48]):

*In a neighborhood of  $(\epsilon, \gamma) = (0, 0)$ , there exists a unique once continuously differentiable function  $(\theta^*(\epsilon, \gamma), \mathbf{u}^*(\epsilon, \gamma))$ , which satisfies (S.62) and  $(\theta^*(\epsilon, \gamma), \mathbf{u}^*(\epsilon, \gamma)) = (\theta^*, \mathbf{u}^*)$  when  $(\epsilon, \gamma) = (0, 0)$ .*

Next, we show that the above  $\theta^*(\epsilon, \gamma)$  always respects the constraints  $R_i(\xi_{(\theta^*(\epsilon, \gamma), \gamma)}, \theta^*(\epsilon, \gamma)) < 0$ ,  $i = 1, 2, \dots, l$ , for any small  $\epsilon > 0$  and any small  $\gamma > 0$ , which is the second-part of Claim (a).

In fact, for any inactive constraint,  $R_i(\xi_{\theta^*}, \theta^*) < 0$ , due to the continuity of  $(\xi_{(\theta^*(\epsilon, \gamma), \gamma)}, \theta^*(\epsilon, \gamma))$ , one has

$$R_i(\xi_{(\theta^*(\epsilon, \gamma), \gamma)}, \theta^*(\epsilon, \gamma)) \rightarrow R_i(\xi_{\theta^*}, \theta^*) < 0 \quad \text{as } (\epsilon, \gamma) \rightarrow (0, 0), \quad (\text{S.63})$$

and thus  $R_i(\xi_{(\theta^*(\epsilon, \gamma), \gamma)}, \theta^*(\epsilon, \gamma)) < 0$  for any small  $\epsilon > 0$  and  $\gamma > 0$ . For any active constraint,  $R_i(\xi_{\theta^*}, \theta^*) = 0$ , and since the corresponding  $u_i^* > 0$  (due to the strict complementarity given in Theorem 3) and the continuity of  $\mathbf{u}^*(\epsilon, \gamma)$ , one has

$$u_i^*(\epsilon, \gamma) \rightarrow u_i^* > 0 \quad \text{as } (\epsilon, \gamma) \rightarrow (0, 0), \quad (\text{S.64})$$

and thus  $u_i^*(\epsilon, \gamma) > 0$  for small  $\epsilon > 0$  and consequently

$$R_i(\xi_{(\theta^*(\epsilon, \gamma), \gamma)}, \theta^*(\epsilon, \gamma)) = -\frac{\epsilon}{u_i^*(\epsilon, \gamma)} < 0 \quad (\text{S.65})$$

because of (S.62). Therefore, we have proved that for any small  $\epsilon > 0$  and  $\gamma > 0$ ,  $\theta^*(\epsilon, \gamma)$  always respect the constraints  $R_i(\xi_{(\theta^*(\epsilon, \gamma), \gamma)}, \theta^*(\epsilon, \gamma)) < 0$ ,  $i = 1, 2, \dots, l$ . This prove the second part of Claim (a).

From now on, we show that the above  $\theta^*(\epsilon, \gamma)$  with any small  $\epsilon > 0$  and  $\gamma > 0$  also is a local isolated minimizer to the unconstrained optimization (S.57). From the last equation in (S.62), we solve

$$u_i^*(\epsilon, \gamma) = -\frac{\epsilon}{R_i(\xi_{(\theta^*(\epsilon, \gamma), \gamma)}, \theta^*(\epsilon, \gamma))}, \quad i = 1, 2, \dots, l, \quad (\text{S.66})$$

and substitute it to the first equation, yielding

$$\nabla \ell(\xi_{(\theta^*(\epsilon, \gamma), \gamma)}, \theta^*(\epsilon, \gamma)) - \sum_{i=1}^l \frac{\epsilon}{R_i(\xi_{(\theta^*(\epsilon, \gamma), \gamma)}, \theta^*(\epsilon, \gamma))} \nabla R_i(\xi_{(\theta^*(\epsilon, \gamma), \gamma)}, \theta^*(\epsilon, \gamma)) = \mathbf{0}. \quad (\text{S.67})$$

One can find that the obtained equation in (S.67) is exactly the first-order optimality condition (KKT condition) for the unconstrained optimization in Problem SP( $\epsilon, \gamma$ ) in (S.57), and this indicates that  $\theta^*(\epsilon, \gamma)$  satisfies the KKT condition for Problem SP( $\epsilon, \gamma$ ). To further show that  $\theta^*(\epsilon, \gamma)$  is a local isolated minimizing solution to Problem SP( $\epsilon, \gamma$ ) in (S.57), we only need to verify the second-order condition, that is, for any nonzero  $\theta \neq \mathbf{0}$ ,

$$\theta'(\nabla^2 W(\theta^*(\epsilon, \gamma), \epsilon, \gamma))\theta > 0, \quad (\text{S.68})$$

for any small  $\epsilon > 0$  and  $\gamma > 0$ , which will be proved next.

Proof by contradiction: suppose that the second-order condition (S.68) is false. Then, there must exist a sequence of  $(\epsilon_k, \gamma_k) > 0$  and a sequence of  $\theta_k$  for  $k = 1, 2, \dots$  such that  $(\epsilon_k, \gamma_k) \rightarrow (0, 0)$  and

$$\theta_k'(\nabla^2 W(\theta^*(\epsilon_k, \gamma_k), \epsilon_k, \gamma_k))\theta_k \leq 0. \quad (\text{S.69})$$

as  $k \rightarrow +\infty$ . Without loss of generality, assume  $\|\boldsymbol{\theta}_k\| = 1$  for all  $k$ . Select a convergent sub-sequence of  $\boldsymbol{\theta}_k$ , relabel the sequence  $\boldsymbol{\theta}_k$  for convenience, and call the limit  $\bar{\boldsymbol{\theta}}$ , that is,  $\boldsymbol{\theta}_k \rightarrow \bar{\boldsymbol{\theta}}$  and  $(\epsilon_k, \gamma_k) \rightarrow 0$  as  $k \rightarrow +\infty$ . Then,

$$\begin{aligned}
& \lim_{k \rightarrow +\infty} \boldsymbol{\theta}'_k (\nabla^2 W(\boldsymbol{\theta}^*(\epsilon_k, \gamma_k), \epsilon_k, \gamma_k)) \boldsymbol{\theta}_k \\
&= \lim_{k \rightarrow +\infty} \left( \boldsymbol{\theta}'_k \left( \nabla^2 L(\boldsymbol{\theta}^*(\epsilon_k, \gamma_k), \mathbf{u}^*(\epsilon_k, \gamma_k)) + \sum_{i=1}^l \frac{\epsilon_k}{(R_i(\epsilon_k, \gamma_k))^2} (\nabla R_i(\epsilon_k, \gamma_k) \nabla R_i(\epsilon_k, \gamma_k)') \right) \boldsymbol{\theta}_k \right) \\
&= \lim_{k \rightarrow +\infty} \left( \boldsymbol{\theta}'_k \left( \nabla^2 L(\boldsymbol{\theta}^*(\epsilon_k, \gamma_k), \mathbf{u}^*(\epsilon_k, \gamma_k)) \right) \boldsymbol{\theta}_k \right) + \lim_{k \rightarrow +\infty} \left( \sum_{i=1}^l \frac{\epsilon_k}{(R_i(\epsilon_k, \gamma_k))^2} (\nabla R_i(\epsilon_k, \gamma_k)') \boldsymbol{\theta}_k \right)^2 \\
&= \bar{\boldsymbol{\theta}}' \left( \nabla^2 L(\boldsymbol{\theta}^*, \mathbf{u}^*) \right) \bar{\boldsymbol{\theta}} + \lim_{k \rightarrow +\infty} \left( \sum_{i=1}^l \frac{\epsilon_k}{(R_i(\epsilon_k, \gamma_k))^2} (\nabla R_i(\epsilon_k, \gamma_k)') \boldsymbol{\theta}_k \right)^2,
\end{aligned} \tag{S.70}$$

where we write  $R_i(\epsilon_k, \gamma_k) = R_i(\boldsymbol{\xi}_{(\boldsymbol{\theta}^*(\epsilon_k, \gamma_k), \gamma_k)}, \boldsymbol{\theta}^*(\epsilon_k, \gamma_k))$  and  $\nabla R_i(\epsilon_k) = \nabla R_i(\boldsymbol{\xi}_{(\boldsymbol{\theta}^*(\epsilon_k, \gamma_k), \gamma_k)}, \boldsymbol{\theta}^*(\epsilon_k, \gamma_k))$  for notation convenience, and the last line is because  $L(\boldsymbol{\theta}, \mathbf{u})$  in (S.60) is twice-continuously differentiable with respect to  $(\boldsymbol{\theta}, \mathbf{u})$  near  $(\boldsymbol{\theta}^*, \mathbf{u}^*)$ , and  $(\boldsymbol{\theta}^*(\epsilon, \gamma), \mathbf{u}^*(\epsilon, \gamma))$  is once-continuously differentiable with respect to  $(\epsilon, \gamma)$  near  $(0, 0)$ . In (S.70), we consider two cases for  $\bar{\boldsymbol{\theta}}$ :

*Case 1:*  $\|\bar{\boldsymbol{\theta}}\| = 1$  and there exists at least an active inequality constraint  $R_i(\boldsymbol{\xi}_{\boldsymbol{\theta}^*}, \boldsymbol{\theta}^*) = 0$ , such that  $\bar{\boldsymbol{\theta}}' \nabla R_i(\boldsymbol{\xi}_{\boldsymbol{\theta}^*}, \boldsymbol{\theta}^*) \neq 0$ . Then,

$$\begin{aligned}
& \lim_{k \rightarrow +\infty} \left( \sum_{i=1}^l \frac{\epsilon_k}{(R_i(\epsilon_k, \gamma_k))^2} (\nabla R_i(\epsilon_k, \gamma_k)') \boldsymbol{\theta}_k \right)^2 \\
&= \lim_{k \rightarrow +\infty} \left( \sum_{i=1}^l \frac{-u_i(\epsilon_k, \gamma_k)}{R_i(\epsilon_k, \gamma_k)} (\nabla R_i(\epsilon_k, \gamma_k)') \boldsymbol{\theta}_k \right)^2 = +\infty.
\end{aligned} \tag{S.71}$$

This is because the following term corresponding to such active constraint has

$$\lim_{k \rightarrow +\infty} \frac{-u_i(\epsilon_k, \gamma_k)}{R_i(\boldsymbol{\xi}_{(\boldsymbol{\theta}^*(\epsilon_k, \gamma_k), \gamma_k)}, \boldsymbol{\theta}^*(\epsilon_k, \gamma_k))} = +\infty. \tag{S.72}$$

due to the strict complementarity given in Theorem 3. Therefore, (S.70) will have

$$\lim_{k \rightarrow +\infty} \boldsymbol{\theta}'_k \left( \nabla^2 W(\boldsymbol{\theta}^*(\epsilon_k, \gamma_k), \epsilon_k, \gamma_k) \right) \boldsymbol{\theta}_k = +\infty, \tag{S.73}$$

which contradicts the assumption in (S.69) in that

$$\lim_{k \rightarrow +\infty} \boldsymbol{\theta}'_k \left( \nabla^2 W(\boldsymbol{\theta}^*(\epsilon_k, \gamma_k), \epsilon_k, \gamma_k) \right) \boldsymbol{\theta}_k \leq 0. \tag{S.74}$$

*Case 2:*  $\|\bar{\boldsymbol{\theta}}\| = 1$  and for any active constraint  $R_i(\boldsymbol{\xi}_{\boldsymbol{\theta}^*}, \boldsymbol{\theta}^*) = 0$  (and  $u_i^* > 0$  due to strict complementarity given in Theorem 3),  $\bar{\boldsymbol{\theta}}' \nabla R_i(\boldsymbol{\xi}_{\boldsymbol{\theta}^*}, \boldsymbol{\theta}^*) = 0$ . Then, from (S.70),

$$\lim_{k \rightarrow +\infty} \boldsymbol{\theta}'_k \left( \nabla^2 W(\boldsymbol{\theta}^*(\epsilon_k, \gamma_k), \epsilon_k, \gamma_k) \right) \boldsymbol{\theta}_k \geq \bar{\boldsymbol{\theta}}' \left( \nabla^2 L(\boldsymbol{\theta}^*, \mathbf{u}^*) \right) \bar{\boldsymbol{\theta}} > 0, \tag{S.75}$$

where the last inequality is because of the second-order condition in (S.61) satisfied for  $\boldsymbol{\theta}^*$  given in Theorem 3. The obtained (S.75) also contradicts the assumption in (S.69).

Combining the above two cases, we can conclude that given any small  $\epsilon > 0$  and  $\gamma > 0$ ,  $\boldsymbol{\theta}^*(\epsilon, \gamma)$  satisfies both the KKT condition (S.67) and the second-order condition (S.68) for  $W(\boldsymbol{\theta}, \epsilon, \gamma)$ . Thus, one can assert that  $\boldsymbol{\theta}^*(\epsilon, \gamma)$  is a local isolated minimizer to the unconstrained optimization  $W(\boldsymbol{\theta}, \epsilon, \gamma)$  in (S.57), i.e., Problem SP( $\epsilon, \gamma$ ). This completes the proof of the Claim (a) in Theorem 3.

## D.2 Proof of Claim (b)

From the previous proof for Claim (a), we have the following conclusions: first, for any  $(\epsilon, \gamma)$  in a neighborhood of  $(0, 0)$ , there exists a *unique* once-continuously differentiable function  $(\boldsymbol{\theta}^*(\epsilon, \gamma), \mathbf{u}^*(\epsilon, \gamma))$ , satisfying (S.62); second, additionally provided small  $\epsilon > 0$  and  $\gamma > 0$ , such  $\boldsymbol{\theta}^*(\epsilon, \gamma)$  is also a local isolated minimizer to the well-defined unconstrained minimization  $W(\boldsymbol{\theta}, \epsilon, \gamma)$  in (S.57); and third, when  $(\epsilon, \gamma) = (0, 0)$ , (S.62) becomes the KKT condition for Problem P, whose solution  $(\boldsymbol{\theta}^*, \mathbf{u}^*)$  must satisfy. Therefore, due to the uniqueness and continuity of the function  $(\boldsymbol{\theta}^*(\epsilon, \gamma), \mathbf{u}^*(\epsilon, \gamma))$  near  $(\epsilon, \gamma) = (0, 0)$ , one can obtain

$$\boldsymbol{\theta}^*(\epsilon, \gamma) \rightarrow \boldsymbol{\theta}^*(0, 0) = \boldsymbol{\theta}^*, \quad \text{as } (\epsilon, \gamma) \rightarrow (0, 0). \quad (\text{S.76})$$

This completes the proof of Claim (b) in Theorem 3.

## D.3 Proof of Claim (c)

To prove Claim (c) in Theorem 3, we use the following facts: first, as proved in Claim (a), for any small  $\epsilon > 0$  and  $\gamma > 0$ ,  $\boldsymbol{\theta}^*(\epsilon, \gamma)$  always respects the constraints  $R_i(\boldsymbol{\xi}_{(\boldsymbol{\theta}^*(\epsilon, \gamma), \gamma)}, \boldsymbol{\theta}^*(\epsilon, \gamma)) < 0$ ,  $i = 1, 2, \dots, l$ ; second, as also proved in Claim (a),  $\boldsymbol{\theta}^*(\epsilon, \gamma)$  is differentiable with respect to  $(\epsilon, \gamma)$  near  $(0, 0)$  and  $\boldsymbol{\theta}^*(\epsilon, \gamma) \rightarrow \boldsymbol{\theta}^*$  as  $(\epsilon, \gamma) \rightarrow (0, 0)$ ; and third, as proved in Theorem 2,  $\boldsymbol{\xi}_{(\boldsymbol{\theta}, \gamma)}$  is a differentiable function of  $(\boldsymbol{\theta}, \gamma)$  near  $(\boldsymbol{\theta}^*, 0)$ . All these facts lead to that for small  $\gamma > 0$ ,  $R_i(\boldsymbol{\xi}_{(\boldsymbol{\theta}, \gamma)}, \boldsymbol{\theta})$ ,  $i = 1, 2, \dots, l$ , is also a continuous function of  $\boldsymbol{\theta}$  near  $\boldsymbol{\theta}^*(\epsilon, \gamma)$ , and

$$R_i(\boldsymbol{\xi}_{(\boldsymbol{\theta}, \gamma)}, \boldsymbol{\theta}) \rightarrow R_i(\boldsymbol{\xi}_{(\boldsymbol{\theta}^*(\epsilon, \gamma), \gamma)}, \boldsymbol{\theta}^*(\epsilon, \gamma)) < 0, \quad \text{as } \boldsymbol{\theta} \rightarrow \boldsymbol{\theta}^*(\epsilon, \gamma), \quad \forall i = 1, 2, \dots, l. \quad (\text{S.77})$$

Thus  $R_i(\boldsymbol{\xi}_{(\boldsymbol{\theta}, \gamma)}, \boldsymbol{\theta}) < 0$ ,  $i = 1, 2, \dots, l$ , holds for any  $\boldsymbol{\theta}$  in a small neighborhood of  $\boldsymbol{\theta}^*(\epsilon, \gamma)$  with small  $\epsilon > 0$  and small  $\gamma > 0$ . This completes the proof of Claim (c) in Theorem 3.

With the above proofs for Claims (a), (b), and (c), we have completed the proof of Theorem 3.  $\square$



## E Algorithms for Safe PDP

We have implemented Safe PDP in Python and made it as a stand-alone package with friendly interfaces. Please download at <https://github.com/wanxinjin/Safe-PDP>.

### E.1 Algorithm for Theorem 1

---

**Algorithm 1:** Solving  $\frac{\partial \xi_\theta}{\partial \theta}$  by establishing auxiliary control system  $\bar{\Sigma}(\xi_\theta)$

---

**Input:**  $\xi_\theta$ , with the costates  $\lambda_{1:T}^\theta$  and multipliers  $v_{0:T}^\theta$  and  $w_{0:T}^\theta$  from solving Problem **B**( $\theta$ )

**def** Identify\_Active\_Inequality\_Constraints (a small threshold  $\delta > 0$ ):

$\bar{g}_t(x_t, u_t, \theta) = \text{col}\{g_{t,i} \mid g_{t,i}(x_t^\theta, u_t^\theta, \theta) \geq -\delta, i = 1, 2, \dots, q_t\}, t = 0, 1, \dots, T-1$ ;

$\bar{g}_T(x_T, \theta) = \text{col}\{g_{T,i} \mid g_{T,i}(x_T^\theta, \theta) \geq -\delta, i = 1, 2, \dots, q_T\}$ ;

**Return:**  $\bar{g}_t(x_t, u_t, \theta)$  and  $\bar{g}_T(x_T, \theta)$

Compute the derivative matrices  $L_t^{xx}, L_t^{xu}, L_t^{uu}, L_t^{x\theta}, L_t^{u\theta}, L_T^{xx}, L_T^{x\theta}, F_t^x, F_t^u, F_t^\theta, H_t^x, H_t^u, H_t^\theta, H_T^x, H_T^u, H_T^\theta, \bar{G}_t^x, \bar{G}_t^u, \bar{G}_t^\theta, \bar{G}_T^x, \bar{G}_T^u, \bar{G}_T^\theta$  to establish  $\bar{\Sigma}(\xi_\theta)$  in (3);

**def** Equality\_Constrained\_LQR\_Solver ( $\bar{\Sigma}(\xi_\theta)$ ):

Implementation of the equality constrained LQR algorithm in [80];

**Return:**  $\{X_{0:T}^\theta, U_{0:T-1}^\theta\}$

**Return:**  $\frac{\partial \xi_\theta}{\partial \theta} = \{X_{0:T}^\theta, U_{0:T-1}^\theta\}$

---

Note that  $\lambda_{1:T}^\theta$ ,  $v_{0:T}^\theta$ , and  $w_{0:T}^\theta$  are normally the by-product outputs of an optimal control solver [77], and can also be obtained by solving a linear equation of C-PMP (S.5) given  $\xi_\theta$ , as done in [71]. Also note that the threshold  $\delta$  to determine the active inequality constraints can be set according to the accuracy of the solver; in our experiments, we use  $\delta = 10^{-3}$ .

### E.2 Algorithm for Theorem 2

---

**Algorithm 2:** Safe unconstrained approximations for  $\xi_\theta$  and  $\frac{\partial \xi_\theta}{\partial \theta}$

---

**Input:** The constrained optimal control system  $\Sigma(\theta)$  and a choice of small  $\gamma > 0$

Convert  $\Sigma(\theta)$  to an unconstrained optimal control system  $\Sigma(\theta, \gamma)$  in (5) by adding all constraints in  $\Sigma(\theta)$  to its control cost through barrier functions with barrier parameter  $\gamma$ ;

*/\* Below is an implementation of unconstrained PDP [71] \*/*

**def** Optimal\_Control\_Solver ( $\Sigma(\theta, \gamma)$ ):

Implementation of any trajectory optimization algorithms, such as iLQR [81] and DDP [82], or use any optimal control solver [77];

**Return:**  $\xi_{(\theta, \gamma)}$

Use  $\xi_{(\theta, \gamma)}$  to compute the derivative matrices  $\hat{L}_t^{xu}, \hat{L}_t^{uu}, \hat{L}_t^{x\theta}, \hat{L}_t^{u\theta}, \hat{L}_T^{xx}, \hat{L}_T^{x\theta}, F_t^x, F_t^u, F_t^\theta$  to establish the auxiliary control system  $\bar{\Sigma}(\xi_{(\theta, \gamma)})$  in (S.78);

**def** LQR\_Solver ( $\bar{\Sigma}(\xi_{(\theta, \gamma)})$ ):

Implementation of any LQR algorithm such as Lemma 2 in [71];

**Return:**  $\{X_{0:T}^{(\theta, \gamma)}, U_{0:T-1}^{(\theta, \gamma)}\} = \frac{\partial \xi_{(\theta, \gamma)}}{\partial \theta}$

**Return:**  $\xi_{(\theta, \gamma)}$  and  $\frac{\partial \xi_{(\theta, \gamma)}}{\partial \theta}$

---

Note that the auxiliary control system  $\bar{\Sigma}(\xi_{(\theta, \gamma)})$  corresponding to  $\Sigma(\theta, \gamma)$  is

$$\bar{\Sigma}(\xi_{(\theta, \gamma)}) : \quad \begin{aligned} \text{control cost} \quad \bar{W} &= \text{Tr} \sum_{t=0}^{T-1} \left( \frac{1}{2} \begin{bmatrix} X_t \\ U_t \end{bmatrix}' \begin{bmatrix} \hat{L}_t^{xx} & \hat{L}_t^{xu} \\ \hat{L}_t^{ux} & \hat{L}_t^{uu} \end{bmatrix} \begin{bmatrix} X_t \\ U_t \end{bmatrix} + \begin{bmatrix} \hat{L}_t^{x\theta} \\ \hat{L}_t^{u\theta} \end{bmatrix}' \begin{bmatrix} X_t \\ U_t \end{bmatrix} \right) \\ &+ \text{Tr} \left( \frac{1}{2} X_T' \hat{L}_T^{xx} X_T + (\hat{L}_T^{x\theta})' X_T \right) \quad (\text{S.78}) \\ \text{subject to} \\ \text{dynamics} \quad X_{t+1} &= F_t^x X_t + F_t^u U_t + F_t^\theta \quad \text{with} \quad X_0 = X_0^\theta. \end{aligned}$$

Here,  $\hat{L}_t$ ,  $t = 0, 1, \dots, T-1$ , and  $\hat{L}_T$  are the Hamiltonian, defined in (S.31), for the unconstrained optimal control system  $\Sigma(\theta, \gamma)$ . The derivative (coefficient) matrices  $\hat{L}_t^{xu}$ ,  $\hat{L}_t^{uu}$ ,  $\hat{L}_t^{x\theta}$ ,  $\hat{L}_t^{u\theta}$ ,  $\hat{L}_T^{xx}$ ,  $\hat{L}_T^{x\theta}$ ,  $F_t^x$ ,  $F_t^u$ ,  $F_t^\theta$  in (S.78) are defined in the similar notation convention as in (3).

### E.3 Algorithm for Theorem 3

---

#### Algorithm 3: Safe PDP to solve Problem P

---

**Input:** Small barrier parameter  $\epsilon > 0$  for outer-level and  $\gamma > 0$  for inner-level, initialization  $\theta_0$

```

/* Convert inner-level into its safe unconstrained approximation */
1 Convert the inner-level constrained control system  $\Sigma(\theta)$  in (1) into an unconstrained
  system  $\Sigma(\theta, \gamma)$  in (5) by adding all constraints to its control cost through barrier
  functions with the inner-level barrier parameter  $\gamma > 0$ ;

/* Convert outer-level into its safe unconstrained approximation */
2 Convert the constrained Problem P to an unconstrained Problem  $\text{SP}(\epsilon, \gamma)$  by adding all
  task constraints  $R_i$  to the task loss through barrier functions with the outer-level barrier
  parameter  $\epsilon > 0$ ;

/* Gradient-based update for  $\theta$  */
for  $k = 0, 1, 2, \dots$  do
3 Apply Algorithm 2 to the inner-level safe unconstrained approximation system
   $\Sigma(\theta_k, \gamma)$  to compute  $\xi_{(\theta_k, \gamma)}$  and  $\frac{\partial \xi_{(\theta, \gamma)}}{\partial \theta} |_{\theta_k}$ ;
4 For the outer-level unconstrained Problem  $\text{SP}(\epsilon, \gamma)$  with objective function
   $W(\theta, \epsilon, \gamma) = \ell(\xi_{(\theta, \gamma)}, \theta) - \epsilon \sum_{i=1}^l \ln(-R_i(\xi_{(\theta, \gamma)}, \theta))$ , compute the partial
  gradients  $\frac{\partial W}{\partial \theta} |_{\theta_k}$  and  $\frac{\partial W}{\partial \xi_{(\theta, \gamma)}} |_{\xi_{(\theta_k, \gamma)}}$ ;
5 Apply the chain rule to obtain the gradient of the outer-level unconstrained objective
   $W(\theta, \epsilon, \gamma)$  with respect to  $\theta$ , i.e.,  $\frac{dW}{d\theta} |_{\theta_k} = \frac{\partial W}{\partial \theta} |_{\theta_k} + \frac{\partial W}{\partial \xi_{(\theta, \gamma)}} |_{\xi_{(\theta_k, \gamma)}} \frac{\partial \xi_{(\theta, \gamma)}}{\partial \theta} |_{\theta_k}$ ;
6 Gradient-based update:  $\theta_{k+1} = \theta_k - \eta \frac{dW}{d\theta} |_{\theta_k}$  with  $\eta$  being the learning rate;
end

```

**Return:**  $\theta^*(\epsilon, \gamma)$  for the given barrier parameters  $\epsilon > 0$  and  $\gamma > 0$

---

Note that after obtaining  $\theta^*(\epsilon, \gamma)$  from Algorithm 3, one can sequentially refine  $\theta^*(\epsilon, \gamma)$  by choosing a sequence of  $\{(\epsilon, \gamma)\}$  such that  $(\epsilon, \gamma) \rightarrow (0, 0)$ .

Also note that in the case where the original inner-level control system  $\Sigma(\theta)$  is already unconstrained, such as in the applications of safe policy optimization and safe motion planning in Section 7, please modify lines 1 and 3 in Algorithm 3 and just compute exact  $\xi_{\theta_k}$  and  $\frac{\partial \xi_{\theta}}{\partial \theta} |_{\theta_k}$  by following PDP [71].

## F Experiment Details

The proposed Safe PDP has been evaluated in different simulated systems in Table 1, where each system has the immediate constraints  $g(\theta_{\text{cstr}})$  on both its state and input during the entire time horizon (around  $T = 50$ ). For the detailed description and physical models of each system in Table 1, we refer the reader to [71] and its accompanying codes. We have developed the Python code of Safe PDP as a stand-alone package, which can be accessed at <https://github.com/wanxinjin/Safe-PDP>.

### F.1 Safe Policy Optimization

In this experiment, we apply Safe PDP to perform safe policy optimization for the systems in Table 1. In Problem P, we set the details of  $\Sigma(\theta)$  as (8), where the dynamics  $f$  is learned from demonstrations in Section F.3, and the policy  $u_t = \pi(x_t, \theta)$  is represented using a neural network (NN) with  $\theta$  the NN parameter. In our experiment, we have used a fully-connected feedforward NN to represent the policy; the number of nodes in the NN is  $n-n-m$  (meaning that the input layer has  $n$  nodes, hidden layer  $n$  nodes, and output layer  $m$  nodes, with  $n$  and  $m$  the dimensions of the system state and input, respectively); and the activation function of the NN is tanh. In Problem P, set the task loss  $\ell(\xi_\theta, \theta)$  as the control cost  $J(\theta_{\text{obj}})$ , and set the task constraints  $R_i(\xi_\theta, \theta)$  as the system constraints  $g(\theta_{\text{cstr}})$ , both in Table 1, with both  $\theta_{\text{obj}}$  and  $\theta_{\text{cstr}}$  known.

Note that since the parameterized  $\Sigma(\theta)$  in (8) does not include the control cost  $J$  anymore, solving Problem B( $\theta$ ) for  $\xi_\theta$  becomes a simple integration of (8) from  $t = 0$  to  $T-1$ , and the auxiliary control system  $\bar{\Sigma}(\xi_\theta)$  in (3) to compute  $\frac{\partial \xi_\theta}{\partial \theta}$  is simplified to a feedback control system [71] below:

$$\bar{\Sigma}(\xi_\theta) : \begin{array}{l} \text{dynamics: } X_{t+1}^\theta = F_t^x X_t^\theta + F_t^u U_t^\theta \quad \text{with } X_0 = \mathbf{0}, \\ \text{control policy: } U_t^\theta = U_t^x X_t^\theta + U_t^e. \end{array} \quad (\text{S.79})$$

Here,  $U_t^x = \frac{\partial \pi_t}{\partial x_t^\theta}$  and  $U_t^e = \frac{\partial \pi_t}{\partial \theta}$ . Integrating (S.79) from  $t = 0$  to  $T-1$  leads to  $\{X_{0:T}^\theta, U_{0:T-1}^\theta\} = \frac{\partial \xi_\theta}{\partial \theta}$ .

In our experiments, in order to make sure the initial NN policy is feasible (safe), we initialize the NN policy using supervised learning from a random demonstration trajectory (note that this demonstration trajectory does not have to be optimal but only to be feasible/safe). For each system in Table 1, we apply Safe PDP Algorithm 3 to optimize the NN policy, and the complete experiment results are shown in Fig. S1-S3. More discussions about how to give a safe initialization are presented in Appendix G.5

For each system, at a fixed barrier parameter  $\epsilon$ , we have applied the vanilla gradient descent to solve Problem SP( $\epsilon$ ) with the step size (learning rate  $\eta$  in Algorithm 3) set around  $10^{-3}$ . We plot the task loss (i.e., control cost)  $\ell(\xi_\theta, \theta)$  versus iteration of the gradient descent in the first panel in Fig. S1-S3, where we only show the results for outer-level barrier parameter  $\epsilon$  taking from  $10^0$  to  $10^{-4}$  because the NN policy has already achieved a good convergence when  $\epsilon \leq 10^{-2}$ . As shown in the first panel in Fig. S1-S3, for each system, the policy achieves a good convergence after a small number of iterations for each  $\epsilon$ , and obtains a good convergence after  $\epsilon \leq 10^{-2}$ .

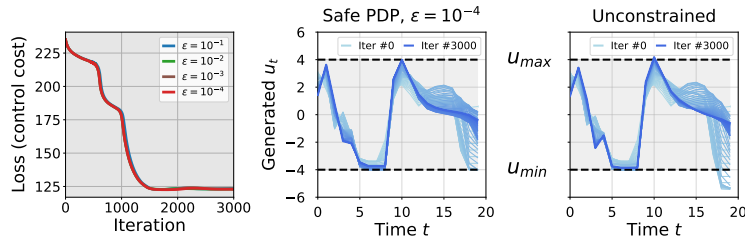


Figure S1: Safe neural policy optimization for cartpole. The first panel plots the loss (control cost) versus gradient-descent iteration under different outer-level barrier parameter  $\epsilon$ ; the second panel plots all intermediate control trajectories generated by the NN policy during the entire gradient-descent iteration ( $\epsilon = 10^{-4}$ ); and the third panel plots all intermediate control trajectories generated by the NN policy for the unconstrained policy optimization under the same experimental conditions. The system constraints are also marked using black dashed lines in the second and third panels.

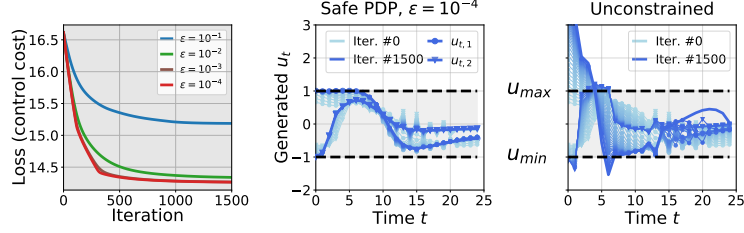


Figure S2: Safe neural policy optimization for robot arm. The first panel plots the loss (control cost) versus gradient-descent iteration under different outer-level barrier parameter  $\epsilon$ ; the second panel plots all intermediate control trajectories generated by the NN policy during the entire gradient-descent iteration ( $\epsilon = 10^{-4}$ ); and the third panel plots all intermediate control trajectories generated by the NN policy for the unconstrained policy optimization under the same experimental conditions. The system constraints are also marked using black dashed lines in the second and third panels.

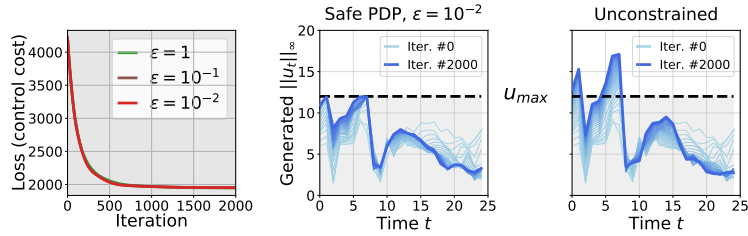


Figure S3: Safe neural policy optimization for 6-DoF maneuvering quadrotor. The first panel plots the loss (control cost) versus gradient-descent iteration under different outer-level barrier parameter  $\epsilon$ ; the second panel plots all intermediate control trajectories generated by the NN policy during the entire gradient-descent iteration ( $\epsilon = 10^{-2}$ ); and the third panel plots all intermediate control trajectories generated by the NN policy for the unconstrained policy optimization under the same experimental conditions. The system constraints are also marked using black dashed lines in the second and third panels.

In order to show the constraint satisfaction of Safe PDP throughout the entire policy optimization process, in the second panel in Fig. S1-S3, respectively, we plot all intermediate control trajectories generated from the NN policy throughout the entire gradient-descent iteration of Safe PDP, as shown from the light to dark blue. From the second panel in Fig. S1-S3, we note that throughout the optimization process, the NN policy is guaranteed safe, meaning that the generated trajectory will never violate the constraints. Under the same experimental conditions (NN configuration, policy initialization, learning rate), we also compare with the unconstrained policy optimization and plot its results in the third panel in Fig. S1-S3, respectively. By comparing the results between Safe PDP and unconstrained policy optimization, we can confirm that Safe PDP enables to achieve an optimal policy while guaranteeing that any intermediate policy throughout optimization is safe, as asserted in Theorem 3.

We have provided the video demonstrations for the above safe policy optimization using Safe PDP; please visit <https://youtu.be/sC81qc2ip8U>. The codes for all experiments here can be downloaded at <https://github.com/wanxinjin/Safe-PDP>.

## F.2 Safe Motion Planning

In this experiment, we apply Safe PDP to solve the safe motion planning problem for the systems in Table 1. In Problem P, we set the details of  $\Sigma(\theta)$  as follows,

$$\Sigma(\theta) : \begin{array}{l} \text{dynamics: } \mathbf{x}_{t+1} = \mathbf{f}(\mathbf{x}_t, \mathbf{u}_t) \text{ with } \mathbf{x}_0, \\ \text{control input: } \mathbf{u}_t = \mathbf{u}(t, \theta), \end{array} \quad (\text{S.80})$$

where the dynamics  $\mathbf{f}$  is learned from demonstrations in Section F.3, and we parameterize the control

input function  $\mathbf{u}_t = \mathbf{u}(t, \boldsymbol{\theta})$  using the Lagrangian polynomial [83] as follows,

$$\mathbf{u}(t, \boldsymbol{\theta}) = \sum_{i=0}^N \mathbf{u}_i b_i(t) \quad \text{with} \quad b_i(t) = \prod_{0 \leq j \leq N, j \neq i} \frac{t - t_j}{t_i - t_j}. \quad (\text{S.81})$$

Here,  $b_i(t)$  is called Lagrange basis, and the policy parameter  $\boldsymbol{\theta}$  is defined as

$$\boldsymbol{\theta} = [\mathbf{u}_0, \dots, \mathbf{u}_N]' \in \mathbb{R}^{m(N+1)}, \quad (\text{S.82})$$

which is the vector of the pivots of the Lagrange polynomial. The benefit of the above parameterization is that the trajectory of system states, which results from integrating (S.80) given the input polynomial trajectory  $\mathbf{u}_t = \mathbf{u}(t, \boldsymbol{\theta})$ , is inherently smooth and dynamics-feasible. In our experiments, the degree  $N$  of the Lagrange polynomial is set as  $N = 10$ . Also in Problem P, we set the task/planning loss  $\ell(\boldsymbol{\xi}_\theta, \boldsymbol{\theta})$  as the control cost  $J(\boldsymbol{\theta}_{\text{obj}})$ , and set the task constraints  $R_i(\boldsymbol{\xi}_\theta, \boldsymbol{\theta})$  as the system constraints  $\mathbf{g}(\boldsymbol{\theta}_{\text{cstr}})$ , both given in Table 1 with  $\boldsymbol{\theta}_{\text{obj}}$  and  $\boldsymbol{\theta}_{\text{cstr}}$  known.

Since the system  $\Sigma(\boldsymbol{\theta})$  in (S.80) now does not include the control cost  $J$  anymore, solving Problem B( $\boldsymbol{\theta}$ ) for  $\boldsymbol{\xi}_\theta$  becomes a simple integration of (S.80) from  $t = 0$  to  $T-1$ , and the auxiliary control system  $\bar{\Sigma}(\boldsymbol{\xi}_\theta)$  in (3) to compute  $\frac{\partial \boldsymbol{\xi}_\theta}{\partial \boldsymbol{\theta}}$  is simplified to a feedback control system [71] below:

|                                           |                                                                                            |        |
|-------------------------------------------|--------------------------------------------------------------------------------------------|--------|
| $\bar{\Sigma}(\boldsymbol{\xi}_\theta) :$ | dynamics: $X_{t+1}^\theta = F_t^x X_t^\theta + F_t^u U_t^\theta$ with $X_0 = \mathbf{0}$ , | (S.83) |
|                                           | control input: $U_t^\theta = U_t^e$ ,                                                      |        |

where  $U_t^e = \frac{\partial \pi_t}{\partial \boldsymbol{\theta}}$ . Integrating (S.83) from  $t = 0$  to  $T - 1$  leads to  $\{X_{0:T}^\theta, U_{0:T-1}^\theta\} = \frac{\partial \boldsymbol{\xi}_\theta}{\partial \boldsymbol{\theta}}$ .

For each system in Table 1, we apply Safe PDP Algorithm 3 to perform safe motion planning, and the complete experiment results are shown in Fig. S4-S6. For each system, at a fixed outer-level barrier parameter  $\epsilon$ , we have applied the vanilla gradient descent to solve Problem SP( $\epsilon$ ) with the step size (learning rate  $\eta$  in Algorithm 3) set to  $10^{-2}$  or  $10^{-1}$ . We plot the planning loss  $\ell(\boldsymbol{\xi}_\theta, \boldsymbol{\theta})$  versus gradient descent iteration in Fig. S4a-S6a, respectively; here we only show the results for  $\epsilon$  taking from  $10^0$  to  $10^{-2}$  because the trajectory has already achieved a good convergence when  $\epsilon \leq 10^{-2}$ . As shown in Fig. S4a-S6a, for each system, the trajectory achieves a good convergence after a small number of iterations given a fixed  $\epsilon$ , and obtains a good convergence after  $\epsilon \leq 10^{-2}$ .

To demonstrate that Safe PDP can guarantee safety throughout the optimization process, we plot all intermediate trajectories during the entire iteration of Safe PDP in S4b-S6b. At the same time, we also show the results of the ALTRO method [21], which is a state-of-the-art method for constrained trajectory optimization. By comparing the results in Fig. S4b-S6b, we can observe that Safe PDP enables to find the optimal trajectory while guaranteeing strict constraint satisfaction throughout the entire optimization process; while for ALTRO, although the trajectory satisfies the constraints at convergence, the intermediate trajectories during optimization may violate the constraints, making it not suitable to handle safety-critical motion planning tasks.

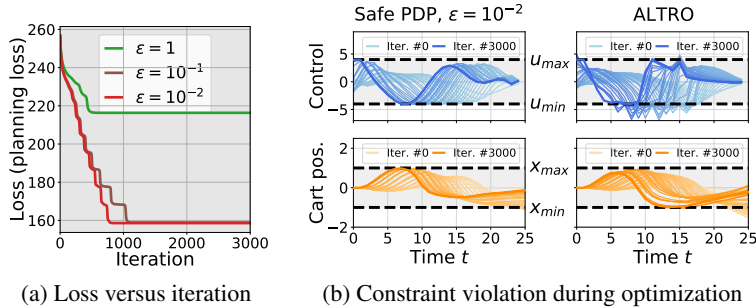


Figure S4: Safe motion planning for cartpole. (a) plots the loss (i.e., planning loss) versus gradient-descent iteration under different outer-level barrier parameter  $\epsilon$ . The left figure in (b) shows all intermediate trajectories during the entire iteration of Safe PDP ( $\epsilon = 10^{-2}$ ), and the right figure in (b) shows all intermediate trajectories during the entire iteration of the ALTRO algorithm [21]. The state and control constraints are also marked in (b).

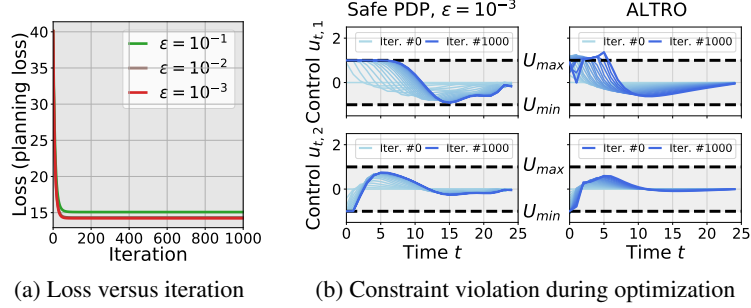


Figure S5: Safe motion planning for robot arm. (a) plots the loss (i.e., planning loss) versus gradient-descent iteration under different outer-level barrier parameter  $\epsilon$ . The left figure in (b) shows all intermediate trajectories during the entire iteration of Safe PDP ( $\epsilon = 10^{-3}$ ), and the right figure in (b) shows all intermediate trajectories during the entire iteration of the ALTRO algorithm [21]. The control constraints are also marked in (b).

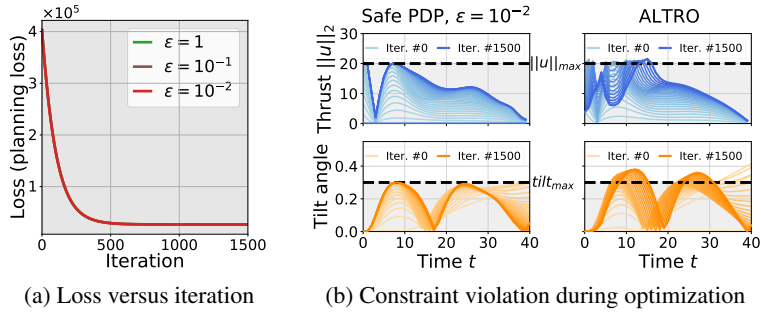


Figure S6: Safe motion planning for 6-DoF rocket powered landing. (a) plots the loss (i.e., planning loss) versus gradient-descent iteration under different outer-level barrier parameter  $\epsilon$ . The left figure in (b) shows all intermediate trajectories during the entire iteration of Safe PDP ( $\epsilon = 10^{-2}$ ), and the right figure in (b) shows all intermediate trajectories during the entire iteration of the ALTRO algorithm [21]. The state and control constraints are also marked in (b).

We have provided the videos for the above safe motion planning using Safe PDP. Please visit the link <https://youtu.be/vZVxgo30mDs>. The codes for all experiments here can be downloaded at <https://github.com/wanxinjin/Safe-PDP>.

### F.3 Learning MPCs from Demonstrations

In this experiment, we apply Safe PDP to learn dynamics  $f$ , constraints  $g$ , or/and control cost  $J$  for the systems in Table 1 from demonstration data. This type of problems has been extensively studied in system identification [88] (neural ODEs [89]), inverse optimal control (inverse reinforcement learning) [90–92], and learning from demonstrations [85, 93]. However, existing methods have the following two technical gaps; first, existing methods are typically developed without considering constraints; second, there are rarely the methods that are capable to *jointly* learn dynamics, state-input constraints, and control cost for continuous control systems. In this part, we will show that the above technical gaps can be addressed by Safe PDP. Throughout this part, we define the task loss in Problem P as the *reproducing loss* as below

$$\ell(\xi_\theta, \theta) = \|\xi^{\text{demo}} - \xi_\theta\|_2^2, \quad (\text{S.84})$$

which is to penalize the distance between the reproduced trajectory  $\xi_\theta$  from the learnable model  $\Sigma(\theta)$  and the given demonstrations  $\xi^{\text{demo}}$ , and there is no task constraint. For  $\Sigma(\theta)$  in Problem P, only the unknown parts (dynamics, control cost, or/and constraints) are parameterized by  $\theta$ . Thus, by solving Problem P, we are able to learn  $\Sigma(\theta)$  such that its trajectory  $\xi_\theta$  has closest distance to the given demonstrations  $\xi^{\text{demo}}$ .

In our experiment, when dealing with  $\xi_\theta$  and  $\frac{\partial \xi_\theta}{\partial \theta}$  for  $\Sigma(\theta)$ , we use the following three strategies.

- *Strategy (A)*: use an optimal control solver [77] to solve the constrained optimal control  $\Sigma(\theta)$  in Problem **B**( $\theta$ ) to obtain  $\xi_\theta$ , and use Theorem 1 (i.e., Algorithm 1) to obtain the trajectory derivative  $\frac{\partial \xi_\theta}{\partial \theta}$  by solving  $\bar{\Sigma}(\xi_\theta)$  in (3).
- *Strategy (B)*: by applying Theorem 2 (i.e., Algorithm 2), approximate  $\xi_\theta$  and  $\frac{\partial \xi_\theta}{\partial \theta}$  using  $\xi_{(\theta, \gamma)}$  and  $\frac{\partial \xi_{(\theta, \gamma)}}{\partial \theta}$ , respectively, with a choice of small barrier parameter  $\gamma > 0$ .
- *Strategy (C)*: obtain  $\xi_\theta$  by solving  $\Sigma(\theta)$  in Problem **B**( $\theta$ ) via a solver [77], and apply Theorem 2 (i.e., Algorithm 2) only to approximate  $\frac{\partial \xi_\theta}{\partial \theta}$  using  $\frac{\partial \xi_{(\theta, \gamma)}}{\partial \theta}$ .

In the following experiments, when using Algorithm 2, we choose  $\gamma = 10^{-2}$  because the corresponding inner-level approximations  $\xi_{(\theta, \gamma)}$  and  $\frac{\partial \xi_{(\theta, \gamma)}}{\partial \theta}$  already achieve a good accuracy, as shown in previous experiments. In practice, the choice of  $\gamma > 0$  is very flexible depending on the desired accuracy (a smaller  $\gamma$  never hurts but would decrease the computational efficiency, as discussed in Appendix G.3).

### F.3.1 Learning Constrained ODEs from Demonstrations

In the first experiment, consider that in  $\Sigma(\theta)$  the control cost  $J$  is known while the dynamics (Ordinary Difference Equation)  $f(\theta_{\text{dyn}})$  and constraints  $g_t(\theta_{\text{cstr}})$  are unknown and parameterized, as in Table 1,  $\theta = \{\theta_{\text{dyn}}, \theta_{\text{cstr}}\}$ . We aim to learn  $\theta$  from given demonstrations  $\xi^{\text{demo}}$  by solving Problem P. Here, the demonstrations are generated by simulating the true system (i.e., expert) with  $\theta$  known; the demonstrations for each system contain two episode trajectories with time horizon around  $T = 50$ .

To solve Problem P, since there are no task constraints, we use the vanilla gradient descent to minimize the reproducing loss (S.84) while using the three strategies as mentioned above to handle the lower-level Problem B( $\theta$ ). The initial condition for the gradient descent is given randomly, and the learning rate for the gradient descent is set as  $10^{-5}$ . The complete results for all systems in Table 1 are given in Fig. S7.

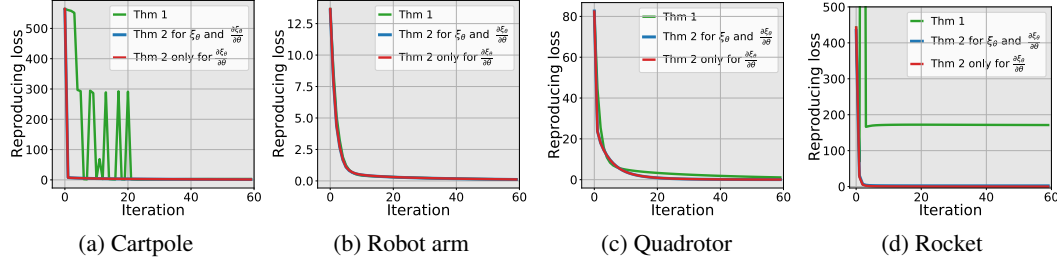


Figure S7: Learning both dynamics and constraints from demonstrations.

Fig. S7a-S7d plot the reproducing loss (S.84) versus gradient-descent iteration. The results show that for Strategies (B) and (C) (in blue and red, respectively), the reproducing loss (S.84) is quickly covering to zeros, indicating that the dynamics and constraints are successfully learned to reproduce the demonstrations. However, we also note that Strategy (A) (in green) suffers from some numerical instability, and this will be discussed later.

### F.3.2 Jointly Learning Dynamics, Constraints, and Control Cost from Demonstrations

In the second experiment, suppose in all systems in Table 1, the control cost  $J(\theta_{\text{cost}})$ , dynamics  $f(\theta_{\text{dyn}})$ , and state and input constraints  $g_t(\theta_{\text{cstr}})$  are all unknown and parameterized as in Table 1. We aim to jointly learn  $\theta = \{\theta_{\text{cost}}, \theta_{\text{dyn}}, \theta_{\text{cstr}}\}$  from given demonstrations  $\xi^{\text{demo}}$  by solving Problem P. Here, the demonstrations are generated by simulating the system (i.e., expert) with  $\theta$  known, the demonstrations for each system contain two episode trajectories for each system with time horizon around  $T = 50$ .

To solve Problem P, since there is no task constraints, we use the vanilla gradient descent to minimize the reproducing loss (S.84) while using the three strategies as mentioned above to handle the lower-level Problem B( $\theta$ ). The initial condition for the gradient descent is given randomly, and the learning

rate for the gradient-descent is set as  $10^{-5}$ . The complete results for all systems in Table 1 are given in Fig. S8 (also see Fig. 4a-4d in the primary text of the paper).

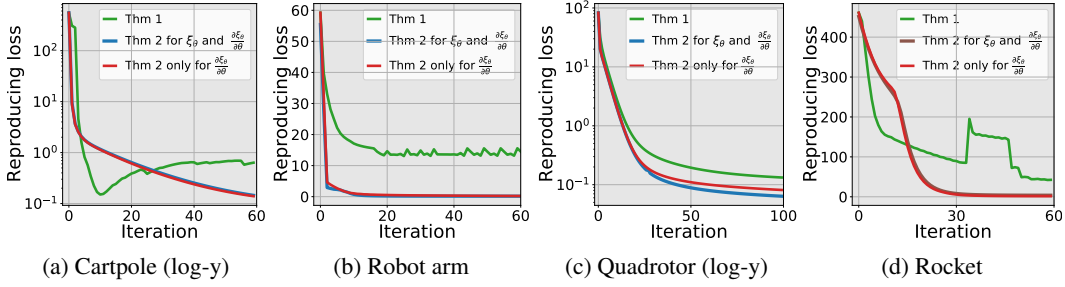


Figure S8: Jointly learning dynamics, constraints, and control cost from demonstrations.

Fig. S8a - Fig. S8d plot the reproducing loss (S.84) versus gradient-descent iteration. The results show that for Strategies (B) and (C) (in blue and red, respectively), the reproducing loss (S.84) is quickly covering to zeros, indicating that the dynamics, constraints, and control cost function are successfully learned to reproduce the demonstrations. However, we also note that Strategy (A) (in green) suffers from some numerical instability, which will be discussed below.

We have provided some videos for the above learning MPCs from demonstrations using Safe PDP. Please visit the link <https://youtu.be/OBiLYY1Wi98>. The codes for all experiments here can be downloaded at <https://github.com/wanxinjin/Safe-PDP>.<sup>1</sup>

**Why implementation of Theorem 1 is not numerically stable?** In both Fig. S7 and S8, we have noted that Strategy (A) suffers from some numerical instability, and this is due to the following reasons. First, Theorem 1 requires to accurately detect the inactive/active inequalities (i.e., whether an inequality constraint is zero or not), which is always difficult accurately due to computational error (in our experiments, we detect the active constraints by applying a brutal threshold, as described in Algorithm 1). Second, although the differentiability of  $\xi_\theta$  holds at the local neighborhood of  $\theta$ ,  $\xi_\theta$  might be extremely discontinuous due to the ‘jumping switch’ of the active and inactive inequality constraints for the large range of  $\theta$ ; thus, such non-smoothness will deteriorate the decrease of loss between iterations.

**Why implementation of Theorem 2 is more numerically stable?** Theorem 2 has perfectly addressed the above numerical issues of Theorem 1. Specifically, first, there is no need to distinguish the active and inactive inequality constraints in Theorem 2; and second, in Theorem 2, by adding all constraints to the control cost function, it introduces the ‘softness’ of the hard constraints and potentially eliminates the discontinuous ‘jumping switch’ between inactive and active inequalities over a large range of  $\theta$ , enabling a stable decrease of loss when applying gradient descent.

<sup>1</sup>All experiments in this paper have been performed on a personal computer with 3.5 GHz Dual-Core Intel Core i7 and macOS Big Sur system.



## G Further Discussion

In this section, we will provide further experiments and discussion on the performance of Safe PDP.

### G.1 Comparison Between Safe PDP and PDP

In this part, we compare Safe PDP and non-safe PDP [71] to show the performance trade-offs between the constraint enforcement of Safe PDP and its resulting computational expense. We use the example of learning MPCs from expert demonstrations for the cartpole system (in Table 1) to show this, and the experiment settings are the same with Appendix F.3. The comparison results between Safe PDP and PDP are given in the following Table S1.

Table S1: Performance comparison between Safe PDP and PDP

| Methods  | Loss at convergence | Timing for Forward Pass | Timing for Backward Pass | Learning constraints? | Constraint Guaranteed? |
|----------|---------------------|-------------------------|--------------------------|-----------------------|------------------------|
| PDP      | 524.02              | 0.10s                   | 0.046s                   | No                    | No                     |
| Safe PDP | 7.42                | 0.21s                   | 0.042s                   | Yes                   | Yes                    |

Based on the results in Table S1, we have the following comments and analysis.

(1) We note that Safe PDP achieves lower training loss. This is because compared to PDP, Safe PDP has introduced the inductive bias of constraints within its model architecture, making it more suited to learn from demonstrations which are the results of a constrained control system (expert). In this sense, Safe PDP architecture (with an inductive bias of constraints) can be thought of as having more expressive power than PDP architecture for the above experiments.

(2) For Safe PDP, its ability to learn and guarantee constraints comes at the cost of lower computational efficiency in the forward pass, as shown in the second column in Table S1. Even though Safe PDP handles constraint enforcement by adding them to the control cost using barrier functions, solving the resulting unconstrained approximation still needs more time than solving the unconstrained PDP. This could be because the added log barrier terms can increase the complex/stiff curvature of the cost/loss landscape, thus taking longer to find the minimizer. Further discussion about how barrier parameter influences the computational efficiency of the forward pass will be given in Appendix G.3.

(3) The running time for the backward pass is almost the same for both PDP and Safe PDP because both methods are solving an unconstrained LQR problem (auxiliary control system) of the same size (see Theorem 2), which can be very efficient based on Riccati equation.

### G.2 Strategies to Accelerate Forward Pass of Safe PDP

In the previous experiments in Appendix F, we have used an NLP solver to solve the trajectory optimization (optimal control) in the forward pass. Since the solver blindly treats an optimal control problem as a general non-linear program without leveraging the (sparse) structures in an optimal control problem. Thus, solving the long-horizon trajectory optimization is not very efficient. To accelerate long-horizon trajectory optimization, one can use plenty of strategies, as described below.

- To solve a long-horizon optimal control problem, one effective method is to scale a (continuous) long time horizon into a smaller one (like a unit) by applying a time-warping function to the system dynamics and control cost [85]. After discretizing and solving this short-horizon optimal control problem, re-scale the obtained optimal trajectory back. This time-scaling strategy is common in many commercial optimal control solvers, such as GPOPS [94].
- There are also the ‘warm-up’ tricks to accelerate the trajectory optimization in the forward pass of Safe PDP. For example, one can initialize the trajectory at the next iteration using the result of the previous iteration.
- One also can use a coarse-to-fine hierarchical strategy to solve long-horizon trajectory optimization. For example, given a long-time horizon optimal control system, first, discretize the trajectory with larger granularity and solve for a coarse-resolution optimal trajectory;

then use the coarse trajectory as initial conditions to solve the trajectory optimization with fine granular discretization.

As an additional experiment based on cartpole system (in Table 1), we tested and compared the above three strategies for accelerating the forward pass of Safe PDP. The timing for each strategy is given in the following Table S2. Here,  $t_f$  is the continuous-time horizon of the cartpole system,  $\Delta$  is the discretization interval, and the discrete-time horizon is  $T = t_f/\Delta$ .

Table S2: Running time for different strategies in accelerating the forward pass of Safe PDP

| Strategies       | $t_f = 2\text{s}, \Delta = 0.1\text{s},$ | $t_f = 6\text{s}, \Delta = 0.1\text{s},$ | $t_f = 10\text{s}, \Delta = 0.1\text{s},$ | $t_f = 20\text{s}, \Delta = 0.1\text{s},$ |
|------------------|------------------------------------------|------------------------------------------|-------------------------------------------|-------------------------------------------|
|                  | $T = t_f/\Delta = 20$                    | $T = t_f/\Delta = 60$                    | $T = t_f/\Delta = 100$                    | $T = t_f/\Delta = 200$                    |
| Plain NPL solver | 0.082s                                   | 0.202s                                   | 0.491s                                    | 1.743s                                    |
| Time scaling     | <b>0.014s</b>                            | <b>0.033s</b>                            | <b>0.055s</b>                             | <b>0.083s</b>                             |
| Warm start       | 0.055s                                   | 0.095s                                   | 0.108s                                    | 0.224s                                    |
| Hierarchical     | 0.021s                                   | 0.055s                                   | 0.074s                                    | 0.133s                                    |

From the results in Table S2, one can see that time-scaling is the most effective way among others to accelerate long-horizon trajectory optimization. Of course, one can combine some of the above strategies to further improve the running performance of the forward pass of Safe PDP.

Additionally, one can also use iLQR [81] and DDP [82] to solve optimal control problems. iLQR can be viewed as the one-and-half-order method—linearizing dynamics and quadratizing cost function. DDP is a second-order method — quadractizing both dynamics and cost function. Both methods solve a local bellman equation to generate the update of the control sequence. But without coding optimization, both methods are slower than the commercial NPL solver (e.g., CasADi [77]). Some ongoing works are trying to take advantage of GPUs for accelerating trajectory optimization, which is also our future research.

### G.3 Trade-off Between Accuracy and Efficiency using Barrier Penalties

In the paper, we have provided both theoretical guarantees (see Theorem 2 and Theorem 3) and empirical experiments (see Fig. 1, Fig. 2a and 2c, Fig. 3a and 3c, and Fig. 4) for the relationship between the accuracy of a solution to an unconstrained approximation and the choice of the barrier parameter. This subsection further investigates the trade-off between accuracy and computational efficiency under different choices of the barrier parameter.

In the experiment below (based on the cartpole system in Table 1), by choosing different barrier parameters  $\gamma$  in the forward pass of Safe PDP, we show the accuracy of the trajectory  $\xi(\gamma)$  solved from an unconstrained approximation system  $\Sigma(\gamma)$  and the corresponding computation time. The results are presented in Table S3.

Table S3: Accuracy of the trajectory  $\xi(\gamma)$  from the unconstrained approximation system  $\Sigma(\gamma)$  and its computation time with different choices of barrier parameter  $\gamma$

|                                                                                                                       | choice of $\gamma$ |           |           |           |           |           |
|-----------------------------------------------------------------------------------------------------------------------|--------------------|-----------|-----------|-----------|-----------|-----------|
|                                                                                                                       | 1                  | $10^{-1}$ | $10^{-2}$ | $10^{-3}$ | $10^{-4}$ | $10^{-5}$ |
| Accuracy of $\xi(\gamma)$ in percentage:<br>$\frac{\ \xi(\gamma) - \xi^*\ _2}{\ \xi^*\ _2} \times 100\%$ <sup>1</sup> | 51.9%              | 12.2%     | 1.6%      | 0.18%     | 0.018%    | 0.0002%   |
| Timing for computing $\xi(\gamma)$                                                                                    | 0.023s             | 0.033s    | 0.035s    | 0.040s    | 0.038s    | 0.047s    |

<sup>1</sup> Note that in the above table,  $\xi^*$  is the ground-truth solution obtained from solving the original constrained trajectory optimization, and the computation time for such a constrained trajectory optimization is 0.062s.

We have the following comments on the above results in Table S3.

- First, the results in the first row of Table S3 show that a smaller barrier parameter leads to higher accuracy of the approximation solution. This again confirms the theoretical guarantee

in Theorem 2 (Claim (b)). The results here are also consistent with the ones in Fig. 1 in the paper.

- Second, the second row of Table S3 shows that a smaller barrier parameter, however, increases the computation time for solving the unconstrained approximation optimization. This could be because using a small barrier parameter, the added barrier terms can increase the complex/stiff curvature of the cost/loss landscape, thus taking Safe PDP longer to find the minimizer. Despite this, the time needed for finding a minimizer is still lower than directly solving a constrained trajectory optimization in the above experiment.
- Third, if one still wants to further increase the computation efficiency of Safe PDP, we have provided some strategies to achieve so, including "time scaling," "warm start," and "coarse-to-fine." Please check the Appendix G.2 for more detailed descriptions and corresponding experiment results.

In summary, we have shown that higher accuracy of the unconstrained approximation solution can be achieved using a smaller barrier parameter, while a smaller barrier parameter would increase the computation time for finding the approximation solution. In practice, one would likely choose an appropriate barrier parameter to balance the trade-off between accuracy and computational efficiency. Also, there are multiple strategies available to increase the computational efficiency of Safe PDP, as discussed in the Appendix G.2.

#### G.4 Learning MPCs from Non-Optimal Demonstrations

In the application of learning MPCs (including objective, dynamics, constraints), given non-optimal demonstrations, Safe PDP can still learn an MPC such that the trajectory reproduced by the learned MPC has the closest discrepancy to the given non-optimal demonstrations (e.g., when the task loss is defined as  $l_2$  norm between the reproduced trajectory and demonstrations). As an illustrative example, the following Table S4 shows learning an MPC from a sub-optimal demonstration for the cartpole system.

Table S4: Safe PDP for learning MPCs from non-optimal demonstrations

|                            | Number of iterations |        |        |        |        |        |        |        |
|----------------------------|----------------------|--------|--------|--------|--------|--------|--------|--------|
|                            | 0                    | 10     | 20     | 50     | 100    | 150    | 200    | 1000   |
| loss with optimal demo     | 779.986              | 2.206  | 1.481  | 0.832  | 0.641  | 0.620  | 0.611  | 0.232  |
| loss with non-optimal demo | 1126.820             | 18.975 | 17.771 | 15.602 | 13.690 | 12.469 | 11.620 | 10.923 |

As shown in S4, the only difference between learning from optimal and non-optimal demonstrations is that the converged loss for the non-optimal demonstrations is relatively higher than for the optimal ones. This is because, for non-optimal demonstrations, there might not necessarily exist an exact MPC model in the parameterized model space which perfectly corresponds to the given demonstration. In such a case, however, Safe PDP can still find the best model in the parametrized model space such that its reproduced trajectory has a minimal distance to the given non-optimal demonstrations. For the extended research of the generalization ability of the learned MPCs from the non-optimal demonstrations, please refer to [85].

#### G.5 Limitation of Safe PDP

Safe PDP requires a safe (feasible) initialization such that the log-barrier-based objectives (cost or task) are well-defined. While this requirement can be restrictive in some cases, we have the following empirical experiences on how to provide safe initialization for different types of problems.

- In safe policy optimization, one could first use supervised learning to learn a safe policy from some safe trajectories/demonstrations (which could not necessarily be optimal). Then, use the learned safe policy to initialize Safe PDP. We have used this strategy in our previous experiments in Appendix F.1.
- In safe motion planning, one could arbitrarily provide a safe trajectory (not necessarily optimal) to initialize Safe PDP. We have used this strategy in the previous experiments in Appendix F.2.

- In learning MPCs from demonstrations (Appendix F.3), the goal includes learning constraint models, and there is no such requirement.

Also, Safe PDP cannot apply to robust learning and control tasks. The goal of robust learning and control concerns achieving or maintaining good performance (such as stability or optimality) in the case of the worst disturbance or attacks to a system. Methods for handling those types of problems, such as robust control and differential game, have been well-developed in both control and machine learning communities. On the other hand, Safe PDP only focuses on guaranteeing the satisfaction of inequality constraints throughout a learning or control process, and such constraints are defined on the system states and inputs.